



University of Kentucky
UKnowledge

Theses and Dissertations--Plant and Soil
Sciences

Plant and Soil Sciences


2021

UNDERSTANDING THE EFFECTS OF COMPLEX TOPOGRAPHY ON COVER CROP DYNAMICS AND MAIZE PRODUCTION IN KENTUCKY AGROECOSYSTEMS

Samuel John Leuthold

University of Kentucky, sam.leuthold@gmail.com

Author ORCID Identifier:

 <https://orcid.org/0000-0003-4180-7081>

Digital Object Identifier: <https://doi.org/10.13023/etd.2021.057>

[Right click to open a feedback form in a new tab to let us know how this document benefits you.](#)

Recommended Citation

Leuthold, Samuel John, "UNDERSTANDING THE EFFECTS OF COMPLEX TOPOGRAPHY ON COVER CROP DYNAMICS AND MAIZE PRODUCTION IN KENTUCKY AGROECOSYSTEMS" (2021). *Theses and Dissertations--Plant and Soil Sciences*. 142.
https://uknowledge.uky.edu/pss_etds/142

This Master's Thesis is brought to you for free and open access by the Plant and Soil Sciences at UKnowledge. It has been accepted for inclusion in Theses and Dissertations--Plant and Soil Sciences by an authorized administrator of UKnowledge. For more information, please contact UKnowledge@lsv.uky.edu.

STUDENT AGREEMENT:

I represent that my thesis or dissertation and abstract are my original work. Proper attribution has been given to all outside sources. I understand that I am solely responsible for obtaining any needed copyright permissions. I have obtained needed written permission statement(s) from the owner(s) of each third-party copyrighted matter to be included in my work, allowing electronic distribution (if such use is not permitted by the fair use doctrine) which will be submitted to UKnowledge as Additional File.

I hereby grant to The University of Kentucky and its agents the irrevocable, non-exclusive, and royalty-free license to archive and make accessible my work in whole or in part in all forms of media, now or hereafter known. I agree that the document mentioned above may be made available immediately for worldwide access unless an embargo applies.

I retain all other ownership rights to the copyright of my work. I also retain the right to use in future works (such as articles or books) all or part of my work. I understand that I am free to register the copyright to my work.

REVIEW, APPROVAL AND ACCEPTANCE

The document mentioned above has been reviewed and accepted by the student's advisor, on behalf of the advisory committee, and by the Director of Graduate Studies (DGS), on behalf of the program; we verify that this is the final, approved version of the student's thesis including all changes required by the advisory committee. The undersigned agree to abide by the statements above.

Samuel John Leuthold, Student

Dr. Hanna J. Poffenbarger, Major Professor

Dr. Mark Coyne, Director of Graduate Studies

UNDERSTANDING THE EFFECTS OF COMPLEX TOPOGRAPHY ON COVER
CROP DYNAMICS AND MAIZE PRODUCTION IN KENTUCKY
AGROECOSYSTEMS

THESIS

A thesis submitted in partial fulfillment of the
requirements for the degree of Master of Science in the
College of Agriculture, Food and the Environment
at the University of Kentucky

By

Samuel John Leuthold

Lexington, Kentucky

Director: Dr. Hanna J. Poffenbarger, Assistant Professor of Soil Nutrient Management

Lexington, Kentucky

2021

Copyright © Samuel John Leuthold 2021
<https://orcid.org/0000-0003-4180-7081>

ABSTRACT OF THESIS

In Central Kentucky, rolling hill cropland presents a number of challenges related to soil sustainability. Increased topographic complexity can lead to increased erosion, inefficient crop nutrient use and increased nutrient loss. Further, grain crop yields can be variable across both space and time in rolling hill fields and are less resilient to changes in weather conditions than flatter, more homogeneous areas. More than 30% of cropland in Kentucky has a slope greater than 3°, which means a large swath of the row crop production land in the state is at increased risk of contribution to soil and water resource degradation. Managing these croplands in a way that secures the economic and environmental sustainability of Kentucky producers is critical to ensuring food system security on a local scale, and increase the viability of Kentucky ecosystems, both managed and natural.

Cover crops, crops grown for ecosystem benefits rather than harvested for profit, may be a way of reducing the impact of complex topography on row crop production. Cover crops have been shown to reduce erosion losses, prevent nutrient loss to groundwater, and improve soil quality. Further when grown in a mixture, such as a cereal-legume biculture, cover crops have been shown to exhibit multifunctional traits, such as coupling N retention and release in synchrony with crop uptake. As such, they may present a management practice that can increase the sustainability of rolling hill agroecosystems, and possibly reduce the spatial and temporal variability in yield and biogeochemical cycling. There has been some research on the interaction between topography and cover crop implementation conducted up to this point. Across these studies however, to the author's knowledge, there has not been a systems level analysis of the landscape position effect on cover crop growth and dynamics, decomposition, and the subsequent interactive effect of cover crop and topography on maize development and yield. Closing this knowledge gap provides an opportunity to increase our understanding of agroecosystem processes beyond individual crop growing seasons and determine how management of winter cover crops can be improved to enhance overall agronomic outcomes.

Understanding how landscape topography impacts cover crop production, and in turn affects maize production, is critical to improving management of cover crops in Central Kentucky, and thus increasing agroecosystem sustainability. Here, we present the results of four experiments, which had the objectives of: 1.) Determining the effect of landscape position on cover crop biomass production and function, including species diversity and nitrogen fixation, 2.) Quantifying the effect of landscape position on the decomposition and N release rate of different cover crop treatments, 3.) Examining the scientific literature to determine how weather influences the relationship between grain production and topography, and 4.) Using field observations to calibrate a soil-crop system model for predictions of cover crop by topography interactions on maize yield and spatiotemporal yield stability under different climate scenarios.

Our results, detailed in the subsequent chapters, indicate that cover crop growth and function respond strongly to topographic factors such as slope, and edaphic factors such as soil texture and inorganic nitrogen. Additionally, landscape position has a significant effect on the spatial distribution of soil water, and the surface soil temperature

throughout the maize growing season, but this does not translate to spatial differences in the rate of cover crop decomposition. Our analysis of the relationships between topography and crop yield indicate that maize yield varies in its response to topographic factors based on growing season precipitation, such that at low precipitation, sloping areas yield poorly, but increase in yield as growing season precipitation increases. When we expanded our field data results to different climate scenarios using a soil-crop system model, we found that the presence of cover crop residue can decrease maize yield variability across time and space by raising yields in sloping positions via increased soil water storage, especially under dry conditions. The results presented here offer further evidence that the integration of cover crops into areas of sloping topography offer outsized benefits compared to areas of homogeneous terrain, including more stable yields, and increased N return. This work provides a means for maximizing the benefits of cover crop functionality for producers and increasing the overall sustainability of Kentucky agroecosystems.

KEYWORDS: Cereal rye, maize, yield stability, crimson clover, decomposition, nitrogen fixation

Samuel John Leuthold

(Name of Student)

3/29/2021

Date

UNDERSTANDING THE INTERACTIVE EFFECTS OF COMPLEX TOPOGRAPHY
ON COVER CROP DYNAMICS AND MAIZE PRODUCTION IN KENTUCKY
AGROECOSYSTEMS

By
Samuel John Leuthold

Hanna J. Poffenbarger, PhD

Director of Thesis

Mark Coyne, PhD

Director of Graduate Studies

3/29/2021

Date

DEDICATION

To John H. Leuthold Jr. A poor old dirt farmer, and an inspiration above all others.

ACKNOWLEDGMENTS

The thesis presented here represents the culmination of hard work from an amazing number of individuals, all of whom deserve more thanks than can be expressed in this section. My thesis advisor, Hanna Poffenbarger, has taught me more than I could have imagined, setting an example for being an excellent scientist, a gracious leader, and a kind and thoughtful person. The additional members of my advisory committee, Montse Salmeron and Ole Wendroth, provided guidance, support, and encouragement at every step of the process, and I could not be more grateful. I owe an exorbitant amount to Laura Harris and the rotating cast of characters in the Agroecosystem Nutrient Cycling Lab, for without whom this project would have continued *ad infinitum*. Your help in the lab and the field was invaluable to the product we present here. Additionally, I'd like to thank Richard Preston, Josh McGrath, Gene Hahn, James Dollarhide, Jason Walton, and Dan Quinn. The collective knowledge these individuals share regarding the act of farming serves to remind me how much I still have to learn and was integral to making sure I actually had data to talk about. My previous advisors, including Stephanie Ewing and Rob Payn, also contributed to shaping me into the scientist I am today; without their mentorship my time at the University of Kentucky would not have been half as fruitful as it has been.

I owe Hunter Howe an immeasurable debt for her support and partnership; she endured countless long drives and early morning flights, and never wavered in her encouragement and backing. Thank you, for everything and more. My family has supported me every step of the way, never questioning why I was so interested in dirt, and understanding when I couldn't answer questions about the lawn or the flowers. Thank you all for your optimism and sage counsel whenever I had a moment of doubt. To my friends, both new and old, thank you for picking up the phone, for sharing a beer, and for offering kind words when I needed them.

Finally, this work would not have been possible without the generous support from the USDA Southern SARE program, the Kentucky Corn Board, the University of Kentucky College of Agriculture, Food, and the Environment, and the Karri Casner Environmental Fellowship.

Thank you all, for your help, your insight, and your mentorship, and your support.
I am immensely grateful, and I wouldn't have made it to this point without it.

TABLE OF CONTENTS

ACKNOWLEDGMENTS	iii
LIST OF TABLES	viii
LIST OF FIGURES	x
CHAPTER 1. Impacts of topography on nitrogen fixation, species composition, and biomass production of cover crops.....	1
1.1 Abstract	1
1.2 Introduction	2
1.3 Materials and Methods.....	5
1.3.1 <i>Field site description and experimental design</i>	5
1.3.2 <i>Cover crop management</i>	7
1.3.3 <i>Field data collection</i>	8
1.3.4 <i>Spatial data analysis and statistics</i>	10
1.4 Results	11
1.4.1 <i>Site edaphic and topographic characteristics</i>	11
1.4.2 <i>Total cover crop biomass production and N uptake</i>	12
1.4.3 <i>Percentage clover and nitrogen fixation</i>	14
1.4.4 <i>Landscape controls on cover crop dynamics</i>	15
1.5 Discussion.....	17
1.5.1 <i>Cover crop biomass production by landscape position and cover crop treatment</i>	17
1.5.2 <i>Cover crop N accumulation by landscape position and cover crop treatment</i>	19
1.5.3 <i>Clover dynamics within mixture</i>	20
1.5.4 <i>Cover crop mixture effect on biomass stability</i>	22
1.5.5 <i>Implications for agroecosystems</i>	23
1.6 Conclusions	24
1.7 Chapter 1 tables and figures	26
CHAPTER 2. Landscape topography effects on soil microclimate and surface cover crop residue decomposition	35
2.1 Abstract	35
2.2 Introduction	36

2.3	Materials and methods	40
2.3.1	<i>Experimental design and management</i>	40
2.3.2	<i>Experimental data collection</i>	41
2.3.2.1	Cover crop biomass.....	41
2.3.2.2	Litterbag construction, deployment, and processing.....	42
2.3.2.3	Weather and soil microclimate measurements.....	43
2.3.3	<i>Calculations and statistics</i>	45
2.3.3.1	Exponential decay models.....	45
2.3.3.2	Soil temperature and moisture analysis.....	46
2.4	Results	47
2.4.1	<i>Topographic and edaphic factors</i>	47
2.4.2	<i>Microclimate</i>	48
2.4.2.1	Air temperature, growing degree days, and decomposition days.....	48
2.4.2.2	Soil temperature and moisture responses to landscape position and cover crop treatment	50
2.4.3	<i>Litterbag experiment results</i>	51
2.4.3.1	Initial litterbag properties	51
2.4.3.2	Litterbag decomposition and nutrient release	51
2.4.3.3	Landscape position adjusted litterbags.....	54
2.5	Discussion.....	55
2.5.1	<i>Landscape position and cover crop effects on microclimate</i>	55
2.5.2	<i>Landscape position and cover crop effects on decomposition</i>	59
2.5.2.1	Landscape position treatment	59
2.5.2.2	Cover crop treatment.....	62
2.6	Conclusions	64
2.7	Chapter 2 tables and figures	66
CHAPTER 3. Weather dependent relationships between topographic variables and yield of maize and soybean: A quantitative review.....		
3.1	Abstract	81
3.2	Introduction	82
3.3	Materials and methods	83
3.4	Results and Discussion.....	85
3.5	Conclusions and Implications.....	90
3.6	Chapter 3 tables and figures	91
CHAPTER 4. Cover crops decrease maize yield variability in sloping landscapes through increased water during reproductive stages		
4.1	Abstract	97
4.2	Introduction	98

4.3	Materials and Methods.....	102
4.3.1	<i>Description of field trial</i>	102
4.3.2	<i>Experimental data collection and analysis</i>	104
4.3.3	<i>Simulation of field study</i>	106
4.3.3.1	Description of software used and model settings.....	106
4.3.3.2	Soil physical parameter calibration.....	107
4.3.3.3	Parameterization of the DSSAT-Century for soil N mineralization.....	107
4.3.3.4	Calibration of crop coefficients	108
4.3.3.5	Model evaluation	110
4.3.4	<i>Sensitivity analysis with historical weather</i>	111
4.4	Results	113
4.4.1	<i>Model performance and comparison to field experiment</i>	113
4.4.1.1	Cover crop biomass and N content	113
4.4.1.2	Maize growth and N content	113
4.4.1.3	Soil moisture dynamics	115
4.4.2	<i>Sensitivity analysis of weather and management effects on simulated maize yield</i>	116
4.4.2.1	Cover crop effects on simulated maize yield and yield stability.....	117
4.4.2.2	Cover crop effect on frequency and size of simulated water-stress yield gap	118
4.4.2.3	Cover crop effects on simulated water balance and water stress	119
4.5	Discussion.....	121
4.5.1	<i>Applications of DSSAT to simulate topography x weather x cover crop interactions</i>	121
4.5.2	<i>Cover crops effect on maize yield</i>	125
4.5.3	<i>Study limitations and future research</i>	127
4.6	Conclusions	128
4.7	Chapter 4 tables and figures	130
	Appendix	147
	REFERENCES.....	150
	VITA.....	175

LIST OF TABLES

Table 1.1 - Soil and topographical characteristics for hillslope fields in 2019 and 2020..	26
Table 1.2 - Cover crop management dates for the four site-years.	27
Table S1.1 - Contribution of each factor to principal components for first 17 PCs in the rye treatment. PC1 and PC2 (presented in main text) are highlighted according to contribution; red: low, green: high.	33
Table 2.1 – Soil and topographic characteristics for hillslope fields in 2019 and 2020....	66
Table 2.2 – Removal dates and days after installation of litterbags in 2019 and 2020.	67
Table 2.3 - Decomposition rate (k) and asymptote (a) predictions and standard errors from non-linear models of cover crop residue decomposition in 2019 and 2020. Units are in percentage decomposed or percentage released, where appropriate. No parameters were significantly different according to pairwise comparisons of model contrasts, except for the k2 parameter for nitrogen release in the backslope position in 2020, and the a2 parameter in 2019.....	68
Table 2.4 - Predictions of N release and mass remaining at the final removal date (i.e., 130 or 132 days after installation for ST1 and ST2, respectively) for each landscape position based on the application of non-linear models to initial biomass measurements.	69
Table S2.1 - Model fitting assessment values for proposed time scales for litter decomposition.....	76
Table S2.2 - Total accumulated growing degree days (sGDD) calculated from soil temperature at each landscape position.....	77
Table S2.3 - Cover crop biomass production and R1 maize aboveground biomass at each landscape position in 2019 and 2020.....	78
Table S 2.4 - Proportion of original litter remaining and percentage of N released from position specific litterbags at the final removal date. No significant differences were present between treatments.	79
Table 3.1 – Definitions of key topographic variables considered in this analysis	91

Table 3.2 - Average correlation coefficients (r), and p-values between selected topographic variables and crop yield from reviewed studies. Significant p-values (bolded correlation coefficients) presented indicate if the correlation coefficient between yield and a given topographic variable was significantly different than zero. Planar curvature was omitted for soybean because the minimal data requirement was not met.....	92
Table S3.1 - Studies included in the analysis, including number of site years, crop species, regions, and correlation type used. Xs in the topographic attribute columns indicate that a correlation between yield and topographic factor was present in that study.....	95
Table 4.1 - Summary of field operations for cover crop and maize management in the 2019 field experiment.	130
Table 4.2 - Measured, estimated, and calculated characteristics of soils used in simulations. Soil layers were provided to the model in 10 cm increments but are average and combined in this table for brevity.	131
Table 4.3 - Simulated water balance components during maize growing season by landscape position, precipitation category, and cover crop treatment, and difference between cover treatments (cover crop – control).	132
Table S 4.1 - Full ANOVA tables for yield sensitivity analysis. Top panel reflects results from baseline soil organic matter treatments, lower panel reflects low soil organic matter treatments. The percent sums of squares represent the fraction of sums of squares apportioned to the face in question compared to the total sums of squares.	142
Table S4.2 - Crop coefficient parameters for the wheat cultivar used to simulate a rye cover crop, and the maize cultivar used in this study	144

LIST OF FIGURES

Figure 1.1 – Plot arrangement for the four site-years presented in this study. Capital letters on the individual plots indicate the cover crop treatment for each plot (R = rye monoculture, M = rye-crimson clover mixture, B = bare). At the HC1 and HC2 sites, replicates were split across three separate hillslopes. To preserve map scale and improve readability, each replicate is presented separately for these site-years.	28
Figure 1.2 – Total cover crop biomass and total N uptake for rye monoculture and rye-crimson clover mixture.	29
Figure 1.3 - Boxplots representing the percentage of N derived from fixation at each landscape position, and the percentage of clover within the mixture treatment at each landscape position. Differences in the letters above each box indicates significant differences between landscape position treatments at the $p < 0.10$ significance level.	30
Figure 1.4 – PCA biplots of the first and second principal components of the rye monoculture and rye-crimson clover mixture treatments. Angles $< 90^{\circ}$ indicate positive correlations between variables, while angles $> 90^{\circ}$ indicate negative correlations. The ellipses represent the 90% confidence interval for the mean value in PC space of each landscape position.	31
Figure 1.5 – Correlations between biomass of cover crop species and important explanatory variables identified in the PCA. Different shapes indicate different field sites, while different colors indicate different landscape positions. Data are pooled across all 4 site-years. Rye biomass includes rye in both monoculture and mixture. .	32
Figure 2.1 - Field orientation and plot layout for 2019 (left) and 2020 (right). Different colored plots indicate different cover crop treatments, green for cereal rye, red for the cereal rye-crimson clover mixture, and tan for the winter fallow. Inset illustration is an example of the plot layout between the center two maize rows for plots with litterbags present.	70

Figure 2.2 - Weather data for the growing season in 2019 (left) and 2020 (right) collected by the UK Ag Weather Station at Spindletop Farm. Blue bars indicate the cumulative weekly rainfall (cm). Connected points indicate the average weekly temperature.....	71
Figure 2.3 - Relative decomposition rate compared to optimum environmental conditions, calculated using the DCD model from Steiner et al. (1999). Shading indicates dominant decomposition control on a given day; red for temperature limitation and blue for moisture limitation. Black line represents the lower value of the two coefficients and indicates how quickly decomposition is occurring relative to optimum temperature and moisture conditions.	72
Figure 2.4 - Soil temperature at 5 cm depth throughout the corn growing season for mixture (left) and rye (right) treatments, at each landscape position. The top panels reflect the 2019 growing season, the bottom panels reflect the 2020 growing season. Horizontal bars indicate the results of GAM analysis and indicate significant differences within a given pairwise comparison. Ribbons surrounding the predictions indicate the 95% confidence interval.....	73
Figure 2.5 - Soil volumetric water (0-10 cm) taken weekly throughout the corn growing season for mixture (left) and rye (right) treatments, at each landscape position. The top panels reflect the 2019 growing season, the bottom panels reflect the 2020 growing season. Horizontal bars indicate the results of GAM analysis and indicate significant differences within a given pairwise comparison. Ribbons surrounding the predictions indicate the 95% confidence interval. The points indicate the average of three measurements on each sampling date, error bars are +/- 1 SE.	74
Figure 2.6 - Left: Proportion of cover crop residue remaining measured in both cover crop treatments at removal dates (circles) and predictions from non-linear models in the 2019 (upper left) and 2020 (bottom left) growing season. Right: Cumulative proportion of N released from the cover residue measured in both cover crop treatments at removal dates (circles) and predictions from non-linear models for the 2019 (upper right) and 2020 growing season (bottom right). Ribbons around predictions indicate the prediction standard error.	75
Figure S2.1 - Relative solar insolation (%) for the period of time litterbags were deployed in the field for 2019 (left) and 2020 (right).....	80

Figure 3.1 – Correlation matrix of yield vs. topography correlations and precipitation categories. The center number indicates the correlation between correlations coefficients and precipitation, with color indicating the direction of the relationship (red: negative, green: positive). The lower number is the p-value of the linear regression.	94
Figure 3.2 – Crop yield (A) and crop yield variability (B) with increasing precipitation. Different points represent observations from an individual site year, while different colors represent the different studies considered in this analysis. Relationships were not significant for soybean, but were significant for maize.	93
Figure S3.1 - Linear regressions of correlation coefficients between yield and topography characteristics (i.e., elevation, planar curvature, profile curvature, and slope), and cumulative precipitation during the three precipitation categories. Different points represent different site years, while different colors indicate different studies. The shaded area indicates the 90% confidence interval.	96
Figure 4.1 - Topographic map with % slope and experimental layout for field experiments in 2019.	133
Figure 4.2 - Observed and simulated rye cover crop aboveground biomass at termination (A), and maize grain yield (B). Closed symbols represent observed and simulated data for experimental trials in 2019, error bars on observed data represent ± 1 standard deviation. Boxplots show data from 30-year simulations with historical weather data (1989 – 2019).	134
Figure 4.3 - Observed and simulated maize aboveground biomass and N content at R1 and R6, grain yield, grain N content, unit kernel weight, and kernels per square meter in maize after fallow (A) and maize after a cereal rye cover crop (B). Different symbols show data by landscape position and N rate. Maize aboveground biomass and N content at R1 was only sampled in treatments receiving 0 and 270 kg N ha ⁻¹	135
Figure 4.4 - Observed and simulated total soil water in the top (0-50 cm) and bottom (50-100 cm) soil profile at each landscape position in maize after fallow and after a cover crop during 2019 experimental trial. Soils in the backslope position did not extend beyond 50 cm. Error bars show the standard error in the observed data. Statistics for	

model performance are presented for fallow treatment and rye treatment, respectively.	136
Figure 4.5 - Treemap indicating the apportionment of sums of squares within the ANOVA models for the baseline soil fertility and the low fertility treatments. Larger areas within the treemap correlate with greater percentage of sums of square apportioned to a particular model term.	137
Figure 4.6 - Smoothed density plots of maize yield at different landscape positions for different cover crop treatments and precipitation categories. Dashed lines indicate the mean yields for each distribution.....	138
Figure 4.7 - Top: Maize grain yield vs. variance plot for the different landscape positions (A) and different precipitation categories (B). Dashed lines connect the fallow and cover cropped treatment within the same landscape position. $\sigma(\text{Yield})$ is equal to one standard deviation in kg ha^{-1} . Bottom: Yield coefficient of variation from 30-year simulations by landscape position (C), precipitation category (D), and total (E), of maize grown after fallow or after a cereal rye cover crop.	139
Figure 4.8 –Percentage of years undergoing 10% or greater yield reduction due to water stress (A) and average annual yield gap due to water stress across all simulation years (B) by landscape position and cover crop treatment. Error bars indicate $\pm 1 \text{ SE}$	140
Figure 4.9 - Simulated daily excess and limited water stress index during the corn growing season by weather scenario (dry, average, and wet) and landscape position for each cover crop treatment. Data averaged across 30-year simulations. The shaded yellow bar indicates the range of simulated anthesis dates across the 30-year simulation study.....	141
Figure S4.1 - Mean measured soil water storage across key developmental stage in the 2019 field experiment for different landscape positions and cover crop treatments. Capital letters indicate significant differences in soil water storage between landscape position, while lowercase letters indicate significant differences in soil water storage between cover crop treatments.	145
Figure S 4.2 - Average soil water storage across 30 years of data for both the cover crop treatments during spring planting period. The first vertical line indicates the date of	

cover crop termination, the second indicates the date of maize planting. Shaded areas
surrounding the lines represent ± 1 SE.146

CHAPTER 1. IMPACTS OF TOPOGRAPHY ON NITROGEN FIXATION, SPECIES COMPOSITION, AND BIOMASS PRODUCTION OF COVER CROPS

1.1 Abstract

Cover crops are a common management practice which can decrease erosion, reduce agricultural impacts on water quality, provide a nitrogen (N) source to subsequent cash crops, and increase overall agroecosystem sustainability. These benefits are especially relevant in areas of rolling hill topography, where variability in edaphic and hydrologic characteristics can create disparate fertility conditions throughout a given field. However, an increased understanding of how the effects of complex topography influence cover crop performance is needed to provide clear management recommendations. In this study, we aimed to determine how landscape position affects biomass production and N uptake of two cover crop treatments: a cereal rye (*Secale cereale* L.) sole crop, and a cereal rye – crimson clover (*Trifolium incarnatum*) mixture. In both the sole crop and the mixture, we aimed to determine how biomass production and N uptake varied across three landscape positions (i.e., summit, backslope, and toeslope positions), all with distinct edaphic characteristics. Within the mixture treatment specifically, we attempted to understand how legume expression within the mixture varied across landscape positions in regard to atmospheric nitrogen fixation rate, and percentage of legume within the total cover crop biomass. Overall, we found evidence that landscape position did influence total cover crop biomass production; toeslope positions produced up to 38% more biomass than backslope and summit positions. Additionally, we found that landscape position and related topographic and edaphic factors influenced legume proportion and nitrogen fixation significantly. The total clover

biomass within the mixture treatment increased by 50 kg ha⁻¹ per degree increase in slope. The percentage of N derived from fixation (NDFA) was strongly correlated with slope and soil sand content; the amount of NDFA increased by 1.75% per 1% increase in sand. Notably, the same factors that drove legume response did not influence the cereal rye cover crop, regardless of whether it was grown in a mixture or a sole crop. Our results illustrate the role topography has in dictating cover crop function and biomass production, providing a means for producers to consider how to best incorporate cover crop practices into their operations.

1.2 Introduction

Cover crops, those planted for agroecosystem benefits rather than for a harvested product, are commonly used to increase the sustainability of crop production (Snapp et al., 2005). Estimates of total nitrogen (N) losses for the primary crop production regions of the United States range between 0.64 – 1.67 Tg N y⁻¹ (Basso et al., 2019), with impacts on water quality and ecosystem sustainability ranging from regional (Nolan et al., 1997) to global scales (Galloway et al., 2003; Vitousek et al., 1997). By assimilating N that would otherwise be susceptible to leaching or other loss pathways, winter cover crops reduce downstream losses of reactive N by 10 – 60%, depending on biomass production and establishment (Kaspar et al., 2012; Strock et al., 2004). Further, the addition of a winter cover crop has been shown to reduce soil erosion (De Baets et al., 2011), increase soil water retention (Basche and DeLonge, 2017), build soil organic matter (SOM) (Chen et al., 2014), and provide an auxiliary source of N to cash crops following cover crop termination (Nevins et al., 2020; Poffenbarger et al., 2015a; Ranells and Waggoner, 1996). While cover crop use has increased over the course of the last decade, improving

management strategies for their use is critical to fostering more widespread adoption by producers.

Rolling hill style topography is a common feature in agricultural land across the United States; in Kentucky, over 35% of cultivated land has a slope greater than 3° (Kentucky Division of Geographic Information, 2017). The accelerated erosional processes that occur in cultivated, rolling hill agroecosystems, coupled with differences in organic matter mineralization rates (Beehler et al., 2017) and soil fertility (Jiang and Thelen, 2004; Kravchenko and Bullock, 2000), create discretized field conditions across hillslopes in regard to edaphic factors such as texture, soil carbon (C), and inorganic N stocks, such that the most fertile regions of the field occur in depression areas, and sloping areas have relatively lower fertility. This heterogeneity can lead to variability in plant production (Martinez-Feria and Basso, 2020), soil nutrient distribution (Dharmakeerthi et al., 2005), and total plant available soil water capacity (Leuthold et al., 2021). Sloping positions tend to be drier, and have poorer and more volatile crop yields than depressional areas (Jiang and Thelen, 2004; Kravchenko and Bullock, 2000; Kumhálová et al., 2011), though depressional areas are more prone to flooding and excess water stress (Maestrini and Basso, 2018a).

Due to the variability in edaphic and fertility characteristics among the landscape positions, growth, N uptake, and the ecosystem services provided by cover crops may differ depending on landscape position (Ladoni et al., 2016; Singh et al., 2019). Ladoni et al. (2015) observed greater cover crop biomass in depression areas compared to sloping and summit areas in a production scale field in MI. In contrast, studies from the same region (Beehler et al., 2017; Negassa et al., 2015) resulted in decreased cover crop

biomass in depressional areas than other positions, due to flooding and poor drainage.

With this diversity in results of cover crop production in complex landscapes, a more thorough understanding of the landscape scale controls on cover crop productivity and function is needed to maximize the benefits and improve management strategies for producers interested in cover crops.

One possible option for ensuring high cover crop productivity and function across the landscape may be to introduce a cereal-legume mixture cover crop, rather than the more common cereal sole crop. Generally, leguminous cover crops encompass a larger proportion of mixture biomass when soil fertility factors (e.g., SOM or soil inorganic N) are low because of their ability to fix atmospheric N (Blesh, 2019; Yu et al., 2016). For example, Blesh (2018) observed that legume biomass decreased within increasing SOM and increased with increasing plant available phosphorus (P) levels. Further to this point, Guretzky et al. (2004) and Harmony et al. (2001) both investigated legume biomass in pasture systems and showed that legume biomass was greatest in sloping areas, compared to depressions and summits. Grass species, in contrast, tend to produce the most biomass in N rich areas, such as topographic depressions (Ladoni et al., 2015; Schipanski and Drinkwater, 2011; Yu et al., 2016), and thus may suppress the legume in these settings. It is possible that a mixture treatment may be able to compensate for differences in soil fertility across hillslopes: increasing legume biomass in low productivity areas and increasing cereal biomass in high productivity areas, thus promoting high cover crop productivity throughout a field. Leveraging the complementary resource use of these two constituent species may therefore allow more consistent ecosystem service provisioning across areas of spatial nutrient variability, such as rolling hill croplands. To date however,

there has been little research investigating the dynamics of mixtures across topographic gradients, which leads to a knowledge gap around how management can be adapted to best incorporate this practice.

The purpose of this study was to describe the response of two cover crop treatments, a legume/cereal mixture and a cereal sole crop, to differences in landscape topography. Our objectives were to determine how landscape position affects biomass production and N uptake, and species composition in mixture. We hypothesized that: 1.) biomass and N uptake of cereal rye would vary by landscape position, with the most biomass production occurring in the toeslope, and the least on the backslope, 2.) the percentage of clover within the mixture would increase in areas of sloping topography, as the clover could better compete with the rye in lower N settings, 3.) N derived from atmospheric fixation would be highest on the slopes, and lowest in the depressions, and 4.) adding a legume to the cereal would moderate cover crop performance across the landscape, such that while species composition may change across the landscape, biomass production would be more similar between landscape positions in the mixture compared to the sole crop.

1.3 Materials and Methods

1.3.1 Field site description and experimental design

Between 2018 and 2020, field trials were conducted at two locations in Central Kentucky to investigate the effects of topography on cover crop biomass production, species composition, N uptake, and N fixation rate for a total of four site-years (**Figure 1.1**). Field sites were selected to represent hillslope settings found in row crop production areas in the Southeastern United States, and three landscape position treatments were identified at each field site based on slope and elevation (**Table 1.1**). One site was located

at the University of Kentucky Spindletop Farm (ST; 38.123° N, -84.490° W), an experimental farm managed by the University of Kentucky College of Agriculture, Food, and Environment (Sites ST1 and ST2). The average annual rainfall at the ST location is 1240 mm, and the average temperature is 13.3 °C (1990 – 2020, <http://weather.uky.edu>). During our field experiments, the total precipitation during the cover crop growing season (Oct. – Mar.) was 883 mm in 2018-2019, and 790 mm in 2019-2020. The average cover crop growing season temperature was 6.3 °C in 2018-2019, and 7.2 °C in 2019-2020. The accumulated growing degree days (base 0 °C, GDD) was 1213 during the 2018-2019 season, and 1347 in the 2019 -2020 season. The second site was located in Hardin County, KY (HC; 37.602° N, -85.906° W) as a part of an on-farm collaboration with a local producer (Sites HC1 and HC2). The average annual rainfall at the HC location is 1321 mm, and the average temperature is 13.2 °C (2009 – 2020; <http://weather.uky.edu/>). During our field experiments, the average temperature during the cover crop growing season was 6.0 °C in 2018-2019, and 7.2 °C in 2019-2020. The accumulated GDD in 2018-2019 was 1181, and in 2019-2020 was 1349. The total rainfall during the cover crop growing season in 2018-2019 was 878 mm, and 873 mm in 2019-2020.

Soils at the ST sites varied across landscape positions, but the arrangement of mapped soil series was consistent between years. At the summit positions, soils were classified as fine-silty, mixed, active mesic Typic Paleudalfs (Bluegrass Series). Soils at the backslope positions were classified as fine, mixed, active, mesic Mollic Hapludalfs (McAfee Series). The toeslope position soils were classified as fine-silty, mixed, active mesic Fluventic Hapludolls (Huntington Series). At the HC field sites, soils did not vary across

landscape positions according to the soil map. The dominant soil at both HC sites was classified as fine silty, mixed, active, mesic Typic Paleudalfs (Crider Series; Soil Survey Staff, 2020) . Soil depth varied across hillslopes, with toeslope positions having deeper soils and backslope soils noticeably shallower. Soil depth was determined via reported soil survey data in summit and toeslope (Soil Survey Staff, 2020), and hand probing in backslope positions. Selected soil fertility, physical components, and topographic attributes for each of the field sites are presented in **Table 1.1**.

Plots were arranged in a split-plot randomized complete block experimental design with three replicates at all field sites. At the ST locations all replicates were located on one hillslope each year, with cover crop treatments randomly assigned within a landscape position-replicate combination (**Figure 1.1**). At the HC sites, each replicate was placed on a separate hillslope within the producer's field each year, and cover crop treatments were continuous strips across landscape positions (**Figure 1.1**). As such, at the ST sites, landscape position was treated as the main plot effect, and cover crop treatment was the subplot effect. At the HC sites, this was reversed, with cover crop treatment acting as the main plot effect, and landscape position as the subplot effect.

1.3.2 *Cover crop management*

Prior to the experiment, both ST sites were in long-term hay production. In preparation for cover crop planting, both fields were sprayed with glyphosate, moldboard plowed, and then disked (ST1 in 2018, ST2 in 2019). Following the initial tillage, ST sites were managed as transitional no-till. The sites at HC were historically managed in no-till maize (*Zea mays* L.), soybean (*Glycine max* (L.) Merr.), and wheat (*Triticum aestivum* L.)

production. Cover crops were planted following soybean and prior to maize in the HC fields in both 2018 and 2019.

Three cover crop treatments were established at the beginning of the experiment for all field sites, a cereal rye (*Secale cereale* L.) sole crop, a cereal rye-crimson clover (*Trifolium incarnatum*) mixture, and no cover. The cereal rye sole crop was drill seeded at a target seeding rate of 73 kg ha⁻¹ at both locations. The mixture treatment was drill seeded at a target seeding rate of 45 kg ha⁻¹ of cereal rye and 13 kg ha⁻¹ of crimson clover at the ST locations, and 45 kg ha⁻¹ of cereal rye and 22 kg ha⁻¹ of crimson clover at the HC locations. The no cover treatments were not chemically controlled during the cover crop growth period. Cover crops were chemically terminated in the spring and left on the soil surface. At the time of termination, the rye cover crop was between the Feekes 7 and Feekes 8 growth stages, and the clover was at an advanced vegetative stage but had not flowered. Cover crop planting, termination, and sampling dates are listed in **Table 1.2**.

1.3.3 Field data collection

Soil samples were taken to a depth of 60 cm at the time of cover crop planting for soil inorganic N analysis. In the spring, prior to cash crop planting, soils were sampled to 20 cm to determine Mehlich 3-extractable nutrients, soil organic C and N, and soil texture. Samples were taken using a hand probe, separated at depths of 0-5, 5-15, 15-30, and 30-60 in the fall, and 0-10 cm and 10-20 cm in the spring. Each sample represent a composite of 9 subsamples taken randomly throughout the entire plot area. An 8 g dry equivalent subsample of fresh soil from the fall sampling was extracted using 40 ml of 1 M KCl and analyzed for total inorganic N using a colorimetric method (Crutchfield and Grove, 2011). The spring samples were subsampled, dried, and ground to 2 mm, then

sent to the University of Kentucky Regulatory Services Soil Lab for Mehlich 3 extractable nutrients, texture, and C and N concentrations (**Table 1.1**). Soil texture analysis was done using the pipette method, and C and N were analyzed via dry combustion.

Cover crop samples were collected immediately prior to chemical termination (**Table 1.2**). Either 2 or 4 subsamples were taken from each cover crop plot, processed individually, and then averaged to obtain a value for each plot. Cover crop samples were obtained by randomly placing a 0.25m² frame into the plot and removing all living biomass as close to the soil surface as possible. Fresh biomass samples were sorted into individual clover, rye, and weed groups, placed in the dryer at 65 °C for approximately one week, and then weighed to obtain a dry matter weight. In 2019, four subsamples were taken from each plot at the ST1 location. At the HC1, ST2, and HC2 locations, two subsamples were taken from each plot. Cover crop aboveground biomass was analyzed for C, N, and ¹⁵N abundance in the University of Kentucky Stable Isotope Geochemistry Laboratory via dry combustion analysis interfaced with isotope ratio mass spectrometry. The amount of N derived from atmospheric fixation for the crimson clover was calculated using the natural abundance method described in equation 1:

$$NDF\text{A}(\%) = \frac{(\text{Reference } ^{15}\text{N} - \text{Clover } ^{15}\text{N})}{(\text{Reference } ^{15}\text{N} - \beta)} \times 100 \quad [1.1]$$

where *Reference* ¹⁵N is the ¹⁵N value of the rye monoculture for a given landscape position and replicate, *Clover* ¹⁵N is the ¹⁵N value of the clover at a given landscape position and replicate, and β is a correction value for the fractionation of the N isotope

that occurs between above and belowground biomass (Schipanski and Drinkwater, 2012). Here we use a β value equal to -1.55 based on the results from (Blesh, 2018).

1.3.4 *Spatial data analysis and statistics*

Digital elevation models were retrieved from the *KentuckyFromAbove* data repository (Kentucky Division of Geographic Information, 2017). Elevation data were collected using light detection and ranging (LiDAR) at a 1 m point spacing and presented as 1.5 m raster grid cells. ArcMap v 10.7.1 was used to calculate the mean elevation, slope, flow accumulation, profile curvature, and planar curvature, at the plot level for all site locations. Zonal statistics were then calculated for each plot from the raster datasets.

Data for cover crop biomass, N uptake, and N derived from fixation were analyzed in R v 4.0.2 (R Core Team, 2020) using linear mixed models from the lme4 package v 1.1-23 (Bates et al., 2015). In the linear mixed models for the ST sites, landscape position, cover crop treatment, and the interaction between landscape position and cover crop treatment were considered fixed effects, replicate and the interaction between landscape position and replicate were considered random effects. In the linear mixed models for HC sites, landscape position, cover crop treatment, and the interaction between landscape position and cover crop treatment were considered fixed effects, replicate and the interaction between cover crop treatment and replicate were considered random effects. A Type III sums of squares ANOVA and a post-hoc Tukey Test were used to identify mean responses that were significantly different between treatments using the multcomp package in R (v. 1.1-13, Hothorn et al., 2008). Due to the heterogeneity in weather, soil, and the limited number of replications possible at each field site, significance was assigned at p-values < 0.10. Site effects and site by year interactions were significant . As

such, we elected to analyze and present the treatment responses separately for all site years.

To identify significant relationships and trends in cover crop performance and landscape topographic variables, we conducted a principal component analysis using the `prcomp` function in the base R stats package (v 4.0.2; R Core Team, 2020). Data were pooled across site years and scaled using Z-scores prior to analysis. Biplots were constructed to visualize variable loading for the first two principle components using the `factoextra` package (Kassambara and Mundt, 2020). Following this analysis, individual regressions of the unscaled, pooled data were conducted to elucidate relationships between factors identified in the PCA to be major drivers of variation or to be highly correlated. In the PCA biplots, variables with acute angles between them were interpreted to be positively correlated, whereas variables arranged in obtuse angles were interpreted to be negatively correlated.

1.4 Results

1.4.1 *Site edaphic and topographic characteristics*

The landscape positions were defined based on slope and elevation – the summit had a low slope and high elevation, the backslope had a high slope and range of intermediate elevation, and the toeslope had a low slope and low elevation (**Table 1.1**). The differences in slopes between positions were more pronounced at the ST sites than the HC sites (**Figure 1.1**). The most significant soil difference between landscape positions was depth, with depth to the largely impermeable epikarst layer ranging from 35 cm to > 150 cm across landscape positions. Solum depth was consistently lower on the backslope than on the toeslope and summit positions. At all locations, the summit and backslope

positions tended to have greater sand and clay content, and lower silt content, in the top 20 cm than the toeslope positions. Averaged across site years, the backslope positions had 35% more clay and 16% less silt than toeslope positions (**Table 1.1**). In general, soil C did not vary substantially across hillslopes. At the HC sites, soil C was either similar across landscape positions (HC1), or numerically higher in depressions (HC2). The ST sites were higher in soil C than the HC sites across all landscape positions and ranged across hillslopes. At the ST sites in both 2019 and 2020, the backslope position numerically had the highest level of soil C, though it was not significantly different than the other two landscape positions. Across all site-years and landscape positions, the 60 cm inorganic N stock ranged from 13 – 60 mg kg⁻¹ N. The ST sites had higher inorganic N on average (34 mg kg⁻¹ N vs. 28 mg kg⁻¹ N, for ST and HC, respectively). Backslope and toeslope positions tended to have higher inorganic N stocks than summit positions (**Table 1.1**), depending on the site-year. The average profile curvature was most positive on the backslope positions (0.03), and generally negative in the depression positions (-0.004). Positive profile curvature indicates concavity of the terrain in the direction of the slope and suggests that flow through that area will be accelerated. Negative values suggest convex terrain and can indicate areas of water accumulation or flow deceleration. As such, it follows that flow accumulation is highest in the toeslope areas at all sites (avg: 42.04), and lowest in the summit positions (avg: 5.51).

1.4.2 *Total cover crop biomass production and N uptake*

Cover crop biomass production varied in response to landscape position and site-year. The ST sites were more productive than the HC sites in both years of the study. Across landscape positions and cover crop treatments, Spindletop sites (ST1 and ST2) produced

between 40 and 45% more overall biomass than the Hardin County sites (HC1 and HC2) (**Figure 1.2A**). The average biomass produced at the HC sites was 1.90 Mg ha^{-1} while the average biomass produced at the ST sites was 3.26 Mg ha^{-1} . The lowest biomass production occurred on the backslope position at HC2 (1.55 Mg ha^{-1}), and the highest biomass production occurred in the summit position at ST1 (3.54 Mg ha^{-1}). Cover crop N uptake mirrored trends in biomass production, with 53 – 54% greater N uptake by the cover crop in the ST sites than the HC sites. The average N uptake by the cover crop was 59.7 kg ha^{-1} at the ST sites, and 28.0 kg ha^{-1} at the HC sites.

The effect of landscape position varied by site-year and was more consistent at the Hardin County field locations than at the Spindletop field locations. When averaged across cover crop treatments, the toeslope produced the greatest amount of biomass in 3 out of 4 site-years. However, this effect was only significant at the HC locations (p-values = 0.06 for HC1, and 0.03 for HC2), and only showed a numerical trend at the ST2 site (p-value = 0.89). In the HC sites, cover crop biomass production in the toeslope was significantly greater than in the summit and the backslope positions in both years (**Figure 1.2A**). Backslope and summit positions at the HC sites were not significantly different from each other. In ST1, the toeslope had significantly lower biomass than the backslope and summit positions, but there was no effect of landscape position in ST2 (**Figure 1.2A**). At the HC sites, the cover crops in the toeslope position assimilated significantly more N than cover crops in the backslope or summit positions in 2019, but not in 2020 (**Figure 1.2B**). At ST1, cover crops in the toeslope position took up significantly less N than those in the backslope and summit positions.

Cover crop treatment was only significant in 1 of the 4 site years, at HC1. Averaged across landscape positions in this site-year, the mixture treatment produced 32% more biomass than the cereal rye monoculture treatment (p -value = 0.03). At all other experimental locations, cover crop treatment did not have a significant effect on biomass production. Additionally, there was not a significant interaction effect between landscape position and cover crop treatment in any site year. Nitrogen uptake was not also significantly impacted by cover crop treatment ($p > 0.10$ in all cases; **Figure 1.2B**).

1.4.3 *Percentage clover and nitrogen fixation*

In addition to differences in the amount of biomass produced and the N recovered among landscape positions, the performance of the clover within the mixture varied considerably among landscape positions. In general, the backslope position had a greater percentage of clover within the cover crop biomass compared to the summit and toeslope positions at the ST sites, and the backslope and toeslope had a greater percentage of clover biomass than the summit at the HC sites. The lowest percentage of clover occurred at the toeslope position at the ST2 site, where the total biomass in the mixture treatment was 3% clover. The highest percentage of clover within the mixture was observed in HC1 at the backslope and toeslope positions, where clover accounted for 22.5-23.3 % of the total cover crop biomass (**Figure 1.3B**). At the ST sites, the backslope and summit positions were significantly different in 2019, but not in 2020. In both years, the percentage of clover on the backslope position at the ST sites was higher than the percentage present at the toeslope (**Figure 1.3B**).

The percentage of N derived from atmospheric fixation (NDFA) showed a different pattern than that of the proportion of clover and was more consistent between sites than

the biomass production or proportion clover. Averaged across sites, NDFA was highest in the sloping areas, followed by the summit position, and then the toeslope (77%, 72%, 60%, respectively). At the HC sites, the percentage of NDFA at summit and backslope positions were similar in both years, and the toeslope position was lower (**Figure 1.3A**). This difference was significant in 2019, but not in 2020. At the ST sites, clover in the backslope position acquired significantly more N via fixation than the summit in 2019, but there were not significant results in 2020. However, a trend persisted across all years that backslope positions consistently had as high or higher percentages of NDFA than the other landscape positions.

1.4.4 *Landscape controls on cover crop dynamics*

To analyze the relationships among landscape variables, soil properties, and cover crop biomass and N accumulation, we used principal component analysis, a multivariate data analysis technique that allows for comparisons of factors across unitless, multidimensional data (**Figure 1.4**). Our results indicated several strong correlations between topographic and edaphic characteristics, and cover crop performance and dynamics. In analyses for both the rye sole crop and the mixture treatments, the variability in the first two principal components was explained largely by the same variables (**Supplemental Tables S1.1A and S1.1B**). In both analyses, PC1 was defined chiefly by variables related to soil fertility and cover crop performance, such as soil C percentage, soil P, rye N uptake, rye biomass production, and total biomass production. In contrast, the highest contributing variables to PC2 were related to landscape position and edaphic characteristics, such as slope, soil pH, and texture components, and in the mixture treatments, clover biomass and performance. In the rye monoculture, landscape

position groups were primarily spread along PC2, and rye biomass was most correlated to inorganic N stocks, soil P, and soil C. In the mixture treatment, landscape positions were more closely clustered, with less spread along PC2. The rye grown in the mixture treatment showed similar relationships to soil fertility traits which it was heavily correlated with in the monoculture. However, high correlations occurred between attributes of the clover within the mixture, such as clover biomass and proportion clover, and the topographic and edaphic characteristics such as slope and soil sand content. Further, variable loadings for the clover biomass were positioned perpendicular to the loadings for the rye biomass and associated soil fertility factors, indicating no significant relationship between clover and soil fertility factors, or rye performance.

Based on the PCA results, we plotted relationships between cereal rye and crimson clover biomass and key explanatory variables (**Figure 1.5**). The relationship between rye biomass and slope was insignificant, with similar biomass levels occurring at slopes ranging from 0 – 6 degrees. However, clover biomass was significantly correlated with slope ($p = 0.004$), showing an increase of 0.05 Mg ha^{-1} , or 19% of the average clover biomass observed in our study, with each 1 degree increase in slope. Similarly, as sand content increased, clover biomass increased significantly ($p < 0.001$). An increase in sand content of 10% led to an increase of 0.2 Mg ha^{-1} in total clover biomass. Rye biomass was not significantly impacted by soil sand content ($p = 0.446$). The total amount of rye biomass showed strong correlations with soil C % ($p < 0.001$) and total inorganic N at planting ($p = 0.006$). Crimson clover biomass was not related to either of these factors, showing numerically negative relationships that were not statistically significant.

1.5 Discussion

1.5.1 *Cover crop biomass production by landscape position and cover crop treatment*

Overall, we found that landscape position did influence total cover crop biomass production; toeslope positions produced between 0 and 38% more biomass than backslope and summit positions. The only site-year that did not show at least a trend towards increased toeslope biomass was ST1. The greater cover crop biomass production in the toeslope relative to other positions is consistent with previous work in moderately well drained soils (Beehler et al., 2017), and consistent with the patterns observed in cash crops in these fields (Leuthold et al., 2021), and across the region (Kaspar et al., 2004; Kravchenko and Bullock, 2000). Unlike some of the water availability reasoning attached to the spatial heterogeneity of crop yields in areas of complex topography, cover crops in this region are typically not limited by evapotranspiration (Ruis et al., 2019). Instead, the primary limitation on cover crop growth is often the available nutrients and growing degree days afforded to them between planting and termination. The 2018 – 2019 cover crop growing season was cooler at both locations than the 2019 – 2020, but the overall accumulation of growing degree days did not vary substantially between site years (1181 – 1349 GDD). Our multivariate analysis of topographic and edaphic factors for both the rye cover crop and the rye-clover mixture indicated the primary controls on rye biomass were soil fertility factors, such as soil C, soil P, and inorganic N stocks at planting, rather than topographic variables such as slope or elevation. Total rye biomass in either cover crop treatment had no relationship with slope, nor the soil sand content, and showed considerably less variability across landscape positions than the clover did (**Figure 1.2, Figure 1.3, Figure 1.5**). However, the topographic arrangement of a given field can lead

to redistribution of soil nutrients downslope, which may give rise to a mosaic of high-productivity areas interspersed with low fertility areas, with depression areas often having higher soil inorganic N stocks and mineralizable SOM (Burke et al., 1995; Dharmakeerthi et al., 2005). The increased biomass in the toeslope positions was likely a result of this discrepancy in soil nutrient status, reflecting a secondary effect of landscape position on cover crop biomass production, one not captured by topographic properties alone. Further, it is possible that the fertility status of areas in rolling hill cropland can enter a feedback loop, in which biomass in areas of lower fertility contribute less residue to the SOM pool, leading to further depressed biomass production, while the opposite occurs in depression areas. That the HC sites saw a more significant increase in cover crop biomass at the toeslope compared to the backslope and summit positions could reflect the effects of long-term crop production at that site, compared to the recently converted ST sites, which have likely not yet developed the discretized soil nutrient status at each landscape position in the same way. The increased soil P, K, and N at the toeslope at the HC sites, compared to more homogenous values among the landscape positions at the ST sites support this possibility (**Table 1.1**).

We did observe that in one site-year (ST1), cover crop productivity was stifled by what we believe to be excess water stress. Average flow accumulation was highest in the toeslope for all of the site-years in this study, and as such, these areas were more susceptible to production variability due to flooding than the upslope areas (Maestrini and Basso, 2018a). As such, the reduced toeslope biomass in ST1 may not be an outlier when compared to the other site-years, but an example of the relationship between topography-induced yield heterogeneity and weather conditions (Martinez-Feria and Basso, 2020),

which likely be exacerbated in coming years as extreme climatic variability becomes more common (Rosenzweig et al., 2002).

1.5.2 *Cover crop N accumulation by landscape position and cover crop treatment*

Trends in total cover crop N uptake mirrored those in biomass production. There were significant differences in the amount of biomass produced, and thus N scavenged, between the two locations. Averaged across year and landscape position, cover crops at the ST sites scavenged 60 kg ha⁻¹ of soil N during their growth. At the HC sites, the average N uptake across landscape position and cover crop treatment was 28 kg ha⁻¹. This discrepancy likely arises from the land use history at either site; ST sites having come out of pasture immediately prior to cover crop planting likely had increased soil N mineralization potential, and high levels of soil solution N. The HC sites had been in long-term cropping, and our experiment followed soybean crops in both years. Given the lack of fertilization to soybean crops, and the small amount of crop residue soybean produces, it is unlikely that mineralizable N stocks were near the same level of the ST sites. The significant differences between landscape positions we observed are especially relevant in relation to water quality; reducing the amount of N in soil solution during the period in which a cash crop is not growing is critical to reducing downstream effects such as eutrophication and groundwater contamination. Cash crop yields in sloping areas are often inconsistent from year to year, leading to spatiotemporal variability in N use efficiency (NUE). As such, when fertilizer is applied at a consistent rate across sloping fields, N losses can be outsized compared to areas with homogeneous topography and more consistent spatial NUE patterns (Basso et al., 2019). Increasing N scavenging in

these locations should therefore be of highest concern for producers interested in increasing sustainability (Tonitto et al., 2006).

We did not observe a significant difference between the cover crop treatments in terms of total N uptake (i.e., total biomass N – NDFA), implying that both treatments scavenged for N equally as well. We did see some evidence that total cover crop N (i.e., the amount of N available to be released to the subsequent cash crop), was often numerically higher in the mixture treatment than the cereal rye. This can be attributed largely to the increased N incorporated into the clover via biological fixation. Overall, our results reaffirm past findings that mixtures of cereals and legumes can provide a range of functions beyond what could be achieved using only one species; the rye was able to scavenge N as well in the mixture as it was alone (**Figure 1.2B**), and the clover provided an added source readily available of N for the subsequent cash crop, balancing ecosystem services and disservices (Finney et al., 2017; Kaye et al., 2019).

1.5.3 *Clover dynamics within mixture*

The clover within the cereal-legume mixture responded strongly to landscape topography, both in terms of total biomass produced, and the percentage of total mixture biomass. At each site year, the backslope typically had the highest proportion clover within the mixture biomass. When we compared slope and the percentage clover, we were able to capture the transitional zones from sloping areas to toeslope or summit to sloping areas better than the categorical analysis of landscape position alone (**Figure 1.5**). We found increasing slope led to significant increases in total amount of clover biomass, and the proportion of clover within the total biomass. Across sites, where average slopes ranged from 0.7° to 6.3°, we found that the percentage of legume within the mixture

increased 2% per degree increase in slope, and that the clover biomass increased 50 kg ha⁻¹ with a one degree increase in slope. The increase in percentage of clover with increasing slope is in line with previous studies of legume abundance in pasture systems. Guretzky et al. (2004) found that legume percentage increased 0.5-1.3% per degree increase in slope, depending on how the system was grazed.

The increase in clover proportion is likely not tied directly to the slope, but rather the impact of sloping landforms on edaphic characteristics. During erosional events in moderate sloping environments, silt particles are often preferentially eroded (Ampontuah et al., 2006), enriching the sand or clay component depending on initial soil composition. In our studies, backslope soils had 31% higher sand contents than toeslope soils, and 19% higher sand content than summit position soils (**Table 1.1**). Schipanski et al. (2010) found that soil sand content explained 20-30% of the variability in biological nitrogen fixation in soybeans, a common leguminous cash crop. This is consistent with our findings, that NDFA of the clover increased by 1.75% per 1% increase in soil sand content. As legume growth and fixation have been shown to be inhibited by excess soil N (Salvagiotti et al., 2008; Schipanski et al., 2010), the shifts in clover biomass production with increasing sand content may reflect the more rapid leaching of inorganic N, or differences in the structure of the SOM pool, as sandy soils have been shown to be dominated by particulate rather than mineral associated organic matter (Haddix et al., 2020). Our multivariate analysis did not indicate a negative relationship between inorganic N and clover biomass or the proportion clover, but it only included soil inorganic N at planting. Shifts that occur in the soil inorganic N pool during the period of cover crop growth such as leaching or uptake by the rye should be investigated further

across soil textural gradients to identify if this mechanism is a significant driver of legume performance within a mixture.

1.5.4 *Cover crop mixture effect on biomass stability*

One of the key hypotheses we aimed to investigate in this study was that the differential response of the clover and cereal rye species to landscape topography would compensate each other and stabilize biomass production and N uptake across landscape positions. We did not find an interactive effect of crop treatment and landscape position on total cover crop biomass production, or N uptake, indicating that our hypothesis lacks support, and may need to be reevaluated. Instead, we found that landscape position tended to have a significant effect on total biomass production, regardless of cover crop treatment (**Figure 1.2A**). The increases in the amount of clover within the mixture in areas with lower overall biomass, such as the backslope, were relatively small, accounting for only 8 – 23% of the total biomass in a given site year. Rather than compensating for decreased rye biomass by increasing clover biomass as we hypothesized, we found the effect to be additive or unrelated; in 2019 we observed increasing clover biomass with increasing rye biomass, and in 2020 there was not a relationship between total rye and total clover biomass.

Although we did not observe a direct compensation effect by the mixture across the landscape positions, it is notable that the two cover crop treatments produced similar levels of total biomass except in one site-year, despite a 40% reduction in the rye seeding rates in the mixture relative to the monoculture. On average, across landscape positions and site-years, the rye in the mixture produced 99% of the biomass that the rye grown in monoculture did. The largest reduction in rye biomass in mixture vs. monoculture was in

the summit position in ST2, where the mixture treatment had 40% less rye biomass than the monoculture, though these results may be due to abnormally high rye monoculture biomass production rather than the mixture underperforming. Without a legume monoculture treatment, we are unable in this study to calculate actual land equivalent ratios for the cover crop treatments, but overall, our examinations of the total biomass and species-specific biomass find similar performance of rye grown in monoculture to rye grown in mixture. The results are consistent with previous studies that have examined mixture biomass potential and found that they often overproduce relative to sole crops of constituent species grown alone (Wortman et al., 2012).

1.5.5 *Implications for agroecosystems*

Our findings that the productivity and function of the constituent species of a cereal rye – crimson clover cover crop mixture show divergent responses to topographic and soil fertility properties may lead to more profitable cover crop management strategies. Across site-years, the total amount of N derived from fixation, in terms of kg ha^{-1} , was highest in the sloping areas, consistent with the increase in legume biomass and NDFA. As we observed that soil N uptake by the cover crop was not hindered by the mixture, the addition of a legume into a cover crop may be most beneficial to environmental sustainability and subsequent cash crop production when implemented in sloping areas. While previous studies have shown that mixtures may better leverage plant functional traits into agronomic outcomes (Blesh, 2018; Finney et al., 2016), our results suggest that relating field fertility and topographic characteristics to cover crop functionality can bolster results towards achieving management outcomes. Similar to precision agriculture's management zone delineation (Albarenque et al., 2016; Basso et al., 2011),

identifying areas throughout heterogeneous fields with different management goals (i.e., increasing cash crop available N vs. reducing N leaching) and adapting cover crop management to fit these areas may lead to increased cover crop performance and lower overall expense. Legumes are typically more costly to establish than cereals; less robust emergence of legumes coupled with increased seed cost can lead to prices up to 10-fold higher than the cost of establishing a cereal rye cover crop (Snapp et al., 2005). In rolling hill systems, targeting the seeding of a cereal-legume mixture to areas where benefits will be realized most vigorously may be a cost-effective management strategy that also improves cover crop function. For instance, flat, silty, and organic matter-rich areas tended to decrease clover biomass and biological nitrogen fixation; these areas may be best suited for cereal monocultures that scavenge N effectively but do not add additional N to the system, while sloping areas can benefit from increased clover proportion and the added N via NDFA and may be more suited for increased seeding rates of legumes. Merging these concepts of precision management and multifunctionality could improve N use efficiency in the subsequent cash crop (Crews and Peoples, 2005), and increase overall agroecosystem health.

1.6 Conclusions

Cover crop mixtures are a popular recommendation for producers attempting to capitalize on several cover crop benefits, such as reduced N leaching and N return to the subsequent crop. This study aimed to demonstrate the effect of landscape topography on cover crop biomass production and N uptake in two cover crop treatments, a cereal monoculture and a cereal-legume mixture. Further, we aimed to elucidate the responses of different cover crop species to landscape factors such as slope, texture, and fertility. We found that cover

crops produced similar levels of biomass whether grown in a mixture or monoculture. Landscape position had a significant effect on biomass production, with depression areas often producing more biomass than sloping and summit areas. We observed that the crimson clover within the mixture was significantly impacted by topography. The proportion clover was greatest in sloping areas, and the amount of NDFA was reduced in depression areas relative to slopes and summits. An analysis of the primary drivers of variations indicated that cereal rye was highly correlated with soil fertility factors such as soil C and inorganic N, while clover biomass was more related to soil texture and field slope. Our results indicate the heterogeneity in cover crop response to landscape factors and provide a baseline for improving cover crop management in areas of rolling hill topography. Future work focused on using a combination of targeted cover crop monocultures and mixtures across a field in response to soil and topographic characteristics variables could yield a method of improving environmental and economic sustainability, while still maximizing cover crop derived ecosystem benefits.

1.7 Chapter 1 tables and figures

Table 1.1 - Soil and topographical characteristics for hillslope fields in 2019 and 2020.

Site	Year	Landscape Position	Soil Characteristics ¹								Topographic Characteristics				
			Silt	Clay	Soil Depth	Soil pH	Organic Carbon	P	K	Inorganic N ²	Slope	Elevation	Profile Curvature	Plan Curvature	Flow Accumulation
			%	%	cm		%	mg kg ⁻¹	mg kg ⁻¹	mg kg ⁻¹	Deg.	masl			
Spindletop	2019	Summit	72	17	100	5.9	2.01	370	146	9.2	2.03	905	0.0221	0.0125	7.9
Spindletop	2019	Backslope	54	26	35	6.6	2.40	472	239	7.5	5.18	899	-0.0029	0.0133	25.4
Spindletop	2019	Toeslope	73	14	150	5.8	2.23	364	125	7.7	1.38	887	-0.0179	-0.0137	63.0
Spindletop	2020	Summit	64	17	90	6.6	3.27	395	352	9.2	1.48	903	0.1083	0.0583	4.9
Spindletop	2020	Backslope	64	17	40	6.7	3.16	366	284	16.5	5.14	891	0.0008	-0.0500	28.8
Spindletop	2020	Toeslope	78	8	150	6.1	2.49	254	117	10.2	1.04	883	-0.0842	0.0250	5.4
Hardin County	2019	Summit	68	16	100	6.2	1.09	38	284	4.2	2.68	668	0.0475	-0.0275	5.2
Hardin County	2019	Backslope	64	16	35	6.3	1.11	28	261	3.9	5.13	661	-0.01916	-0.0141	15.1
Hardin County	2019	Toeslope	70	12	150	6.4	1.25	62	248	4.8	2.68	656	-0.0441	0.0316	57.8
Hardin County	2020	Summit	68	20	90	6.1	1.17	12	91	7.0	1.94	674	0.0808	-0.0600	2.9
Hardin County	2020	Backslope	68	17	40	6.1	1.19	9	104	6.9	4.04	668	0.0725	0.0033	9.3
Hardin County	2020	Toeslope	78	11	150	6.0	1.16	18	103	11.4	1.65	664	-0.0200	0.0492	41.9

1: Soil characteristics, unless noted, are from samples from 0 – 20 cm depth.

2: Soil inorganic N was measured to a 60 cm depth near the time of cover crop planting.

Table 1.2 - Cover crop management dates for the four site-years.

Site	Year	Planting Date	Sampling Date	Termination Date
Spindletop	1	10/12/2018	04/11/2019	04/13/2019
Spindletop	2	10/15/2019	04/01/2020	04/02/2020
Hardin County	1	10/09/2018	04/14/2019	04/16/2019
Hardin County	2	10/21/2019	04/14/2020	04/16/2020

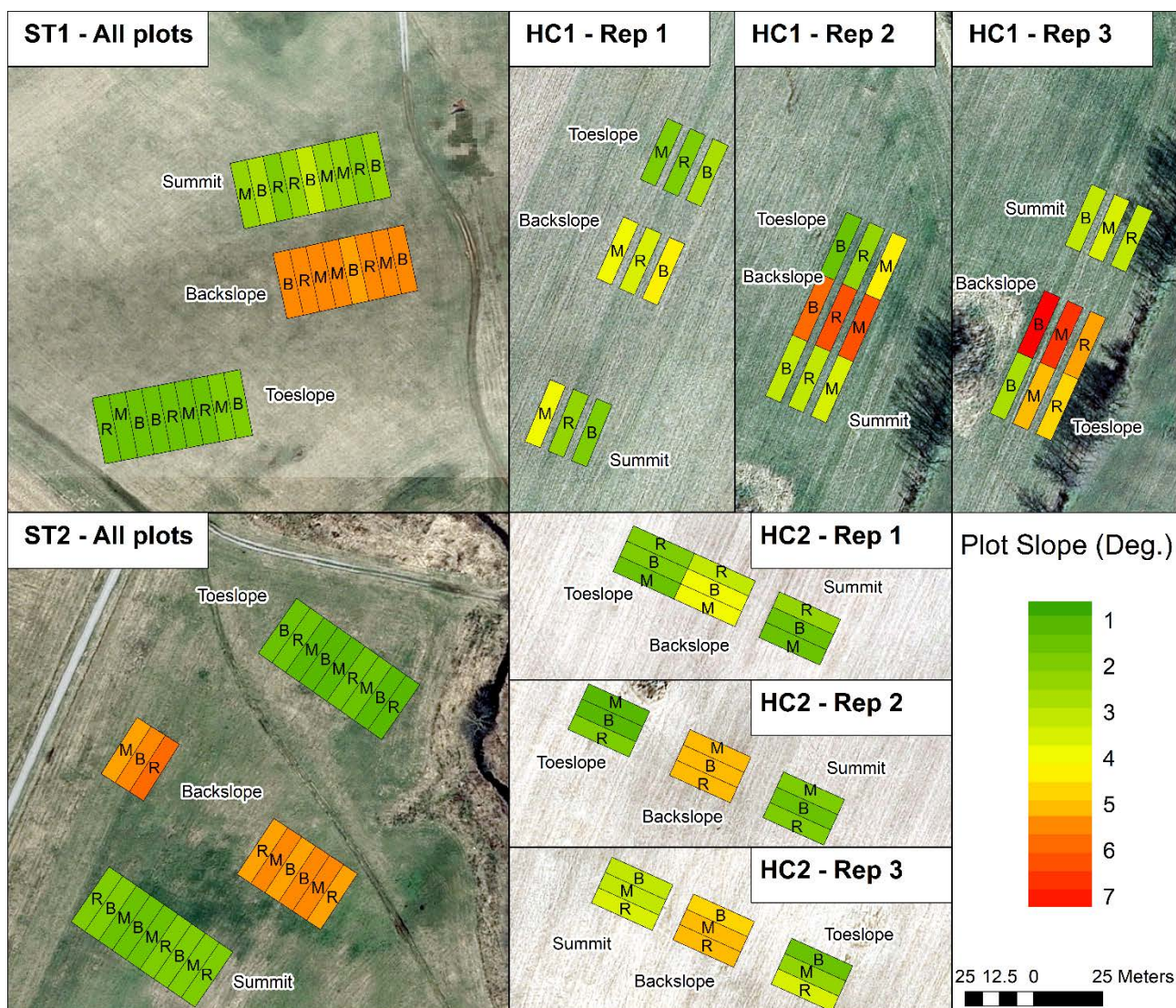


Figure 1.1 – Plot arrangement for the four site-years presented in this study. Spindletop (ST) field sites were located at the University of Kentucky experimental farm in Central KY, Hardin County (HC) field sites were located in a farmer-collaborators field in West Central KY. Capital letters on the individual plots indicate the cover crop treatment for each plot (R = rye monoculture, M = rye-crimson clover mixture, B = bare). At the HC1 and HC2 sites, replicates were split across three separate hillslopes. To preserve map scale and improve readability, each replicate is presented separately for these site-years.

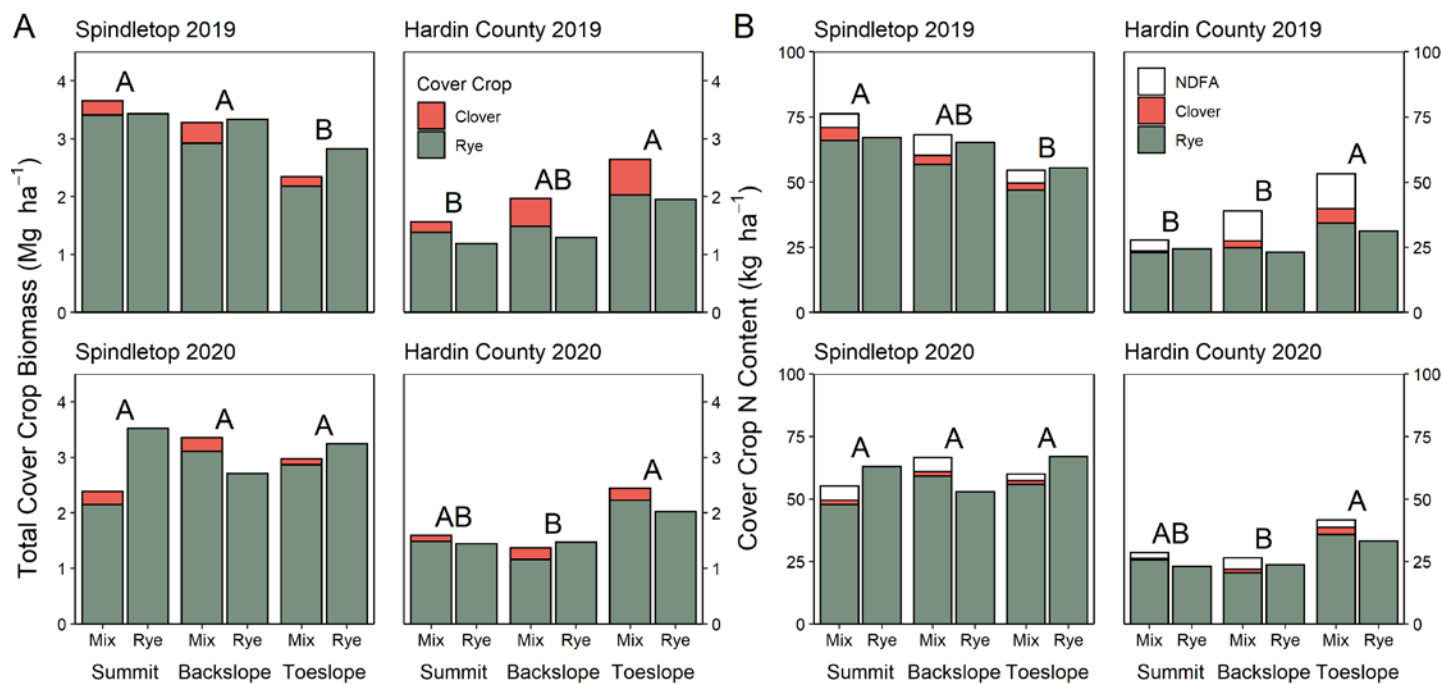


Figure 1.2 – Total cover crop biomass and total N uptake for rye monoculture and rye-crimson clover mixture. Bar plots with different letters above indicates significant differences in biomass or N uptake between landscape positions. Cover crop was not significant except in the biomass of HC1 (2019).

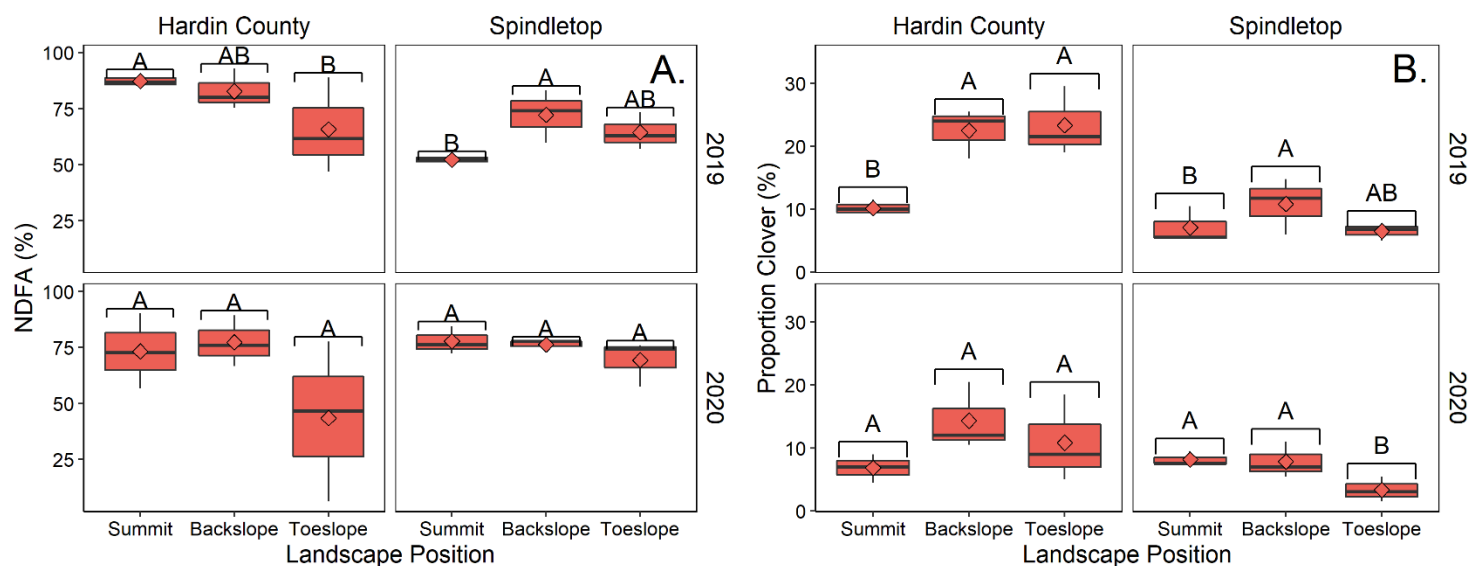


Figure 1.3 - Boxplots representing the percentage of N derived from fixation at each landscape position, and the percentage of clover within the mixture treatment at each landscape position. Differences in the letters above each box indicates significant differences between landscape position treatments at the $p < 0.10$ significance level.

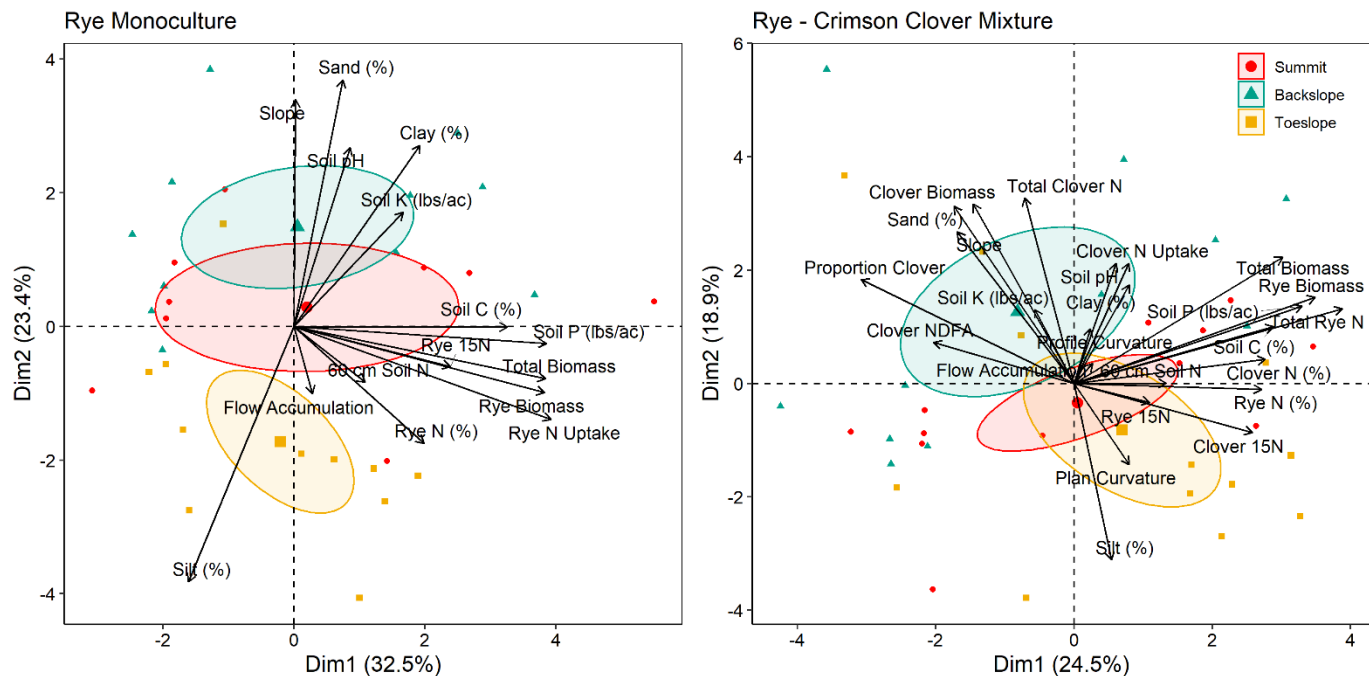


Figure 1.4 – PCA biplots of the first and second principal components of the rye monoculture and rye-crimson clover mixture treatments. Angles $< 90^{\circ}$ indicate positive correlations between variables, while angles $> 90^{\circ}$ indicate negative correlations. The ellipses represent the 90% confidence interval for the mean value in PC space of each landscape position.

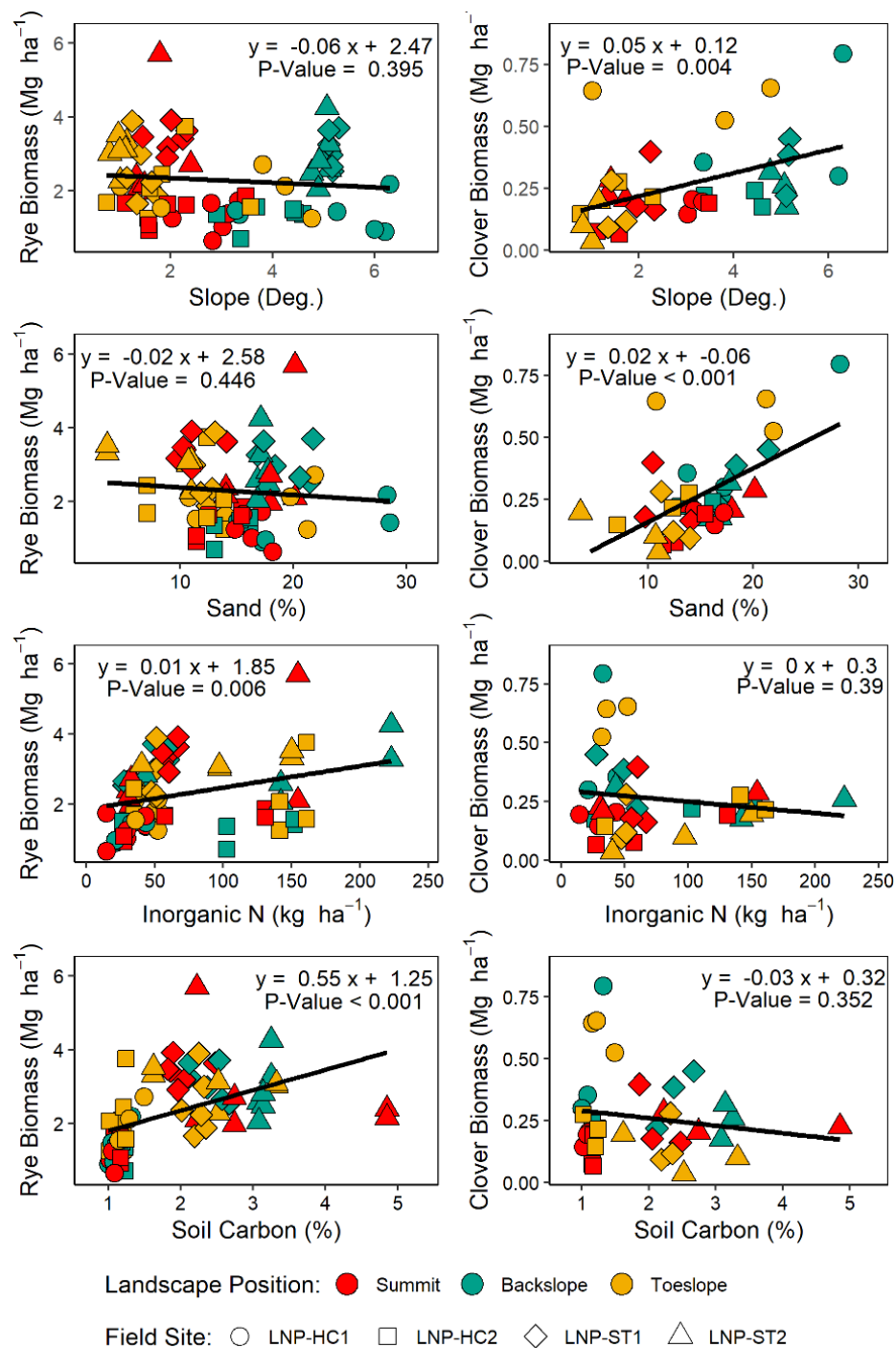


Figure 1.5 – Correlations between biomass of cover crop species and important explanatory variables identified in the PCA. Different shapes indicate different field sites, while different colors indicate different landscape positions. Data are pooled across all 4 site-years. Rye biomass includes rye in both sole crop and mixture.

Table S1.1 - Contribution of each factor to principal components for first 17 PCs in the rye treatment. PC1 and PC2 (presented in main text) are highlighted according to contribution; red: low, green: high.

Factor	PC1	PC2	PC3	PC4	PC5	PC6	PC7	PC8	PC9	PC10	PC11	PC12	PC13	PC14	PC15	PC16	PC17
60 cm Soil N	0.9	1.0	5.4	0.0	30.6	19.3	8.5	5.7	1.0	18.2	1.9	3.7	3.6	0.0	0.1	0.0	0.0
Sand (%)	0.6	20.7	1.0	0.1	1.0	3.1	0.1	17.7	17.7	0.0	1.5	0.8	14.6	0.9	0.2	0.1	20.0
Silt (%)	2.6	22.4	0.3	1.7	0.2	0.7	2.8	1.0	0.5	0.3	2.6	0.9	6.1	0.0	0.0	0.0	58.1
Clay (%)	3.6	11.4	0.0	5.6	2.6	9.1	9.0	5.5	27.1	0.4	2.1	0.5	0.1	1.1	0.0	0.0	21.9
Soil pH	0.8	10.8	13.1	4.3	3.8	0.3	4.3	19.4	4.5	9.0	5.3	11.0	3.0	9.0	1.3	0.1	0.0
Soil C (%)	10.9	0.0	14.0	0.2	3.4	0.4	6.3	1.7	8.5	0.5	14.6	7.6	0.0	30.9	0.9	0.0	0.0
Soil P (lbs/ac)	15.4	0.1	0.0	4.7	3.3	0.2	0.5	0.4	0.7	0.2	1.5	28.3	5.6	38.8	0.0	0.2	0.0
Soil K (lbs/ac)	3.3	4.4	8.3	5.0	14.5	5.0	8.9	5.0	1.3	14.6	0.4	0.2	24.8	0.9	3.0	0.4	0.0
Rye Biomass	15.3	1.4	3.5	2.4	2.0	0.1	0.0	2.7	1.7	1.5	2.2	5.5	0.9	0.0	26.5	34.3	0.0
Total Biomass	15.6	0.9	4.0	0.6	4.6	0.3	0.3	0.6	0.3	3.2	0.4	1.1	0.5	1.3	63.4	2.9	0.0
Rye N (%)	4.2	4.6	10.4	0.3	8.4	0.3	11.8	32.9	0.2	10.4	2.2	3.3	3.1	1.8	0.6	5.5	0.0
Rye 15N	6.0	0.5	14.0	6.9	2.4	0.1	16.2	4.9	25.6	8.9	0.2	1.4	6.7	5.9	0.1	0.1	0.0
Rye N Uptake	16.1	2.8	0.4	1.5	0.2	0.2	2.0	0.1	1.4	0.4	6.3	8.7	0.0	0.7	3.2	56.1	0.0
Slope	0.0	17.4	0.4	0.0	0.0	29.3	0.3	0.2	2.8	14.5	13.2	3.5	11.5	6.5	0.2	0.2	0.0
Flow Accumulation	0.1	1.5	11.1	5.2	14.1	28.9	14.5	0.0	5.3	7.2	7.7	3.7	0.0	0.2	0.2	0.1	0.0
Plan Curvature	0.6	0.1	4.1	39.0	1.1	2.7	14.5	1.4	0.0	6.7	20.9	4.5	3.6	0.7	0.1	0.0	0.0
Profile Curvature	4.1	0.0	10.0	22.5	8.0	0.1	0.0	0.9	1.1	4.0	17.0	15.2	15.9	1.1	0.1	0.0	0.0
Standard deviation	2.25	1.87	1.32	1.31	1.25	0.96	0.85	0.72	0.60	0.54	0.45	0.42	0.38	0.21	0.11	0.04	0.00
Proportion of Variance	29.7%	20.7%	10.3%	10.0%	9.2%	5.5%	4.3%	3.1%	2.1%	1.7%	1.2%	1.0%	0.8%	0.3%	0.1%	0.0%	0.0%
Cumulative Proportion	30%	50%	61%	71%	80%	85%	90%	93%	95%	97%	98%	99%	100%	100%	100%	100%	100%

Table S1.1B - Contribution of each factor to principal components for first 17 PCs in the mixture treatment. PC1 and PC2 (presented in main text) are highlighted according to contribution; red: low, green: high.

Factor	PC1	PC2	PC3	PC4	PC5	PC6	PC7	PC8	PC9	PC10	PC11	PC12	PC13	PC14	PC15	PC16	PC17
60 cm Soil N	1.7	0.0	0.2	9.2	10.7	4.7	15.5	5.2	13.2	7.2	22.0	0.6	0.1	4.5	0.0	2.2	0.7
Sand (%)	2.9	12.0	2.0	0.3	1.8	0.2	1.0	0.1	0.0	9.0	15.5	3.4	7.1	0.9	5.3	1.3	11.3
Silt (%)	0.3	11.9	8.3	1.1	0.7	0.8	0.9	6.0	2.5	0.0	0.2	0.7	0.8	1.6	6.3	0.1	2.1
Clay (%)	0.6	3.7	9.0	1.1	6.3	3.2	0.2	15.3	5.5	6.1	8.7	9.2	1.3	1.1	2.5	0.4	0.9
Soil pH	0.3	5.5	3.7	0.6	3.0	2.6	28.8	1.4	7.4	5.5	7.9	0.1	2.1	4.6	16.1	6.2	0.0
Soil C (%)	7.9	1.2	4.7	0.1	0.6	4.0	6.4	0.6	1.8	1.2	5.2	13.2	16.6	3.1	16.3	0.0	4.4
Soil P (lbs/ac)	10.3	2.3	1.8	2.1	3.2	0.8	1.1	0.6	2.2	0.2	0.3	5.0	10.1	8.0	8.6	0.3	0.2
Soil K (lbs/ac)	0.3	2.1	1.8	7.1	15.2	0.9	19.7	11.0	1.0	0.8	0.0	10.3	0.1	0.4	13.5	0.5	3.1
Rye Biomass	11.5	2.9	0.8	1.5	0.3	4.1	0.3	0.9	0.0	6.5	2.9	0.3	1.7	0.3	0.0	0.1	0.4
Clover Biomass	2.0	12.4	6.9	0.6	0.3	1.3	0.1	0.5	0.8	1.5	1.2	0.0	1.0	0.5	3.8	3.7	2.8
Total Biomass	8.6	6.1	1.3	1.5	2.2	2.3	0.0	0.9	0.1	6.5	1.8	0.0	0.9	0.5	0.1	0.7	1.6
Proportion Clover	9.0	4.2	4.0	1.6	0.1	0.7	0.0	3.0	0.2	0.6	7.8	0.0	3.3	0.5	0.4	3.3	9.9
Rye N (%)	7.0	0.0	4.0	3.7	0.7	14.3	0.1	0.2	1.7	16.3	0.1	2.1	5.7	0.9	0.0	22.5	11.8
Rye 15N	1.1	0.1	1.6	0.4	29.7	10.7	0.0	0.7	0.1	4.0	0.3	36.2	1.3	0.4	0.1	0.0	5.9
Total Rye N	14.3	2.2	0.0	0.3	0.0	0.7	0.2	1.1	0.3	1.6	1.6	0.1	2.1	0.1	0.1	3.0	0.8
Clover N (%)	7.3	0.2	0.0	1.4	14.3	3.3	7.4	7.9	0.0	2.6	0.1	3.6	0.8	3.1	1.2	29.1	0.6
Clover 15N	6.3	0.9	7.7	0.9	6.5	0.3	0.0	7.8	0.2	6.6	1.0	1.9	3.4	0.1	12.3	15.3	8.0
Total Clover N	0.5	13.2	7.7	0.9	0.4	1.7	0.3	1.4	1.1	1.8	1.8	0.2	0.6	0.4	1.1	0.0	0.8
Clover NDFA	3.9	0.6	12.2	1.3	0.1	4.1	0.0	15.2	0.4	9.6	1.8	0.0	0.0	0.0	0.0	3.2	0.3
Clover N Uptake	0.6	5.6	15.6	0.9	1.7	0.0	0.8	1.6	3.5	0.7	2.7	2.6	3.1	0.2	5.3	3.8	29.0
Slope	2.7	8.9	0.8	0.1	0.1	8.0	1.0	5.9	7.8	11.0	7.8	7.3	7.4	12.3	3.6	1.4	3.0
Flow Accumulation	0.1	0.2	5.8	2.5	0.4	14.6	14.6	1.2	47.5	0.2	0.2	2.5	0.3	4.9	2.7	0.1	0.5
Plan Curvature	0.6	2.5	0.0	28.9	0.9	7.5	1.2	2.5	1.5	0.0	7.6	0.0	19.8	22.8	0.7	0.7	1.8
Profile Curvature	0.1	1.1	0.1	31.8	0.7	9.1	0.2	9.1	1.0	0.6	1.7	0.4	10.4	29.0	0.2	2.2	0.1
Standard deviation	2.43	2.13	1.88	1.38	1.34	1.22	1.07	0.97	0.80	0.72	0.65	0.60	0.49	0.43	0.37	0.30	0.25
Proportion of Variance	24.5%	18.9%	14.8%	7.9%	7.5%	6.2%	4.8%	3.9%	2.7%	2.1%	1.8%	1.5%	1.0%	0.8%	0.6%	0.4%	0.3%
Cumulative Proportion	25%	43%	58%	66%	74%	80%	85%	89%	91%	93%	95%	97%	98%	98%	99%	99%	100%

CHAPTER 2. LANDSCAPE TOPOGRAPHY EFFECTS ON SOIL MICROCLIMATE AND SURFACE COVER CROP RESIDUE DECOMPOSITION

2.1 Abstract

Rolling hill topography is common in agricultural land throughout the Southeastern United States. Differences in water and nutrient availability across the landscape can lead to high spatial and temporal variability in crop biomass and yield. Downslope movement of soil nutrients and water can lead to nutrient losses and soil degradation, as well as spatial yield variability. Additionally, differences in the accumulation of water, slope aspect, and crop biomass production can lead to disparate conditions of soil moisture and soil temperature across the landscape. Winter cover crops can reduce erosion and mitigate nutrient losses, while also potentially providing a source of nitrogen (N) to the cash crop as the cover crop residue decomposes. However, given that a combination of the moisture and temperature of residue and topsoil layers, as well as litter quality, are primary controls on litter decomposition, topographic heterogeneity may lead to variable rates of cover crop breakdown and nitrogen return to the system within a given field. Here we examine the effect of landscape position on soil volumetric moisture and temperature at 5 cm depth, and the decomposition and N release rate of two cover crop residues, a cereal rye (*Secale cereale* L.) monoculture, and a cereal rye/crimson clover (*Trifolium incarnatum*) mixture in an attempt to determine the effect of topographic complexity on soil microclimate and surface residue decomposition. We found differences in soil moisture and soil temperature across landscape positions, indicating

that different microclimates co-exist at different points in time and space throughout rolling hill fields. However, differences in microclimate were not sufficient to cause significant differences in decomposition or residue nitrogen release rate between landscape position or cover crop treatments. Instead, our results indicate that decomposition and N release rate of surface residues are homogeneous across space. Our results emphasize the inherent variability present in abiotic factors in rolling hill systems but indicate that the benefits of surface cover crop residue may be consistent across sloping systems.

2.2 Introduction

Cover crops provide a suite of ecosystem services to agricultural systems during their growth and decomposition (Blanco-Canqui et al., 2015; Snapp et al., 2005). While growing, cover crops protect soils from erosion (De Baets et al., 2011), reduce the nitrogen (N) loss from agroecosystems (Basche et al., 2016; Kaspar et al., 2012), suppress the development of winter weeds (Osipitan et al., 2018), and improve soil structure and water retention (Basche and DeLonge, 2017). After termination, cover crop residue left on the soil continues to provide benefits to the subsequent crop, including decreasing moisture loss (Leuthold et al., 2021), suppressing weeds, and continuing to reduce erosive soil losses. Importantly, as residue decomposes, it can also provide an auxiliary N source to the subsequent cash crop (Crews and Peoples, 2005; Nevins et al., 2020). As some of the most important cash crop benefits from cover crops are derived from residue during decomposition, it is important to understand the factors that affect residue persistence and N release.

Species selection is a critical component of managing cover crops, and can vary by region, producer experience, and management goals. Grass cover crop species like cereal rye accumulate a large amount of biomass and N, making them effective at protecting the soil and reducing N losses. Grass cover crops also have a relatively high C:N ratio, which can lead to microbial N immobilization and limit decomposition rate (Kuo and Jellum, 2002). While persistent grass cover crop residue protects the soil, retains water, and suppresses weeds during cash crop growth, it releases N slowly, or even immobilizes N, causing N stress during the early vegetative phase of non-leguminous grain crops such as maize (Kuo and Jellum, 2002). Alternatively, legume cover crop species like crimson clover fix N from the atmosphere, adding external N to the cropping system. The additional nitrogen available via fixation leads to a lower residue C:N ratio and allows for rapid decomposition of legume residue. Increasingly, legumes are being grown along with grass cover crops to capitalize on the high biomass and residue persistence of the grass (Finney and Kaye, 2017), while avoiding N limitation (White et al., 2017). Cereal-legume bicultures are a common management practice, both in the scientific literature (e.g., Florence and McGuire, 2020) and with agricultural producers—more than 75% of farmers who have used cover crops responded that they had planted cover crop mixtures in their operation at some point when surveyed (USDA SARE Farmers Survey, 2020). In the bi-culture, the cereal maintains high biomass production and N scavenging ability during cover crop growth, while the N fixing legume, with a low C:N, moderates the effect of N immobilization during the decomposition.

Apart from the residue chemical composition, cover crop decomposition is also controlled by temperature and moisture (Parr and Papendick, 1978; Schlesinger and

Bernhardt, 2013). In intact surface residue, the temperature and moisture of the topsoil has been shown to influence decomposition rates linearly (Stott et al., 1986), and have interactive effects in which the effect of soil moisture on surface residue decomposition is enhanced as soil temperatures increase (Quemada and Cabrera, 1997). During later stages of decomposition, after the majority of organic matter has been decomposed, environmental variables such as soil temperature and soil moisture are thought to be more important controls of decomposition rate than residue chemistry (Canessa et al., 2020). Spatiotemporal variability in temperature and moisture therefore can lead to variability in cover crop residue decomposition rates across time and space, especially at later stages of decay.

While the bulk of cover crop residue decomposition studies have taken place in homogeneous field sites, limited research suggests that in areas with complex topography, such as rolling hill cropland, residue decomposition rates may vary throughout space and time. For instance, differences in soil water and temperature conditions across areas of topographic complexity can influence microbial community (Cavigelli et al., 2005) and biogeochemical cycling, such as the flux of NO_2 (Reyes et al., 2017). In addition, some authors have shown that the rate of soil carbon (C) accrual from cover crop residue varies across rolling hill environments, with the greatest contributions from buried cover crop residue to the soil C balance occurring in sloping and summit areas (Ladoni et al., 2016). Beehler et al. (2017) found that the most rapid decomposition of an incorporated cover crop residue occurred in the depression areas of a field and was linked to increased soil water accumulation in these areas. However, little research has examined the effect of complex topography on cover crop residue left on the surface

following termination, despite the growing popularity of no-till systems, especially in erosion prone areas. Tillage and the burial of litter residues introduces more microbial access to litter, and leads to a more consistent decomposition environment that speeds up degradation compared to surface residue (Lupwayi et al., 2004; Poffenbarger et al., 2015a). As such, the topographic variability in decomposition may be accentuated in surface residue, where environmental differences are less buffered against change.

A better understanding of the role topography plays in dictating decomposition rates and N release from surface cover crop residues may help to explain spatial variability in ecosystem services provided by cover crops and is crucial for improving management strategies for farmers to maximize benefits. The purpose of this study was to quantify the influence of landscape topography on the rate of above-ground cover crop biomass decomposition in a rolling hill field throughout the subsequent cash crop growing season. The primary objectives of the study were to determine decomposition rates for a cereal rye (*Secale cereale* L.) cover crop and a cereal rye/crimson clover (*Trifolium incarnatum*) mixture at three different landscape positions (i.e., summit, backslope, and toeslope positions) of a rolling hill agricultural production field in Central Kentucky. We hypothesized that decomposition would be primarily limited by moisture during the cash crop growing season. As such, we hypothesized that the backslope position would have the highest soil temperatures and the lowest volumetric soil water in the top layers, and thus would have the slowest decomposition rate, whereas the toeslope position would have the lower soil temperatures and highest volumetric soil water in the top layers, corresponding to the fastest decomposition rate. Further, we hypothesized that the

mixture treatment would decompose more quickly than the monoculture treatment across all landscape positions due to a lower C:N ratio.

2.3 Materials and methods

2.3.1 Experimental design and management

In 2019 and 2020, field trials were conducted at the University of Kentucky Spindletop Farm (38.123° N, -84.490° W), near Lexington, KY USA, to investigate the effects of cover crop species composition and landscape topography on cover crop decomposition rates during maize growth. Two sites were identified to represent hillslope settings found in row crop production fields in the region (**Figure 2.1**). Three topographic positions within each site were delineated based on their slope and elevation (summit, backslope, and toeslope; **Table 2.1**). Soils at the summit positions were classified as fine-silty, mixed, active, mesic Typic Paleudalfs (Bluegrass series). Soils at the backslope positions were classified as fine, mixed, active, mesic Mollic Hapludalfs (McAfee series). Soils at the toeslope positions were classified as fine-silty, mixed, active, mesic Fluventic Hapludolls (Huntington series) (National Cooperative Soil Survey, 2020). Soil depth to the root-restrictive rock layer varied across the hillslopes, with average soil depths of \geq 150 cm in the toeslope, 90 - 100 cm in the summit, and 35-40 cm in the backslope (**Table 2.1**). Average annual precipitation at the research farm is 1088 mm and average annual temperature is 13.1° C (1981-2010; <http://weather.uky.edu/>).

The field experiment was arranged in a split plot randomized complete block design, with three replicates. Landscape position was the main-plot factor, and cover crop treatment was the subplot factor.

Both ST1 and ST2 were in long-term hay production prior to cultivation for this study. In the fall of 2018 and 2019 for ST1 and ST2, respectively, these fields were sprayed with glyphosate, moldboard plowed, and then disked to prepare for cover crop planting. Three cover crop treatments were established following field preparation: a cereal rye cover crop treatment at a target seeding rate of 73 kg ha^{-1} , a cereal rye – crimson clover mixture at a target seeding rate of 45 kg ha^{-1} of cereal rye and 13 kg ha^{-1} of crimson clover, and a winter fallow, which was not chemically controlled during cover crop growth. Cover crops were drill seeded into 19 cm rows on 10/12/2018 at ST1, and 10/15/2019 at ST2. The cover crop was chemically terminated in the spring, (4/13/2019 at ST1, and 4/2/2020 at ST2), and left on the soil surface. At termination, the cereal rye was between the Feekes 7 and Feekes 8 growth stage, and the crimson clover was at an advanced vegetative stage (Knott, 2016).

Following cover crop termination, lime and muriate of potash or sulfate of potash were applied according to University of Kentucky recommendations based on soil test results. Soil tests did not indicate any other nutrient deficiencies for maize growth. Maize was no-till planted on 5/8/2019 at ST1, and 5/11/2020 at ST2 on 76 cm rows at a target population of 78,000 plants ha^{-1} . Nitrogen fertilizer was managed as a split application, with 45 kg N ha^{-1} as 32% UAN fertilizer subsurface banded (5 cm below and 5 cm to the side of the seed) at planting, and 225 kg N ha^{-1} as 32% UAN dribbled on the surface at the V5 growth stage. The V5 sidedress application occurred on 6/4/2019 at ST1, and 6/10/2020 at ST2.

2.3.2 Experimental data collection

2.3.2.1 Cover crop biomass

Just prior to termination, we collected cover crop aboveground biomass from a 0.25 m² frame within each plot (4/11/2019 at ST1, 4/1/2020 at ST2). Four subsamples were taken from each cover crop subplot in ST1 in 2019 (n = 108). COVID-19 restrictions limited the availability of resources during the 2020 sampling, and only two subsamples were taken from each cover crop subplot in ST2 in 2020 (n = 54). Fresh biomass samples were sorted into constituent species and weighed. A subsample of the sorted biomass material was weighed fresh, dried at 65 °C to constant weight, weighed dry, ground, and analyzed for C and N via dry combustion analysis. The remainder of the fresh material was stored at 4°C to prevent decomposition until litter bag construction.

2.3.2.2 Litterbag construction, deployment, and processing

We used a litterbag method to measure cover crop decomposition during the maize growing season. The litterbags measured 40 cm x 18 cm and were made using 1 mm nylon mesh. The amount of fresh litter placed in each bag was constant across landscape positions in each year and was determined based on the average aboveground biomass across landscape positions, scaled to the area of one litterbag (Supplemental Table 1). In 2019, the rye monoculture litterbags contained 21 g dry weight equivalent (DWE) fresh rye litter, and the rye-crimson clover mixture litterbags contained 17 g DWE fresh rye, and 2 g DWE fresh clover. In 2020, rye monoculture bags contained 24 g DWE fresh rye, and the mixture litterbags contained 22 g DWE fresh rye, and 2g DWE fresh clover. Following litterbag preparation, the residue present at the site of litterbag placement was removed, and the litterbags were secured to the soil surface using landscape staples. Litterbags were installed prior to maize planting, approximately one week after chemical termination of the cover crop (**Table 2.2**). The litterbags were removed briefly during

maize planting and pre-emergent herbicide application, after which they were installed in their final position in the middle of the center rows of the plot (**Figure 2.1**). Six litterbags were prepared per plot ($n = 108$). One litterbag per plot served as an indication of initial conditions of the litter and the litter was removed from the litterbag, placed in a paper bag, and placed directly into the drying oven at 65 °C; the other five were removed sequentially throughout the maize growing season (**Table 2.2**).

In 2020, two additional litterbags were added - one at the initial installation and one at the final removal date. These additional bags contained litter amounts representative of landscape position average biomass levels, instead of field averages (**Supplemental Table S2.2**). Following removal from the field, the litter was dried at 65 °C, weighed, ground, and analyzed for C and N via dry combustion. A 1-gram subsample was ashed for 4 hours at 450 °C to account for possible soil contamination of the cover crop residue, and dry weight and C and N content were adjusted to an ash free basis.

2.3.2.3 Weather and soil microclimate measurements

Daily minimum and maximum air temperature and precipitation were measured at the Spindletop Farm station of the University of Kentucky Ag Weather Center, located within 1 km of both field sites. Growing Degree Days (GDDs) for model evaluation were calculated from the mean daily air temperature data and accumulated over the period between initial litterbag installation and the final litterbag removal, using a base temperature of 0 °C. A second set of GDDs was also calculated from the average daily soil temperature at each landscape position to capture the difference in thermal energy across the landscape (sGDD). Additionally, we calculated Decomposition Days (DCD) following the methods described by Steiner *et al.* (1999) and Quemada (2004) to derive

an estimate of the limiting factor to decomposition across time. Decomposition Days take both daily precipitation and temperature into account to calculate what fraction of decomposition occurs on a given day, relative to optimum conditions. Two coefficients are calculated, one for temperature and one for moisture. These daily environment coefficients are constrained between 0 and 1, with 0 indicating no decomposition occurring, and 1 indicating optimum decomposition conditions. The temperature factor was calculated as:

$$TC = \frac{2 \cdot T_{mean}^2 \cdot T_{Optimum}^2 - T_{mean}^4}{T_{Optimum}^4} \quad [2.1]$$

where TC is the temperature coefficient, T_{mean} is the average daily air temperature, and $T_{Optimum}$ is the optimum air temperature for decomposition (defined as 32 °C). The moisture coefficient (MC) was calculated based on rainfall; if on a given day total rainfall > 4mm, MC was set equal to 1. If precipitation occurred on a given day, but was not > 4mm, the MC was equal to the precipitation divided by 4. If no precipitation occurred, the MC was calculated as half the MC of the previous day. The DCD for a given day was then equal to the lower of the two values, indicating which was more limiting to decomposition.

Soil temperature sensors (HOBO TidbiT v2 Temperature Loggers; ONSET, MA USA) were installed after maize planting at 5 cm depth in the center rows of all plots in which litterbags were present, adjacent to the position of the litterbags. Temperature sensors logged soil temperature at a 10-minute time interval throughout the maize growing season. Volumetric soil water content was measured at 10 cm depth increments down to 100 cm or bedrock, depending on the soil profile, using a Sentek Diviner 2000

Capacitance probe (Sentek Technologies, South Australia). In the data presented here, we focus on only the top 10 cm moisture measurements. Each measurement was taken as the average from three readings per sampling. Moisture measurements were calibrated for our site by estimating parameters for the non-linear equation relating volumetric moisture measurements taken at probe installation and scaled frequency measurements taken at the same time for each field site (see Paltineanu and Starr, 1997 for further discussion of calibration methods).

2.3.3 *Calculations and statistics*

2.3.3.1 *Exponential decay models*

The percentages of ash-free cover crop mass remaining (MR) and the N remaining (NR) of our measured field samples at a given litterbag removal date were calculated as:

$$MR \text{ or } NR = 100 \times \left(\frac{X_{RD}}{X_{Int}} \right) \quad [2.2]$$

where X_{RD} is the mass of litter or the amount of N in the biomass at a given removal date, and X_{Int} is the mass of litter or the mass of litter N at Time 0. To calculate the percentage of N released, the percentage of N remaining was subtracted from 100. The percentage of mass remaining of the cover crop residue over time was modeled using a two-component asymptotic exponential decay model:

$$PMR = a_m + (1 - a_m) \times \exp^{-k_m t} \quad [2.3]$$

where PMR is the predicted percentage of litter remaining at a given time point, k_m is the decomposition rate of the residue, and a_m is the (asymptotic) percentage of mass that is resistant to further decomposition. Models were constructed for days after installation,

GDD, and DCD, and compared using Akaike's Information Criterion (AIC), Bayesian Information Criterion (BIC) and the models log likelihood value to determine the most appropriate timescale for the data (**Supplemental Table S2.1**). Model fitting was performed in R v. 4.0.2 (R Core Team, 2020), using nlraa v 0.73 and nlme v. 3.1-148 (Miguez, 2020, Pinheiro et al., 2020). The model structure considered the fixed effects of cover crop treatment, the landscape position and the interaction. A random effect due to replicate was also included in the model. Model inference was based on the parameters of the non-linear model: the decomposition rate (k_m) and resistant fraction (a_m) using pairwise comparisons. To analyze N release of the cover crop residue over time, we used an exponential rise to maximum model:

$$PNR = a_n \times (1 - \exp^{-k_n t}) \quad [2.4]$$

where PNR represents the predicted percentage of N released at a given point in time, a_n is the maximum percentage of N released over the growing season, k_n is a release constant, and t is time in days. A similar procedure of model evaluation to the method described above was used to evaluate treatment effects on the rate of N release from the cover crops at different landscape positions.

2.3.3.2 Soil temperature and moisture analysis

Measurements of soil temperature and volumetric moisture exhibited temporal autocorrelation, meaning that the value of a given day is highly dependent on the value of the previous day, and will influence the following day. To account for this autocorrelation when examining differences among landscape position and cover crop treatments on these microclimate variables, we used general additive models (GAMs),

which have been shown to be a robust method of analyzing this type of soil moisture data (Basche et al., 2016). All GAM analyses were performed in R v. 4.0.2 (R Core Team, 2020) using the mgcv v 1.8 (Wood, 2011) and the itsadug v 2.4 (van Rij et al., 2020) packages. In our models, the interaction between cover crop and landscape position was used to generate separate splines for each possible combination. A separate spline term was added to include the random effect of replicate in the model. Post-hoc comparisons of model predictions for each treatment were performed using a non-parametric Wald test. To account for different weather conditions during our two field seasons, we analyzed our microclimate data separately for each year. The soil moisture measurements at one replicate/landscape position combination (ST2 Summit, Block 1) had results outside the bounds of what could be expected for soils in this region. Point measurements indicated poor agreement with measured gravimetric water samples, and high variability compared to replicates 2 and 3. As such, this replicate/landscape position combination was not included in the final analysis of topsoil moisture presented here.

2.4 Results

2.4.1 *Topographic and edaphic factors*

The landscape position treatments had discrete edaphic and topographic characteristics both field sites that litterbags were installed in (**Table 2.1**). The most significant difference among landscape positions was depth, with depth to the impermeable layer ranging from 35 cm on the backslopes to > 150 cm at the toeslopes. Backslope positions were consistently shallower than toeslope and summit positions. In 2019, the hillslope was oriented towards the southeast, while in 2020, the hillslope was oriented northwest (**Table 2.1**). The orientation impacted the clear sky solar radiation; landscape positions in

ST2 received 2-6% less clear sky growing season radiation than in ST1 (**Supplemental Figure S2.1**). In both 2019 and 2020, the toeslope position tended to have more silt and less clay or sand content than the summit and backslope positions. In general, soil C did not vary substantially across hillslopes. The backslope position at both ST1 and ST2 had numerically the highest level of soil C, however this difference was not statistically significant. The amount of inorganic N in the top 20 cm of soil was similar among landscape position and cover crop treatments but was higher in 2019 than 2020. In 2019, the top 20 cm inorganic N at maize planting ranged between 16.3 and 23.1 kg N ha⁻¹, and the average among cover crop treatments and landscape positions was 19.5 kg N ha⁻¹. In 2020, the average inorganic N in the top layer of soil was 6.2 kg N ha⁻¹, and values ranged from 4.6 – 7.5 kg N ha⁻¹ among treatments (**Table 2.1**).

2.4.2 *Microclimate*

2.4.2.1 *Air temperature, growing degree days, and decomposition days*

In 2019, the maximum daily mean air temperature during the period when litterbags were deployed (between 4/29/2019 and 9/06/2019) was 29 °C, and the mean daily air temperature for the maize growing season was 23 °C. Air temperature was at its highest at the end of July, and its lowest at the beginning of the season in April. The 2020 growing season (between 4/16/2020 and 8/29/2020) was cooler, with a maximum air temperature of 29 °C, but an average temperature of 21 °C. The pattern observed in 2019 was repeated in 2020, with highest air temperatures occurring in the final week of July, and lowest temperatures occurring prior to maize planting in April. Air temperature was more variable in 2020 than in 2019. The coefficient of variation in average daily temperature was 15.5% in 2019, and 27.7% in 2020. Higher variability in the 2020

growing season was driven by a prolonged period of cool temperatures in the spring period (**Figure 2.2**). Because of the lower temperature in April and May in 2020 relative to 2019, total accumulated growing degree days were lower in the 2020 season (**Table 2.2**, 3085 GDD vs. 2770 GDD for 2019 and 2020, respectively). The GDD based on soil temperature (sGDD) varied across the landscape positions in 2019 but were more similar to each other in 2020. The backslope position accumulated the most sGDD in both years (3094 and 2899, for 2019 and 2020, respectively). The difference between years in sGDD occurred primarily between July 15 and August 15 of 2019, when elevated backslope soil temperatures accelerated the accumulation of sGDD in that position. The toeslope and summit positions were similar to each other in 2019 and accumulated 3010 (summit) and 3019 (toeslope) sGDD. In 2020, the toeslope position accumulated 2861 sGDD, and the summit position accumulated 2851 sGDD (**Table 2.2**).

The DCD model was used to determine the relative amount of decomposition occurring on each day compared to an optimum set of temperature and moisture conditions, to identify which climate factor was more limiting to residue decomposition. Similar to GDD and sGDD, decomposition days were higher in the 2019 growing season as well (**Table 2.2**, 29.65 DCD vs. 24.68 DCD for 2019 and 2020, respectively). Overall, the highest values tended to occur sporadically later in the season immediately following rainfall; temperatures were warm and moisture conditions were near optimum. In 2019, decomposition was limited by moisture for 69.9% of the season and limited by temperature for 30.1% of the season. In 2020, decomposition was limited by moisture for 66.9% of the season and limited by temperature for 33.1% of the season (**Figure 2.3**).

The average relative rate of decomposition in comparison to optimum conditions in 2019

was 34%. Values throughout the year varied between from 0 to 94%. The average relative rate of decomposition in 2020 was 29% of that at optimum conditions, though across the year the relative rate spanned a similar range of values to 2019, from 0 to 94%.

2.4.2.2 Soil temperature and moisture responses to landscape position and cover crop treatment

Overall, soil temperature at 5 cm depth followed the trends in air temperature in both 2019 and 2020 (**Figure 2.2, Figure 2.4**). Soil temperature ranged from 15.5 to 31.3 °C in 2019, and between 9.3 and 28.7 °C in 2020. The highest soil temperatures occurred at the beginning of August in 2019 (31.3 °C) and in mid-July in 2020 (28.7 °C). In both years, the highest temperature was observed at the backslope position. Landscape position, cover crop, and their interaction had a significant influence on soil temperature during both years of the study (**Figure 2.4**). The frequency of significant differences was greater in 2019 than in 2020, but the trends in temperature were consistent between years. Based the results of the GAM analysis, the backslope position was generally warmer than the toeslope and the summit positions in both years. The cover crop influenced soil temperature at different time points at each landscape position. In both years however, the rye/crimson clover mixture was significantly warmer than the rye monoculture treatment in the toeslope but cooler than the rye monoculture treatment in the summit at the beginning of the season. Similarly, in both years, the mixture treatment was significantly cooler than the rye monoculture in all landscape positions at the in the middle and end of the season (**Figure 2.4**).

Soil volumetric water content in the top 10 cm ranged from 10% to 23% in 2019 and from 11% to 21% in 2020. In both years of our study, the highest volumetric water

content of the top ten centimeters of the soil profile occurred in the spring, with soil water content decreasing throughout the course of the season (**Figure 2.5**). Landscape position had a significant impact on topsoil volumetric water in the spring of 2019 (p-value < 0.001), and in 2020 (p-value < 0.001), however the effect was much more subdued in 2020 (**Figure 2.5**). The toeslope position was significantly wetter than the backslope and the summit throughout the season in 2019, and significantly wetter than the summit position in 2020. Cover crop treatment did not have a significant effect on topsoil moisture in either year, though landscape position effects were slightly different between the monoculture and mixture at different times throughout the season.

2.4.3 *Litterbag experiment results*

2.4.3.1 *Initial litterbag properties*

At the time of litterbag installation, the average C:N ratio of the cover crop residue in the 2019 litterbags for the rye monoculture treatments was 19.2, and for the mixture treatment was 17.2. The initial N content of the cover crop residue was 2.3% for the rye monoculture treatment and 2.5% for the mixture treatment. In 2020, the average C:N ratio of the litterbag residue for the monoculture treatment was 20.7, and for the mixture treatment was 20.1. The initial N content of the cover crop residue was 2.0% for the monoculture treatment, and 2.1% for the mixture treatment in 2020.

2.4.3.2 *Litterbag decomposition and nutrient release*

Among the three time scales evaluated, natural days had the lowest AIC and BIC values, and the highest log likelihood values, for decomposition and N release models in 2019. In 2020, decomposition days had the lowest AIC and BIC values, but the improvement was

marginal compared to natural days and did not supersede the improved fit of natural days in 2019 (**Supplemental Table S2.1**). Growing degree days based on air temperature consistently had the highest AIC and BIC values, and lowest log likelihood values in across models in both 2019 and 2020. Natural days most consistently had the lowest AIC and BIC values and the highest log likelihood values when considered across both years, indicating the most accurate model fit.

Averaged across treatments, residue decomposed faster in 2019 than in 2020. Cover crop residue decomposed at an average rate (k_m) of 3.2% per day in 2019, and 1.7% per day in 2020 (**Table 2.3**). In 2019, it took 45 days to decompose 50% or more of the residue, whereas it took 56 days in 2020, though the date at which 50% was reached was similar, between June 10 and 12. The most rapid decomposition occurred between the installation and the first removal date, a period of 14 days during which 25% and 15% of the litter decomposed in 2019 and 2020, respectively (**Figure 2.6**). The percentage of residue resistant to further decomposition (model parameter a_m) averaged 32% of the original mass across all treatments in 2019, and 16% in 2020 (**Table 2.3**). The decreased a_m parameter in 2020 relative to 2019 partially explains why the decomposition curve for 2020 appears steeper overall than what was observed in 2019, despite having a lower average k_m constant (**Figure 2.6, Table 2.3**). The average percentage cover crop residue remaining across treatments measured at the end of the growing season was 34% in 2019, and 25% in 2020, indicating that the model estimated asymptote was close to the final value in 2019, but not in 2020. Pairwise comparisons between the landscape position treatments did not indicate significant differences between any two landscape positions in the decomposition rate (k_m) or percentage of residue resistant to decomposition (a_m) in

2019 or 2020 (**Table 2.3**). Similarly, pairwise comparisons of the cover crop treatments at individual landscape positions did not indicate significant differences in either the k_m or a_m parameters.

The average nitrogen release constants (k_n) were 4.6% per day in 2019 and 1.8% per day in 2020. The average model-predicted asymptotic N release (a_n) was lower in 2019 than in 2020 (74% and 85%, respectively; **Table 2.3**). Despite differences in a_n parameters, the measured percentage of residue N released was similar in 2019 and 2020, with 74% of biomass N released by the end of the growing season in 2019, and 77% in 2020.

Nitrogen release from cover crop residue was largely unaffected by cover crop treatment or landscape position in both the 2019 and 2020 growing seasons (**Table 2.3, Figure 2.6**). The rye monoculture released N more rapidly than the mixture treatment in 2020, but only in the backslope position (p-value = 0.02; **Table 2.3**). The actual magnitude of this effect was moderate (k_n = 1.1% and 2.5% for the mixture and rye monoculture, respectively), but was not repeated at any other landscape position in either site year.

In 2019, N release proceeded faster than mass loss. Averaged across landscape positions and cover crop treatments, 50% of the biomass N release occurred by the 25th day after installation, on May 24th, which was 20 days earlier than 50% of biomass decomposition occurred. Similar to the decomposition model, the most rapid N release occurred at the beginning of the season; 35% of the N in the cover crop residue was released between installation and the first removal date 14 days later (**Figure 2.6**). The N release reached the model predicted asymptote (74%) by end of the season, 130 days after installation on September 6th, consistent with the pattern observed in decomposition which also reached the asymptote by the end of the final removal date. In 2020, N release from the litterbags

was not more rapid than mass loss. Model predictions averaged across all treatments indicated that 50% of the biomass N was released by June 7th, 52 days after installation. The average N released did not reach the model-predicted asymptote ($a_n = 85\%$) in 2020, on the final removal date the average N released across treatments was 75% (**Figure 2.6**). This further mirrors trends in the decomposition; the a_m parameter in 2020 was also ~ 10% lower than the observed decomposition.

2.4.3.3 Landscape position adjusted litterbags

In 2020, a secondary set of litterbags was added to evaluate the effect of initial litter mass on decomposition and N release using only an initial (Removal Date 0) and final removal date (Removal Date 5). For these bags, we used the average biomass of each landscape position rather than the average biomass of the overall site year to determine the mass of residue placed in each bag (**Supplementary Table S2.2**). We did not observe a significant effect of landscape position (p-value = 0.86), cover crop treatment (p-value = 0.96), or the interaction of the landscape position and cover crop treatments on the total amount of residue decomposed over the season (p-value = 0.13). The average full season residue decomposition for the position averaged litterbags was similar to the site averaged residue decomposition for 2020; 75% of the residue had decomposed between installation and the final removal date.

Observing no effect of initial biomass on the results of the decomposition rate, we elected to apply our non-linear models to the initial biomass and nitrogen content observed at each landscape position to estimate the amount of N released from the cover crop (**Table 2.4**). Despite differences in the decomposition rate, the average total amount of N released was similar between years. In 2019, across landscape positions and cover crop

treatments, 47 kg N ha⁻¹ was released; 46 kg N ha⁻¹ was released on average in 2020. The estimated total amount of N released from the residue varied numerically by landscape position and cover crop, though at the summit and toeslope position these differences were not significant. Overall, we observed that the mixture treatment, on average, exhibited a trend of releasing more overall N (48 kg ha⁻¹ vs. 44 kg ha⁻¹, for the mix and the rye, respectively). This effect was strongest on the backslope position (51 kg ha⁻¹ vs 41 kg ha⁻¹, for the mix and the rye, respectively), and examinations of the contrasts between the mixture and rye indicated a significant effect of cover crop at this position (p-value = 0.02). In contrast, at the toeslope position the rye and mixture treatments were similar; the rye treatment released 45 kg ha⁻¹ N, and the mixture 44 kg ha⁻¹ N (p-value = 0.67). The summit varied in its response to cover crop treatment between years. The mixture released 14% more N in 2019 at the summit position (58 kg N ha⁻¹ for the mix, 49 kg N ha⁻¹ for the rye), but was more similar in 2020, with the rye numerically higher (41 kg N ha⁻¹ vs 46 kg N ha⁻¹ for the mix and rye, respectively) (p-value = 0.62).

2.5 Discussion

2.5.1 Landscape position and cover crop effects on microclimate

In both years, the backslope position was as warm or warmer than the toeslope and summit positions for at least part of the year. This finding supports our original hypothesis, that sloping positions would generally be warmer than summit or toeslope areas. The landscape position effect on surface soil temperature was more pronounced in 2019 than 2020 (**Figure 2.4**). In 2019, the study site was oriented towards the southeast, and clear sky estimates of solar insolation indicate that the backslope position received more direct sunlight than the toeslope or summit positions. In contrast, the study site in

2020 was oriented towards the northeast, and the sloping position received similar or less amounts of insolation than the summit and toeslope positions (**Table 2.1, Supplemental Figure S2.1**). Thus, the different hillslope aspects between site-years may partially explain the greater warming of the backslope position in 2019 than in 2020.

When combined across our two site years, we found that soil temperature varied by as much as 1.92 °C between the backslope and summit or toeslope positions on a particular day. Further, on average, the backslope position was 0.5 °C warmer than the toeslope and summit positions throughout the growing season. When examined in terms of cumulative heat units based on soil temperature (sGDD), the backslope accumulated 90-100 more cumulative sGDD in 2019, and 40-50 more sGDD in 2020 than the other landscape positions. The spatially variable soil temperatures observed may have led to differences in the rates of microbial reactions and biogeochemical cycles among landscape positions, such as N mineralization (Miller and Geisseler, 2018), C mineralization and sequestration (Craine et al., 2010), and greenhouse gas emissions (Negassa et al., 2015). In both years of our study, the maximum temperatures that we observed fell within or just above the optimum range of fungal and bacterial growth in agricultural soils (25-30 °C; Pietikäinen *et al.*, 2005), indicating that the greatest amount of microbial activity may have occurred on the backslope, at least during periods when topsoil moisture was similar among landscape positions. Sloping positions are thought to have greater potential for C storage relative to downslope areas, due to their typically degraded condition (Ladoni et al., 2016). However, warmer temperatures that are more optimal for microbial decomposition in these landscape positions may actually limit soil C accrual, limiting yield and increasing the need for mineral fertilizers that are easily lost from shallow soils.

We found that volumetric water content in the top 10 cm of the toeslope position was generally as high or higher than soil moisture in the backslope and summit across our study, offering further evidence in support of our original hypothesis regarding microclimate differences. Similar to soil temperature, the differences in soil moisture among landscape positions were more pronounced in 2019 than in 2020. In 2019, the toeslope position was significantly wetter than the summit and backslope position through the first half of the growing season, and not significantly different in the latter half. In 2020, the toeslope position was significantly wetter than the summit position during the first half of the season, but not the backslope. One possible explanation for the different moisture patterns between site-years is that the cumulative spring rainfall between the two seasons differed substantially. In 2019, between cover crop termination and the V5 stage in maize, the field received 114 mm of precipitation. In contrast, between cover crop termination and V5 maize stage in 2020, the field received 227 mm of rain (**Figure 2.2**). The increased rainfall in 2020 during the period in which significant differences between the backslope and toeslope positions were observed in 2019 may have muted a landscape position effect if the rate of lateral redistribution of water was lower than the rate of incoming precipitation. The spatial variation of soil water content in areas of complex topography has been well documented (Kravchenko and Bullock, 2000; Kumhálová et al., 2011; Maestrini and Basso, 2018b), and is a major driver of yield variability across areas of rolling hill topography (Leuthold et al., 2021). While our results do not examine the full profile water storage, they do indicate that at least in the topsoil, landscape position effects are somewhat ephemeral, and likely dependent on the weather of a given year. Previous work examining the interactions between

microtopographic gradients and soil water found inconsistencies in the occurrence of spatiotemporal hot moments in N₂O production that could not be explained by topographic variables alone (Suriyavirun et al., 2019)..

When moisture and temperature are considered in tandem, the distribution of soil water that we observed among landscape positions in either year may also help to explain the differences in soil temperature among the landscape positions. Because wet soils require more energy to warm than do dry soils, soil water content and soil temperature are often negatively correlated (Sauer and Horton, 2005). In 2019 especially, the specific heat capacity of the soils at the three different landscape positions was likely impacted by the significant differences in soil moisture throughout the field. The shallow soils of the backslope position had limited water storage capacity and exhibited high variability in the amount of water stored, and therefore the amount of energy necessary to increase the soil temperature. Accordingly, the midseason drought that occurred in 2019 (**Figure 2.2**), affected the backslope position to a greater degree than the summit or toeslope positions. Evidence of water limitation was present in the maize crop; maize aboveground biomass at the backslope position by R1 (9 Mg ha⁻¹) was severely reduced compared to the summit and toeslope positions (10.5 and 11.7 Mg ha⁻¹) (Leuthold et al., 2021). In 2020, the more consistent rainfall throughout the season, coupled with a more consistent crop canopy among landscape positions, likely led to more homogeneous heat capacity conditions across the landscape, and may further explain why landscape position effects on temperature were muted relative to 2019.

The minor differences in soil temperature between cover crop treatments were largely not significant (**Figure 2.4**). The lack of a cover crop treatment effect on soil temperature was

somewhat expected, as both the rye and the mixture produced similar amounts of biomass and residue coverage (**Supplemental Table S2.1**). Though not directly measured in this study, there is a possibility that the clover within the mixture decomposed more rapidly than the rye, which could lead to more rapid reduction of soil cover and subsequently less buffering against changes in temperature. However, these changes would likely occur later in the season, which is incongruous with our results that showed slight deviations towards elevated temperatures in the mixture compared to the rye early in the season.

2.5.2 Landscape position and cover crop effects on decomposition

2.5.2.1 Landscape position treatment

Despite differences in soil moisture and soil temperature among landscape positions throughout the two growing seasons, we did not find evidence that decomposition rate differed by landscape position. In both 2019 and 2020, there was not a strong effect of landscape position on decomposition rate (k_m), or the N release rate (k_n) for the cover crop residue. This was contradictory to our hypotheses that rapid decomposition would occur in the toeslope and slower decomposition would occur in the backslope. Instead, two new alternative hypotheses arise from this observation: 1.) The relatively warm/dry soil of the backslope, cool/moist soil of the toeslope, and moderately warm/moderately moist soil of the summit all led to similar limitations on microbial activity and the same net effect on decomposition rate, or 2.) soil microclimate is not a primary control on the decomposition rate of surface cover crop residue.

Given that temperature and moisture have an important influence on the decomposition rate of crop residue, it is possible that the increased temperature at the backslope

accelerated decomposition of the residue, but the effect was limited by moisture. Similarly, the increased soil moisture at the toeslope may have accelerated decomposition, but the effect was stifled by lower temperatures. Therefore, across the topographic gradient, decomposition occurred at similar rates, but may have occurred for dissimilar reasons. Previous studies that have examined the decomposition of cover crop residue at different landscape positions have found that differences in microclimate do shift decomposition rates. For instance, Beehler et al. (2017) found that decomposition after 40 days of buried rye cover crop litterbags was significantly higher in depressional areas compared to sloping and summit areas, which was attributed to increased soil moisture and improved conditions for microbial activity. Similarly, Nguyen and Kravchenko (2020) found that the greatest CO₂ flux in a topographically diverse system occurred in depression areas that had cover crop residue chisel tilled in to a depth of 30 – 45 cm, due to differences in hydrologic characteristics between landscape positions. However, one key difference between the results presented here and these studies is the differing tillage systems. Buried litterbags and incorporated residue are much more connected to the soil microclimate, while surface residue is in a constant flux of wetting and drying. The more direct connection to environmental variability may have homogenized the decomposition rate across the hillslope in our study (Steiner et al., 1999). However, our analysis of DCD accumulation indicated that moisture was the major limiting factor to decomposition in both years (**Figure 2.3**), especially later in the season when decomposition is typically more controlled by environmental conditions than labile N content. We would therefore expect that decomposition rate would be

accelerated in the toeslope position and slowed on the backslope, especially in 2019, which is not what we observed.

A second possibility is that while the soil under the residue in our study did vary in temperature and moisture by landscape position, the soil microclimate may not impact the microclimate of surface residue enough to impart a landscape position signal on decomposition or nitrogen release rates. Chemical termination of cover crops prior to the cash crop growing season in no-till agricultural systems typically leaves cover crops standing, as opposed to roller-crimper termination style or tillage. Over the course of the season the residue falls and stacks on the soil surface, but in moderate to high residue areas, the majority of the residue is likely in contact with other residue, and not soil (Steiner et al., 1999). Previous soil column experiments examining decomposition controls have shown that the proportion of residue in contact with the soil is an important factor in modeling residue decomposition rates, with increasing proportion of residue in contact with the soil surface correlating with increasing decomposition (Findeling et al., 2007). Other studies have highlighted the limited extent to which subsurface banded fertilization impacts decomposition rate of residues, due to a spatial disconnection between the applied nutrient, microbial activity, and the residue (Lacey et al., 2020; Poffenbarger et al., 2015). As such, it is possible that a lack of soil-residue contact limited the influence of soil characteristics on surface residue in our study. Ma et al. (1999) examined the decomposition of surface residue over 13 years in dryland agroecosystems in Eastern Colorado and found that landscape position had no effect on the decomposition of crop residue, similar to our findings. Further, an examination of models incorporating soil temperature and water content was not found to be any more predictive

than models that employed days after termination or growing degree days, underscoring the possible disconnect between abiotic soil conditions and surface residue behavior (Ma et al., 1999). Surface residue dries quickly after wetting and is more dynamic in its microclimatic state than soil water pools, such that the decomposition rate is likely more linked to rain-evaporation cycles rather than soil water status (Coppens et al., 2006). Recent research by Thapa et al. (2021) has highlighted the significant interactive effects of residue moisture and temperature on decomposition rate, which impact surface residue to a greater effect than soil temperature or moisture alone. However, residue moisture and temperature require frequent, destructive field measurements to estimate or model, while soil temperature and moisture are relatively easy to continuously monitor. Developing robust, dynamic models of the relationship between measured soil microclimate data and weather data, and residue microclimate is therefore imperative to improving our understanding of decomposition dynamics in surface residue.

2.5.2.2 Cover crop treatment

In addition to the landscape position treatment not imparting a significant effect on decomposition, we also did not observe a significant effect of cover crop treatment, which is in contrast to our original hypothesis. The addition of a low C:N ratio legume accelerating decomposition compared to cereal monocultures is well documented (Poffenbarger et al., 2015; Ranells and Waggoner, 1996; Sievers and Cook, 2018), and follows the paradigm of N availability as a primary determinant of cover crop residue decomposition. A lower C:N ratio of the overall litter allows for increased mineralization and limits the need for immobilization of residue N in the microbial biomass. We did not find an effect of the legume addition on decomposition rate. While this is somewhat

surprising, it mirrors the results of Ranells and Waggoner (1996), in which they found that the decomposition constant for a rye cover crop and a rye crimson clover mixture were similar across two years of study. Other legume species that accumulate more N throughout the season, such as hairy vetch, may impart a more significant cover crop signal on decomposition rate than the crimson clover used here. Additionally, it is possible that the site average of crimson clover was too low to significantly impact decomposition. Poffenbarger et al. (2015) tested the effect of changing proportions of hairy vetch – cereal rye in a decomposing cover crop residue and found a positive relationship between the proportion of hairy vetch and the rate at which the mixture decomposed. The proportion used in this study, 12.2% and 10.9% for 2019 and 2020, respectively, while reflecting the results of the cover crop growth, may not have reached the threshold at which litter decomposition is significantly altered by the presence of a legume. Crimson clover is a well-suited leguminous winter annual cover crop for this region, as it can overwinter through the moderate winters of the southeast and provide rapid spring growth (Clark, 2007). If managing bicultures such as the cereal rye/crimson clover presented in this study with N return to the crop as a primary goal though, seeding rates or planting and termination timing may need to be adjusted to increase the amount of clover at termination for a worthwhile N credit.

Though landscape position and cover crop treatment did not impact the decomposition rate of cover crop residue in our field study, both had significant effects on total cover crop biomass production (**Supplemental Table S2.1**). When we apply the models derived from our litterbag experiment to the residue amounts measured at each landscape position, we observe differences in amount of residue remaining and the amount of N

released across the landscape positions. If, as our results suggest, the rate of surface residue decomposition is similar throughout the field, differences in the total amount of residue will lead to heterogeneity in the ecosystem benefits provided by the cover crop. Applying our non-linear models to the measured residue amounts shows that in the backslope position, the mixture treatment released 14-25% more N than the rye monoculture in both 2019 and 2020. The increased N content of cereal/legume mixtures compared to cereal monocultures is well documented (Thapa et al., 2018). Cereal rye is totally dependent on soil N stocks for plant available N, whereas in the mixture, additional N is added to the system via atmospheric fixation by the clover. In our study, the backslope position had a relatively low total profile N stock, and the addition of an N fixing legume likely allowed for more N return than the monoculture was able to muster by soil scavenging alone. This finding implies an interactive effect that exists beyond decomposition alone, involving winter cover crop growth and landscape position that should be investigated further as a facet of cover crop management and nutrient release in areas of rolling hill terrain. Variable rate seeding of cover crop and cover crop mixtures may provide an avenue to capitalize on consistent decomposition rates while maximizing ecosystem benefits to the cash crop.

2.6 Conclusions

Because cover crop services relate to the persistence and N release of cover crop surface residues, understanding cover crop decomposition dynamics is critical to maximizing potential benefits of cover crops and ensuring the sustainable management of agroecosystems. The purpose of this study was to investigate the effect of landscape position on soil temperature and moisture and identify potential linkages between

microclimate and sub-field variability in decomposition rates of a cereal rye monoculture and a cereal rye/crimson clover mixture cover crop. We found that landscape position did significantly impact topsoil moisture and soil temperature, but that the results varied in intensity by weather year and hillslope orientation. Despite differences in microclimate factors, we did not observe significant differences between landscape positions in regard to the decomposition rate of cover crop residue. In addition, we did not observe an effect of cover crop species composition on decomposition rate. Our results suggest that in cover crop-maize sequences in the southeastern U.S., decomposition of surface residue in no-till fields is likely controlled by larger scale factors such as weather, tillage, and cover crop developmental stages and termination date, rather than landscape position-specific indices. When our non-linear models were applied to field data of measured residue amounts, we observed significantly more N deposition from mixture treatments compared to rye monoculture treatments on sloping positions. Producers should leverage the consistency in decomposition rates to focus on cover crop production in areas of need; increasing legumes in N poor areas to improve N release or increasing total biomass in weed prone areas to improve weed control, for instance. Future research focusing on the interactions between weather, management, and soil heterogeneity derived controls of surface residue decomposition will further increase our understanding of decomposition dynamics in no-till, rolling hill systems.

2.7 Chapter 2 tables and figures

Table 2.1 – Soil and topographic characteristics for hillslope fields in 2019 and 2020.

Year	Landscape Position	Soil Characteristics ¹							Topographic Characteristics		
		Silt	Clay	Soil Depth	Soil pH	SOC	Inorganic N ²		Slope	Aspect	Elevation
							Rye	Mix			
		%	%	cm		%	(kg ha ⁻¹)		Deg.	Deg. ³	masl
2019	Summit	72	17	100	6.0	2.0	23.0	17.4	2.01	221	902
2019	Backslope	54	26	35	6.7	2.4	16.7	23.1	5.08	180	900
2019	Toeslope	73	14	>150	5.9	2.2	20.6	16.3	1.47	216	887
2020	Summit	64	17	90	6.1	2.1	4.6	5.7	1.63	44	903
2020	Backslope	64	17	40	6.7	2.2	5.7	6.6	4.96	94	897
2020	Toeslope	79	8	>150	6.1	1.8	7.5	7.2	1.02	70	883

1: Soil characteristics represent average values from 0-10 cm samples taken at the main plot level, averaged across cover crop treatments.

2: Inorganic N measurements were taken at maize planting, extracted using a 1M KCl extraction, and analyzed using a colorimetric method (Crutchfield and Grove, 2001).

3: Aspect measured in degrees where N is equal to 0, W is equal to 90, S is equal to 180, and E is equal to 270.

Table 2.2 – Removal dates and days after installation of litterbags in 2019 and 2020.

Removal Date	Date		Days after installation		Growing Degree Days		Decomposition Days	
	2019	2020	2019	2020	2019	2020	2019	2020
0	April 29	April 16	0	0	0	0	0.0	0.0
1	May 13	April 27	14	11	253	120	3.0	1.5
2	May 29	May 11	30	25	625	293	7.5	2.9
3	June 30	June 15	62	60	1355	1015	16.1	8.0
4	July 30	July 16	92	91	2141	1759	23.5	18.2
5	September 6	August 29	130	132	3085	2770	29.9	25.6

Table 2.3 - Decomposition rate (k) and asymptote (a) predictions and standard errors from non-linear models of cover crop residue decomposition in 2019 and 2020. Units are in percentage decomposed or percentage released, where appropriate. No parameters were significantly different according to pairwise comparisons of model contrasts, except for the k2 parameter for nitrogen release in the backslope position in 2020, and the a2 parameter in 2019.

Decomposition					
2019					
Landscape Position	Cover Crop	k_1	k_1 SE	a_1	a_1 SE
Summit	Rye	3.60	0.47	25.3	5.20
	Mix	2.75	0.68	36.8	3.62
Backslope	Rye	3.49	0.67	36.4	3.91
	Mix	3.38	0.64	35.5	3.80
Toeslope	Rye	3.34	0.60	31.8	3.84
	Mix	2.75	0.52	30.6	4.63
2020					
Landscape Position	Cover Crop	k_1	k_1 SE	a_1	a_1 SE
Summit	Rye	1.40	0.35	13.4	11.00
	Mix	2.22	0.42	23.9	5.68
Backslope	Rye	2.17	0.41	22.3	5.71
	Mix	1.50	0.35	12.2	9.83
Toeslope	Rye	1.83	0.37	16.5	7.23
	Mix	1.27	0.34	9.2	12.99

Nitrogen Release					
2019					
Landscape Position	Cover Crop	k_2	k_2 SE	a_2	a_2 SE
Summit	Rye	3.18	0.59	80.9	3.29
	Mix	4.55	0.74	71.1	2.57
Backslope	Rye	4.76	0.81	66.3 ⁺	2.71
	Mix	5.89	0.91	69.7 ⁺	2.29
Toeslope	Rye	4.83	0.72	79.8	2.49
	Mix	4.49	0.69	79.5	2.59
2020					
Landscape Position	Cover Crop	k_2	k_2 SE	a_2	a_2 SE
Summit	Rye	1.68	0.44	82.7	9.87
	Mix	2.01	0.46	81.1	7.74
Backslope	Rye	2.53*	0.52	77.2	5.68
	Mix	1.08*	0.36	106.1	20.34
Toeslope	Rye	2.28	0.49	78.3	6.40
	Mix	1.75	0.42	86.4	9.24

*: Cover crop treatments were significantly different in the backslope position for the k_2 .

+: The backslope position a_2 value was significantly less than the summit and toeslope position in 2019.

Table 2.4 - Predictions of N release and mass remaining at the final removal date (i.e., 130 or 132 days after installation for ST1 and ST2, respectively) for each landscape position based on the application of non-linear models to initial biomass measurements.

Site	Landscape Position	Cover Crop	N Release Estimate (kg ha ⁻¹)	SE	Mass Remaining Estimate (kg ha ⁻¹)	SE
ST1	Summit	Mix	57.5	3.3	1365	120
ST1	Summit	Rye	49.3	3.0	975	123
ST1	Backslope*	Mix	49.4	4.4	1189	107
ST1	Backslope*	Rye	42.4	2.2	1248	112
ST1	Toeslope	Mix	42.0	2.4	764	81
ST1	Toeslope	Rye	40.5	2.1	921	95
ST2	Summit	Mix	41.1	2.5	801	110
ST2	Summit	Rye	45.9	2.7	1207	216
ST2	Backslope*	Mix	52.3	4.6	982	173
ST2	Backslope*	Rye	39.0	2.0	828	121
ST2	Toeslope	Mix	46.3	2.6	848	164
ST2	Toeslope	Rye	49.2	2.8	800	127

* : Significant differences in N release estimates occurred between rye and mixture treatments at the backslope position (p-value = 0.02).

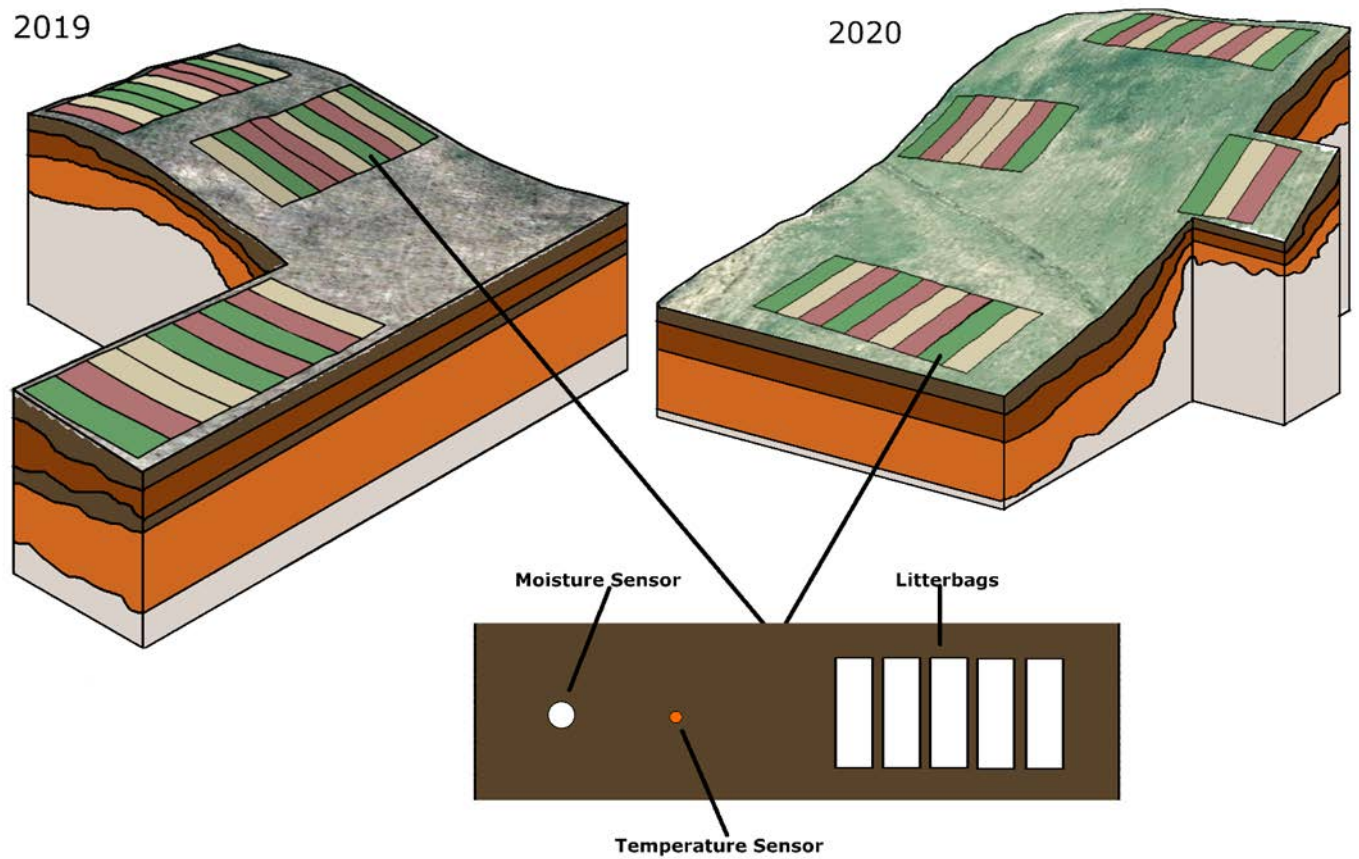


Figure 2.1 - Field orientation and plot layout for 2019 (left) and 2020 (right). Different colored plots indicate different cover crop treatments, green for cereal rye, red for the cereal rye-crimson clover mixture, and tan for the winter fallow. Inset illustration is an example of the plot layout between the center two maize rows for plots with litterbags present.

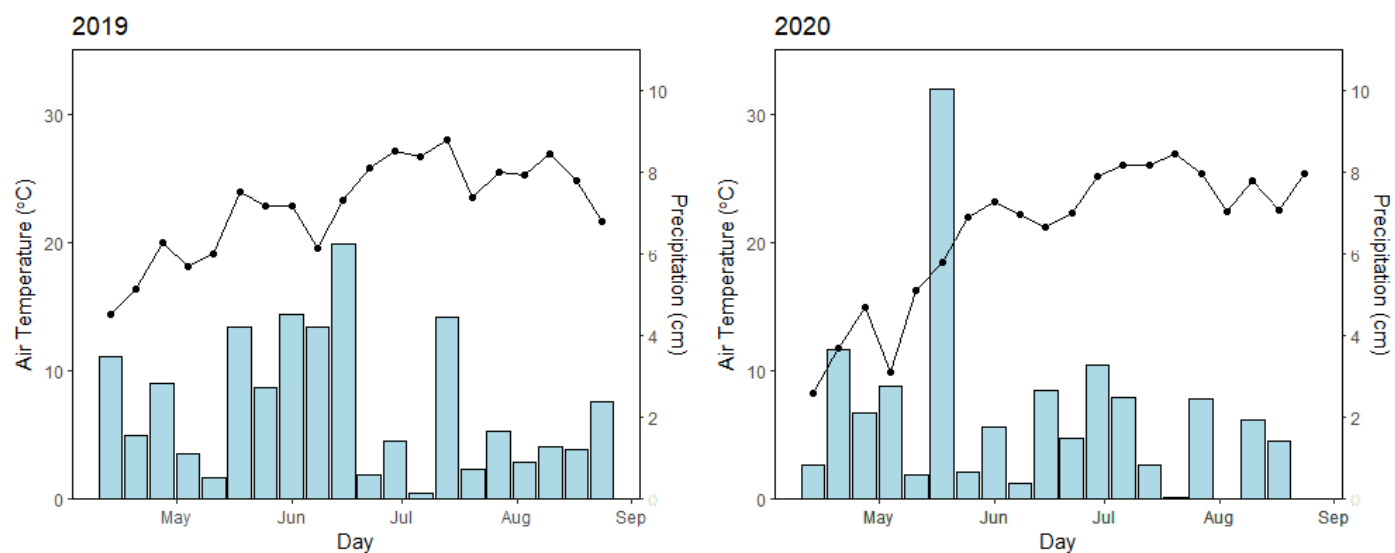


Figure 2.2 - Weather data for the growing season in 2019 (left) and 2020 (right) collected by the UK Ag Weather Station at Spindletop Farm. Blue bars indicate the cumulative weekly rainfall (cm). Connected points indicate the average weekly temperature.

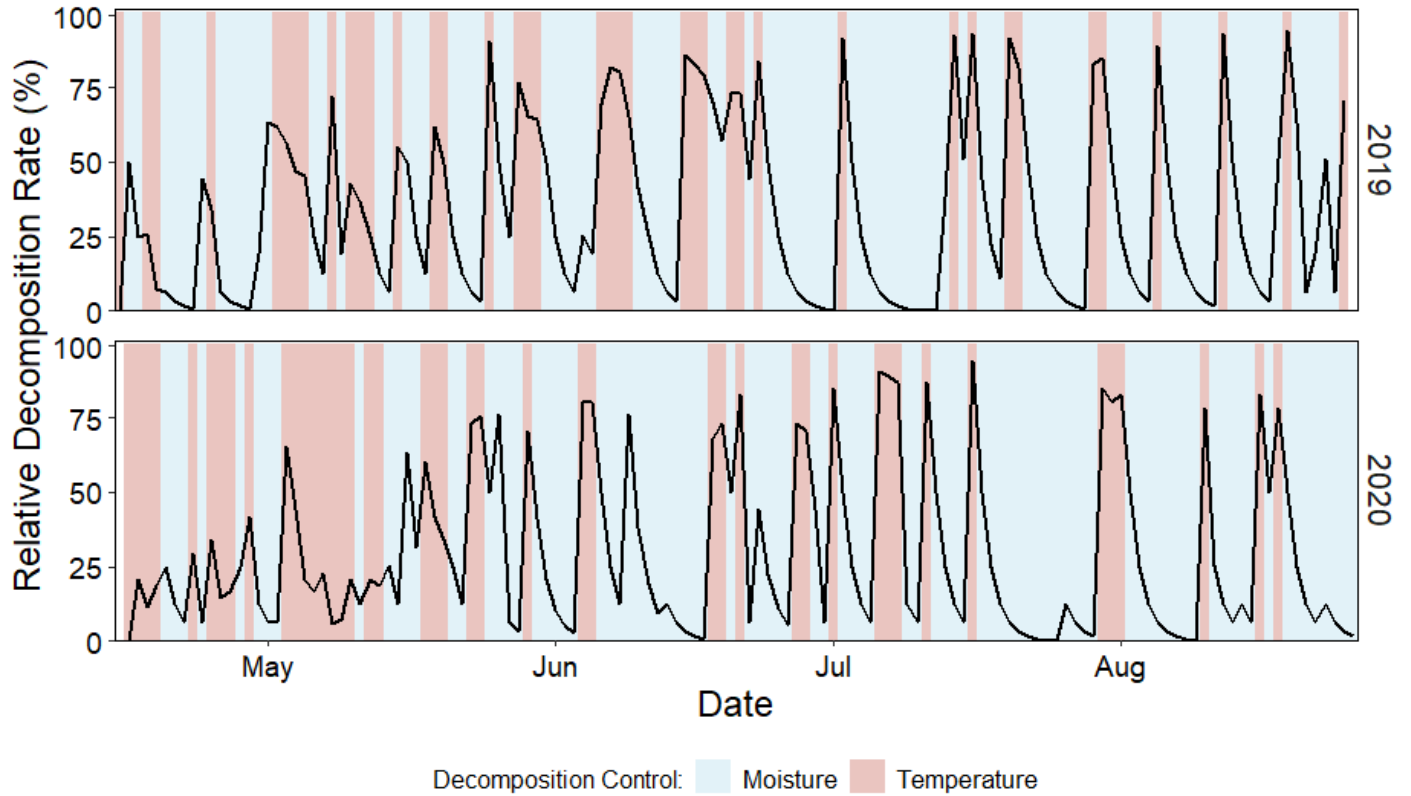


Figure 2.3 - Relative decomposition rate compared to optimum environmental conditions, calculated using the DCD model from Steiner et al. (1999). Shading indicates dominant decomposition control on a given day; red for temperature limitation and blue for moisture limitation. Black line represents the lower value of the two coefficients and indicates how quickly decomposition is occurring relative to optimum temperature and moisture conditions.

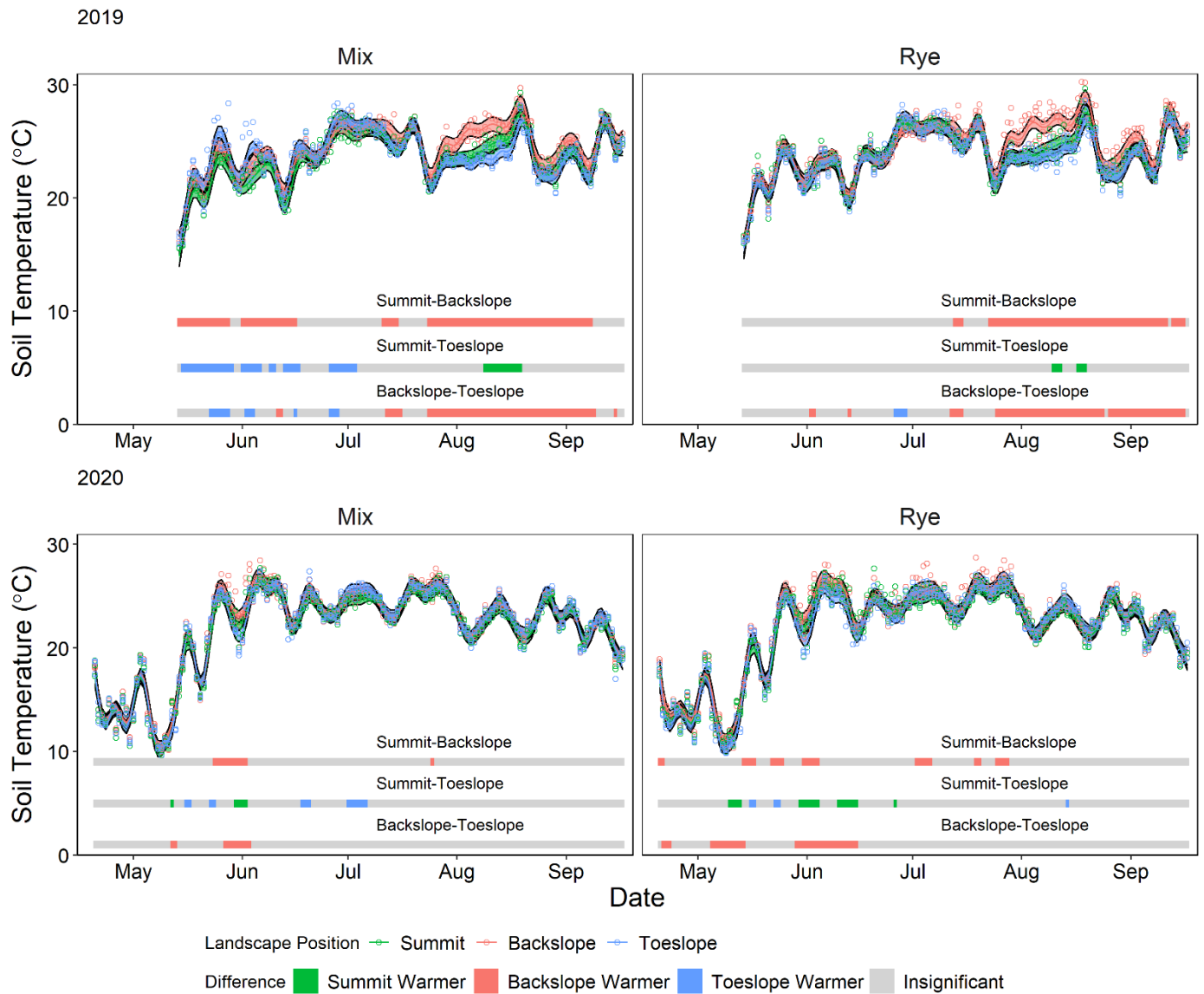


Figure 2.4 - Soil temperature at 5 cm depth throughout the corn growing season for mixture (left) and rye (right) treatments, at each landscape position. The top panels reflect the 2019 growing season, the bottom panels reflect the 2020 growing season. Horizontal bars indicate the results of GAM analysis and indicate significant differences within a given pairwise comparison. Ribbons surrounding the predictions indicate the 90% confidence interval.

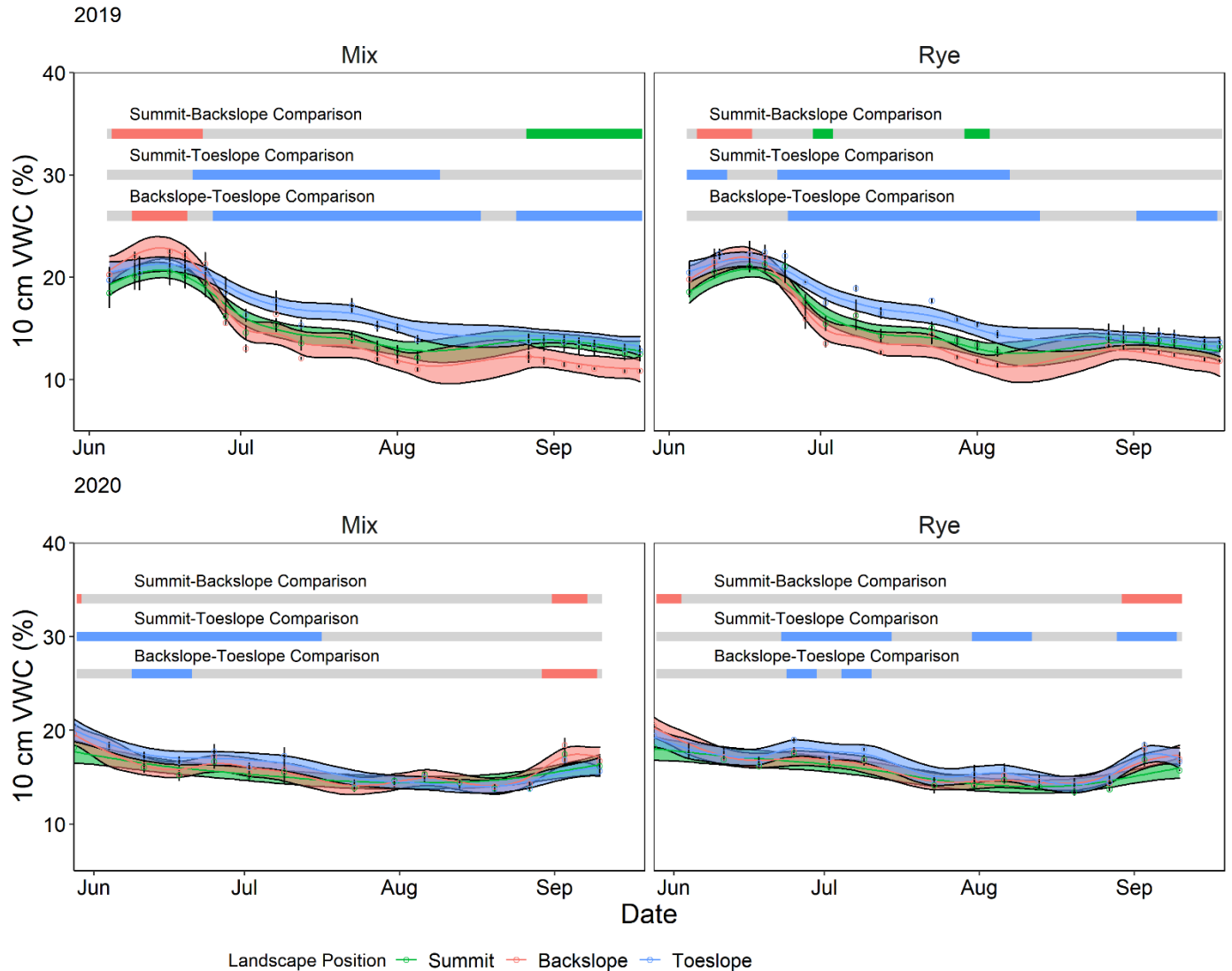


Figure 2.5 - Soil volumetric water (0-10 cm) taken weekly throughout the corn growing season for mixture (left) and rye (right) treatments, at each landscape position. The top panels reflect the 2019 growing season, the bottom panels reflect the 2020 growing season. Horizontal bars indicate the results of GAM analysis and indicate significant differences within a given pairwise comparison. Ribbons surrounding the predictions indicate the 95% confidence interval. The points indicate the average of three measurements on each sampling date, error bars are ± 1 SE.

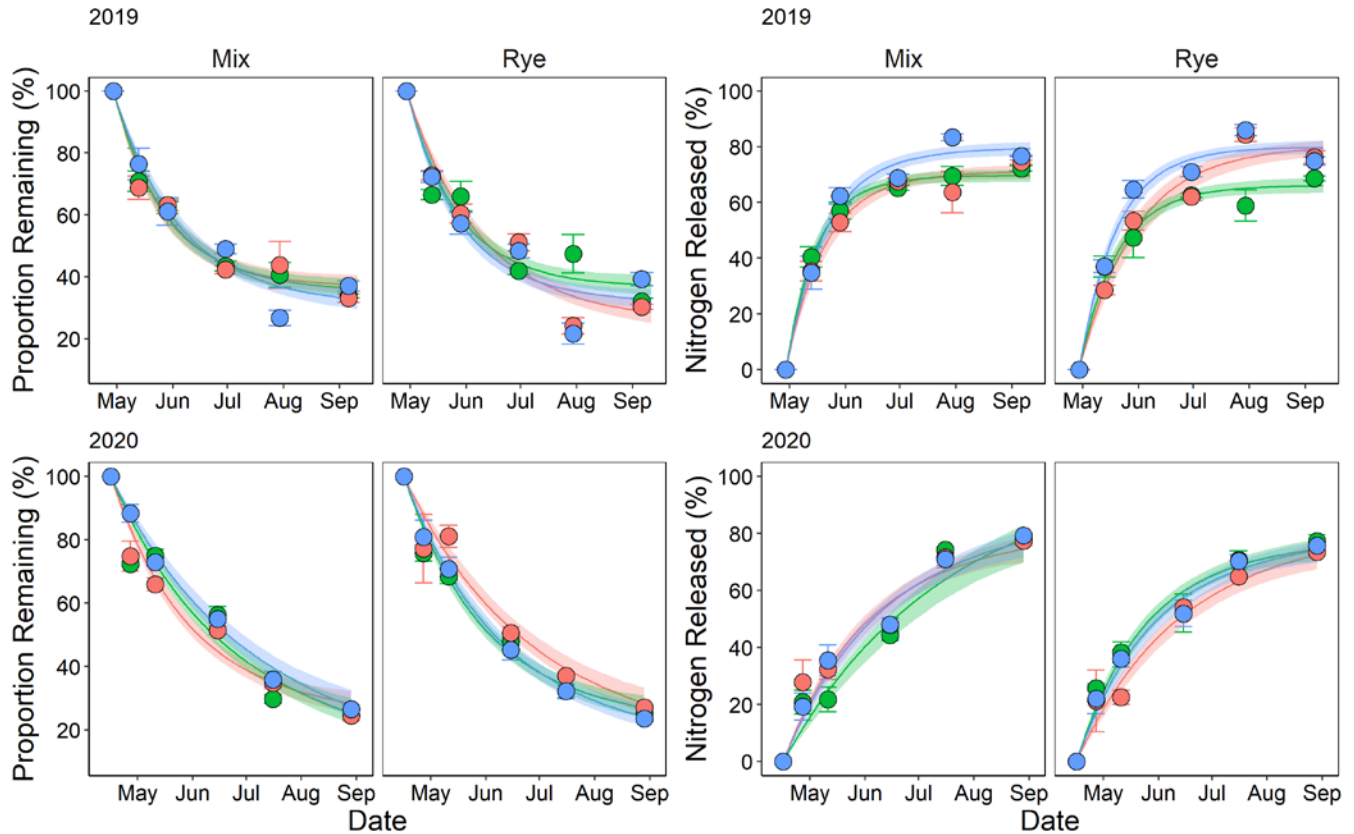


Figure 2.6 - Left: Proportion of cover crop residue remaining measured in both cover crop treatments at removal dates (circles) and predictions from non-linear models in the 2019 (upper left) and 2020 (bottom left) growing season. Right: Cumulative proportion of N released from the cover residue measured in both cover crop treatments at removal dates (circles) and predictions from non-linear models for the 2019 (upper right) and 2020 growing season (bottom right). Ribbons around predictions indicate the prediction standard error.

Table S2.1 - Model fitting assessment values for proposed time scales for litter decomposition

Field	Analysis	Time Scale	AIC	BIC	Log Likelihood
LNP_ST1	Mass Loss	Natural Days	-215.34	-175.25	122.67
LNP_ST1	Mass Loss	Growing Degree Days	-206.87	-166.78	118.44
LNP_ST1	Mass Loss	Decomposition Days	-205.58	-165.49	117.79
LNP_ST1	Nitrogen Release	Natural Days	-243.74	-203.64	136.87
LNP_ST1	Nitrogen Release	Growing Degree Days	-241.50	-201.41	135.75
LNP_ST1	Nitrogen Release	Decomposition Days	-240.82	-200.72	135.41
LNP_ST2	Mass Loss	Natural Days	-230.01	-189.92	130.01
LNP_ST2	Mass Loss	Growing Degree Days	-203.41	-162.95	116.52
LNP_ST2	Mass Loss	Decomposition Days	-234.81	-194.72	132.40
LNP_ST2	Nitrogen Release	Natural Days	-191.50	-151.41	110.75
LNP_ST2	Nitrogen Release	Growing Degree Days	-168.4	-128.31	99.20
LNP_ST2	Nitrogen Release	Decomposition Days	-199.94	-159.84	114.97

Table S2.2 - Total accumulated growing degree days (sGDD) calculated from soil temperature at each landscape position.

Year	Landscape Position	Accumulated sGDD
2019	Summit	3019
2019	Backslope	3094
2019	Toeslope	3010
2020	Summit	2852
2020	Backslope	2899
2020	Toeslope	2862

Table S2.3 - Cover crop biomass production and R1 maize aboveground biomass at each landscape position in 2019 and 2020.

Year	Landscape Position	Cover Crop Biomass ¹				Maize R1 Aboveground Biomass ²			
		Rye		Mixture		Rye		Mixture	
		Mg ha ⁻¹	SE (Mg ha ⁻¹)	Mg ha ⁻¹	SE (Mg ha ⁻¹)	Mg ha ⁻¹	SE (Mg ha ⁻¹)	Mg ha ⁻¹	SE (Mg ha ⁻¹)
2019	Summit	3.43	0.54	3.65	0.61	10.9	0.89	11.4	0.64
2019	Backslope	3.34	0.46	3.28	0.35	9.1	0.98	9.2	1.38
2019	Toeslope	2.82	0.74	2.34	0.65	11.7	1.21	10.6	1.08
2020	Summit	4.26	1.20	2.28	0.26	11.8	0.58	12.3	0.45
2020	Backslope	3.07	0.44	3.67	1.10	12.2	0.33	11.8	0.76
2020	Toeslope	3.31	0.31	3.11	1.03	10.6	0.29	10.3	0.48

1- Cover crop biomass calculated from 0.25 m² samples taken ~1 week before chemical termination.

2- Maize biomass calculated from six plant destructive sampling at the R1 stage in either year, averaged across N rates.

Table S 2.4 - Proportion of original litter remaining and percentage of N released from position specific litterbags at the final removal date. No significant differences were present between treatments.

Year	Landscape Position	Proportion Remaining				Nitrogen Released			
		Rye		Mixture		Rye		Mixture	
		(%)	SE (%)	(%)	SE (%)	(%)	SE (%)	(%)	SE (%)
2020	Summit	27.3	1.23	24.3	1.53	75.0	1.57	78.7	2.1
2020	Backslope	25.3	1.73	24.5	1.15	77.3	2.05	77.5	0.5
2020	Toeslope	23.3	1.81	27.3	1.35	74.3	1.43	74.3	1.8

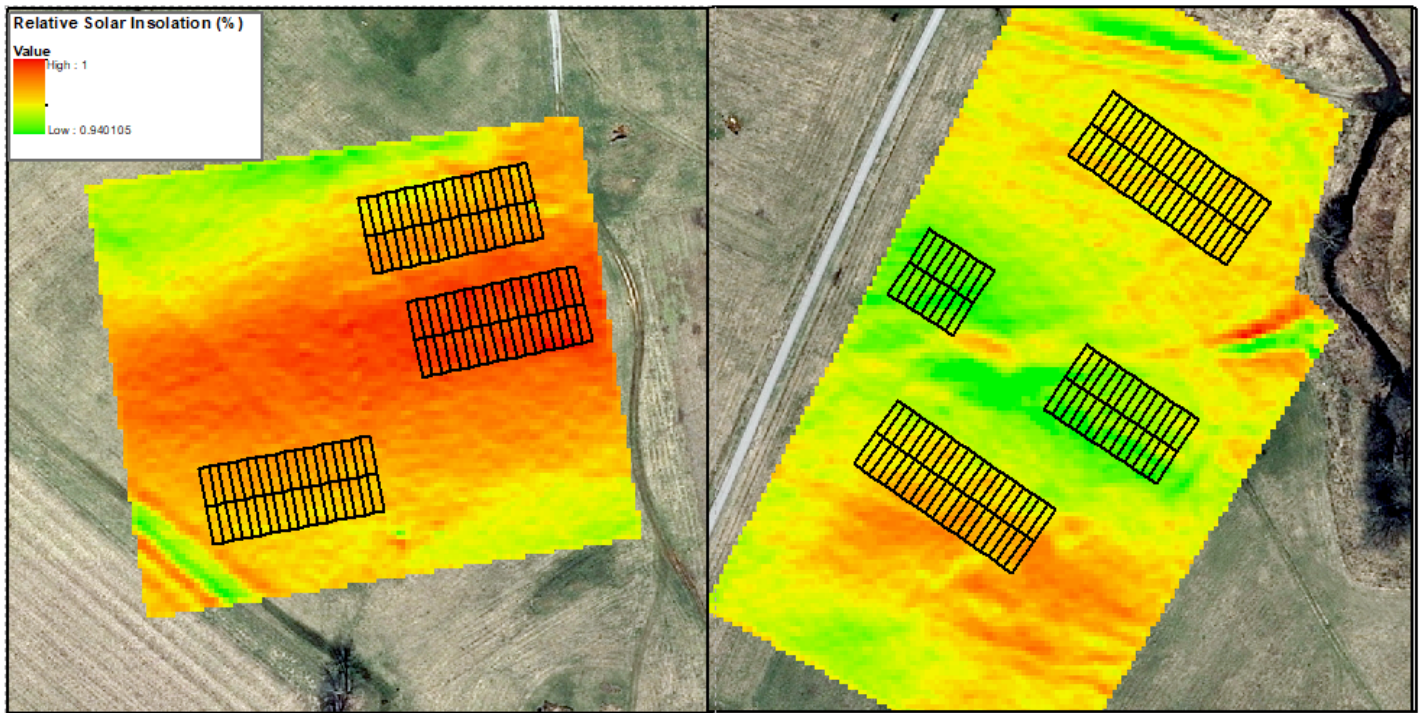


Figure S2.1 - Relative solar insolation (%) for the period of time litterbags were deployed in the field for 2019 (left) and 2020 (right).

CHAPTER 3. WEATHER DEPENDENT RELATIONSHIPS BETWEEN TOPOGRAPHIC VARIABLES AND YIELD OF MAIZE AND SOYBEAN: A QUANTITATIVE REVIEW

3.1 Abstract

The yield response of row crops to landscape topographic factors has been well documented in the literature, but the spatial pattern of this response is dependent on rainfall timing and amount. For example, low lying areas may be highly productive during drought years due to accumulation of water that has been transported downslope but may become flooded and low yielding during wet years. This review synthesizes the research surrounding relationships between topography and crop yield in two major row crops, maize (*Zea mays* L.), and soybean (*Glycine max* (L.) Merr), to determine how weather conditions affect the relationships between yield and topographic factors, such as slope, elevation, and curvature. We identified 10 studies that examined yield response to topography, which provided correlations between yield and topographic variables for up to 59 individual site-years. We then assessed the response of yield-topography correlations to the spring, critical period, and total growing season precipitation. The correlations between yield and slope, yield and elevation, and yield and planar curvature were generally negative but became weaker or even positive with increasing growing season precipitation and critical season precipitation in maize. However, the correlations between soybean yield or soybean yield variability and topographic factors did not show any significant pattern with increasing precipitation. Our results indicate that the relationship between topography and yield is highly dependent on weather in maize but that the response of soybean yields to topographic variables is consistent across weather conditions. A better understanding of the drivers of interannual variability in row crops

grown in areas of complex topography will help to inform future research in these areas and should be considered when managing crops in rolling hill environments.

3.2 Introduction

Rolling hill topography is a common feature in agricultural land across the Central and Southeastern United States. With sloping land comes a number of challenges, including erosion, shallow soils, and a risk of nutrient loss to the environment. Hydrologic and geomorphic processes operating on hillslopes, exacerbated by anthropogenic activities such as cultivation and machine traffic, can give rise to the development of a mosaic of low and high productivity zones interspersed throughout a given production field.

Additional complexity is added when a temporal element is considered, as these productivity zones are not consistent through time (Martinez-Feria and Basso, 2020).

Abnormally wet years may penalize low lying positions as root growth is inhibited by oxygen limitation and soil saturation via water accumulation from upslope positions and shallow water tables (Wankert et al., 1981), while upslope positions may perform well during wet years, but rapidly become water stressed from low soil water storage during dry years. In essence the capacity for producing high yields that are stable over both space and time decreases with increasing landscape heterogeneity (Basso et al., 2019). As such, we need a better understanding of how topography affects yield under different weather conditions to improve the management of rolling hill systems for high and productivity.

Since the introduction of yield mapping in the early 1990s, several researchers have investigated the relationship between observed crop yield and soil and landscape characteristics using Geographic Information System (GIS) tools (Green and Erskine,

2004; Kravchenko et al., 2005; Kumhalova et al., 2011; Singh et al., 2019). Several different metrics and indices have been evaluated as predictors of crop yield, such as slope, landscape position, topographic wetness index (TWI), surface curvature, and upslope area, each performing well in some instances and failing to correlate in others (Chi et al., 2009; Huang et al., 2008; Kravchenko and Bullock, 2000; Thelemann et al., 2010; Wendroth et al., 2003). Although studies have been performed at different scales, ranging from regional (Maestrini and Basso, 2018b), to watershed (Singh et al., 2019), down to the field level (Thelemann et al., 2010) here we focus on the field level studies, with site specific weather conditions. Throughout the course of a two to three-year field study, expecting to capture the full range of interactions between topography and weather conditions is unrealistic. As such, field studies have the potential to be limited in the scope of their inference as to yield – topography traits under different climate conditions, but broader patterns can emerge when several studies are examined in concert.

Although spatial variability in yield is inevitable, a better understanding of the drivers of variability will allow tailored management practices that limit nutrient loss and increase total cropping system efficiency. Here, using the published scientific literature, we explore the relationship between topographic variables and yield across a variety of edaphic and climatic environments. Our goal is to determine how precipitation affects the spatial patterns in crop yield by evaluating published research from the primary agricultural regions of the United States.

3.3 Materials and methods

A search of agricultural scientific literature was conducted using Google Scholar and the Agricola database using the key words, “topography”, “yield”, “slope”, “landscape

position”, “elevation differences”, “spatial variability”, and “field variability”. The suitability of individual research articles was then evaluated based on their inclusion of correlations between yield and at least one topographic variable (i.e., slope, elevation, planar curvature, or profile curvature (**Table 3.1**). We focused our analysis on the major warm-season crops of the central US, maize and soybean, and limited the scope to systems under rain-fed conditions. The correlation coefficients between crop yield and topographic variables for each site-year of each study were compiled into a single spreadsheet. After the initial review of the literature, precipitation data were compiled for each site-year based either on reported data or publicly available data from the region (e.g., NOAA data, local Mesonet data, etc.). To investigate the role that timing of rainfall played in driving yield-topography relationships throughout the season, the precipitation data were further separated into three discrete precipitation categories: spring precipitation, growing season precipitation, and critical period precipitation. The springtime was defined as the period between March through May, the period during which the majority of full season maize and soybean are planted and emerge in the Northern Hemisphere. The growing season was defined as the beginning of March through the end of August. The critical period was defined as the months of July and August, the time during which the majority of maize in the Northern Hemisphere is entering the pollen drop and grain filling stages of development and drought stress can be most detrimental to maize and soybean yield components (Abendroth et al., 2011; Desclaux et al., 2000).

Linear mixed models were used to determine the effect of crop species, i.e., maize or soybean, on the correlation coefficients, with “study” included as a random effect. An

additional mixed model was used to determine whether the method of correlation analysis (i.e., Spearman vs. Pearson) had a significant effect on correlation significance.

Observing no effect of correlation methodology, we elected to pool these correlation coefficients when calculating means and performing linear regression. The correlation coefficients for the yield-topography variable for each of the site years were then regressed against the total rainfall in each of the three precipitation categories to ascertain the conditions under which spatial topographic variability was the greatest driver of total yield variability. These regressions were used to generate Pearson correlation coefficients and test for the significance of linear trends between rainfall and the correlation coefficients of topography vs. yield relationships. To assess the spatial variability of yield withing a given site year, we calculated the coefficient of variation (CV) for yield in all studies where the necessary data was present. We assessed the relationship with total spatial variability (i.e., CV) with increasing precipitation using linear regressions in the same manner described for yield-topography correlations. Statistics were performed in R using the lme4 package (Bates *et al.*, 2014; R Core Team, 2020). Because integrating data from a diversity of production settings generated high variability in the correlation coefficients, an alpha level of 0.10 was used to assess statistical significance.

3.4 Results and Discussion

We found ten studies that fit our criteria (2 theses and 8 peer-reviewed articles; **Supplemental Table S3.1**), for a total of 59 possible site years. Studies ranged across the central and southeastern United States and represented the majority of the major row crop production areas in the US. Due to variable reporting of the topographic factors of

interest, the number of site years varied for each crop yield – topography combination (**Table 3.2**).

Across the studies surveyed, the average soybean yield was 3.06 Mg ha^{-1} , with values spanning from $1.67 - 3.97 \text{ Mg ha}^{-1}$. The average CV of soybean yield across site-years was 22%. The lowest CV in any study of soybean yield was 8.5%, and the highest was 47%. Soybean yield and soybean yield CV were not significantly related to the total growing season precipitation (p-value = 0.4925 and 0.8432, respectively) (**Figure 3.1**).

The average reported maize yield was 9.11 Mg ha^{-1} , with a range of $5.02 - 14.22 \text{ Mg ha}^{-1}$. The maize yield CV was similar to that observed in soybean; the average CV across all studies was 21%, the minimum CV was 9.5%, and the maximum 43%. Linear regression of reported maize yield against total growing season precipitation indicated a slight negative relationship (slope = $-0.003 \text{ Mg mm}^{-1}$, p-value = 0.04). The CV of maize yield was also significantly correlated to growing season precipitation; CV increased as the total cumulative growing season precipitation increased (p-value = 0.0149, **Figure 3.1**).

The average slope reported in the studies we surveyed was 1.4° , the minimum was 0.23° , and the maximum was 5.00° . Both maize and soybean showed significant negative relationships with increasing slope, though only 5 of the site-years surveyed in the studies presented here had an average slope $> 3^\circ$. When these studies were removed from the analysis, the relationship between total yield and slope was not significant. **Table 3.2** shows the average reported correlations between yield and selected topographic variables across all studies surveyed. Averaged across studies, there were significant negative correlations between maize yield and elevation, slope, and profile curvature. The

correlations between soybean yield and elevation and slope were numerically negative though less strong than those for maize and not statistically significant.

The negative correlations for maize show that, on average, low-lying areas tended to yield higher relative to higher elevations areas within a field. Additionally, as slope and concavity along the primary sloping surfaces increased, average yield decreased. Soil water availability likely explains these relationships, at least in part. Eroded landscape positions tend to have lower soil water storage, due to the loss of fine and medium sized particles and soil organic matter through erosion (Brubaker et al., 1990; Rosenbloom et al., 2001), shallower soil depth relative to depositional environments, and possibly greater potential evapotranspiration due to greater amounts of solar radiation, depending on aspect (Hanna et al., 1982). Additionally, lateral subsurface flow may direct mobile soil nutrients such as inorganic N downslope causing nutrient stress in a non-nitrogen fixing crop on the upslope positions and high nutrient supply in the receiving downslope positions.

For maize, the relationships between the yield-topography correlation and cumulative precipitation during critical period and total growing season precipitation were positive, indicating that the negative correlation between yield and slope, elevation, and curvature, became weaker or even positive with increasing rainfall (**Figures 3.1 and 3.2**). The yield-slope correlation was also positively related to springtime precipitation, but no other significant relationship between yield-topography correlation and spring precipitation was observed for maize. In the studies that we identified that investigated soybeans, the yield-topography correlations were less responsive to precipitation in general (**Figures 3.1 and 3.2**). However, yield-elevation and yield-profile curvature correlations were

negatively correlated with increasing springtime precipitation, and the yield-elevation correlation was negatively correlated with growing season precipitation (**Figure 3.1**). With that said, an examination of leverage of points in the linear regression of yield-profile curvature correlation vs. springtime precipitation indicated that three observations drove the response, and thus more data are needed to confirm that relationship (**Supplemental Figure S3.1**).

Our analysis shows that maize and soybean have similar coefficients of variability within a given field, which aligns with the results of previous examinations of yield variability in the literature (Khakural et al., 1996; Smith et al., 2007; Williams et al., 2008). However, our analysis of yield-topography correlations reveals that variability of maize yield is more predictable based on topography than that of soybean yield. Moreover, the correlation between yield and topographic variables appears to be more dependent upon precipitation for maize than soybean (**Figure 3.2**). These differences in spatiotemporal yield response between species may be a reflection of differences in the two species' responses to water and other soil resources. For example, soybeans are generally less sensitive to water deficit, water storage, and solum thickness and more sensitive to soil water-saturated conditions than maize (Khakural et al., 1996; Sadras and Calviño, 2001; Williams et al., 2008). In addition, since soybeans fix their own N, they are less responsive to soil N supply and mineralizable soil organic matter content than maize (Williams et al., 2008). Soybeans are expected to show less of a yield increase than maize in low-lying positions where soil water storage, solum thickness, water-saturated conditions, and soil organic matter content tend to be high, whereas these areas are highly unstable for maize yield—high yielding in drier years, and low yielding in wet years.

Further, soybeans are more sensitive than maize to soil properties that do not predictably vary with topography such as pH, iron, and potassium deficiency (Kaspar et al., 2004).

Thus, it is logical that topographic variables and their interaction with precipitation explained less of the variation in soybean yield than maize yield in our analysis.

Spring precipitation has been posited as an important control on productivity in topographically complex settings, with high levels of spring precipitation limiting germination in depressional areas and causing stand loss (Maestrini and Basso, 2018b).

However, we did not observe a significant relationship between yield-topography correlations and cumulative spring precipitation, indicating early season stand loss did not occur to a significant level in the studies we surveyed. This could be because our range of spring precipitation data did not include possible flooding conditions, or that the variable surveyed did not totally capture the landscape scale effects of increased precipitation at planting. Additionally, it is possible that plot scale research studies do not fully capture the range of conditions in a producer's field and/or are more intensively managed to avoid crop failure.

Two of the studies surveyed here presented data concerning flow length or flow accumulation correlations with yields but did not constitute a large enough sample size to derive meaningful inferences. Da Silva and Silva (2008) highlight some of these secondary topographic variables as crucial to furthering our understanding of crop response to landscape complexity, as they often better capture the redistribution of water across the landscape and can highlight areas of accumulation that slope and elevation alone cannot. The employment of these complex variables such as flow length, topographic wetness index and other model-based wetness indices that have the ability to

incorporate downslope movement and variable contributing areas will likely continue to improve our understanding of landscape scale crop/topography/water dynamics beyond the variables presented here.

3.5 Conclusions and Implications

There continues to be a growing interest by researchers and agricultural practitioners in creating management zones within crop fields to minimize inputs and maximize yield. In the data presented here, we observed that most commonly analyzed terrain attributes, such as slope, elevation, and curvature, were negatively correlated with yield. However, in maize cropping systems we observed a decrease in the strength of the correlation with increasing growing season precipitation, as well as moderately increased spatial variability in yield. Our analysis of topography by weather interactions showed that the strength of the yield-topography correlation was predicted better by cumulative total growing season and critical period precipitation than springtime precipitation. Thus, in maize-soybean cropping systems that are dominant across the US Midwest and Southeast, overall return may be maximized by using terrain attributes to define management zones during the maize period of the rotation, particularly in low-rainfall settings. Management adaptations including planting drought resistant hybrids, decreasing planting population, and varying the nutrient application rate on sloping upland positions could safeguard against the detrimental effects of complex topography, and stabilize yields in these rolling hill systems.

3.6 Chapter 3 tables and figures

Table 3.1 – Definitions of key topographic variables considered in this analysis

Variable	Definition
Slope	Steepness of each cell on a raster surface, given in either degrees of percent of slope (i.e. $\frac{Rise}{Run} \times 100$)
Elevation	Height values of each cell across a raster surface, typically derived from DEM or LiDAR data.
Planar Curvature	The shape of a given slope when viewed perpendicular to the direction of maximum slope. Planar, also called plan or planform curvature, indicates the convergence or divergence of flow across a surface. Values of zero indicate no lateral curvature, positive values indicate convex lateral curvature, and negative values indicate concave lateral curvature.
Profile Curvature	The shape of a given slope when examined parallel to the direction of maximum slope. Profile curvature controls the acceleration of flow across a sloped surface. Positive values indicate a slope that is upwardly concave, accelerating flow. Negative values indicate a slope that is upwardly convex, decelerating flow. Values of zero indicate a linear surface with no effect on flow acceleration.

Table 3.2 - Average correlation coefficients (r), and p-values between selected topographic variables and crop yield from reviewed studies. Significant p-values (bolded correlation coefficients) presented indicate if the correlation coefficient between yield and a given topographic variable was significantly different than zero. Planar curvature was omitted for soybean because the minimal data requirement was not met.

		Elevation	Slope	Planar Curvature	Profile Curvature
Maize	Mean r	-0.169	-0.184	-0.245	-0.190
	p-value	0.022	0.067	0.325	0.008
	Site years	57	55	40	46
Soybean	Mean r	-0.158	-0.04	-	-0.113
	p-value	0.596	0.454	-	0.021
	Site years	59	54	-	38

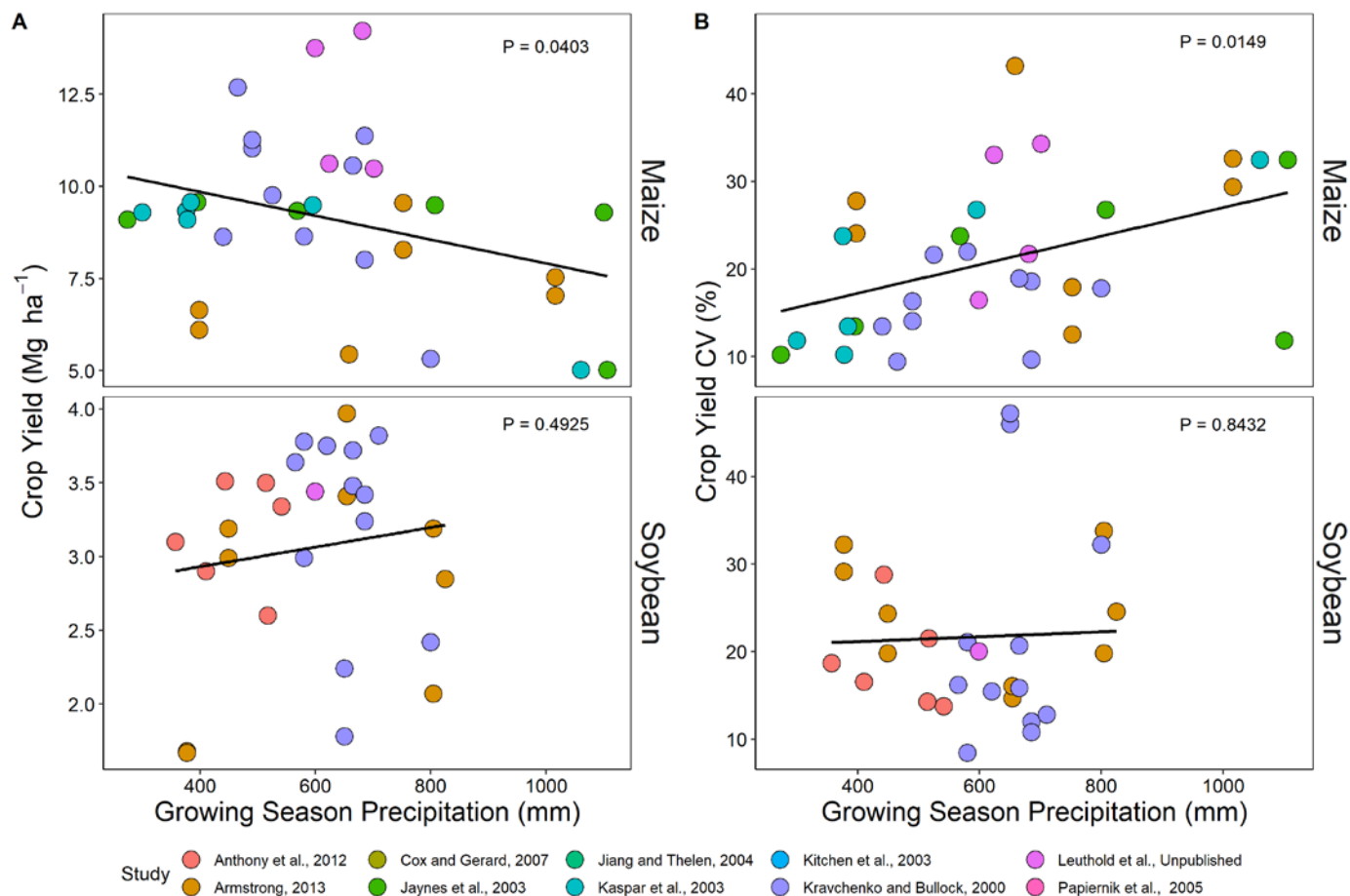


Figure 3.1 – Crop yield (A) and crop yield variability (B) with increasing precipitation. Different points represent observations from an individual site year, while different colors represent the different studies considered in this analysis. Relationships were not significant for soybean, but were significant for maize.

	Corn				Soybean			
Spring Precip.	-0.014 0.9391	-0.005 0.9842	-0.11 0.6263	0.3 0.1012	-0.316 0.0498	-0.267 0.4016	-0.584 0.0087	-0.195 0.2608
Growing Season Precip.	0.349 0.0463	0.593 0.0156	0.152 0.4992	0.607 < 0.001	-0.381 0.0166	-0.288 0.3633	-0.307 0.2007	-0.117 0.502
Critical Period Precip.	0.541 0.0012	0.558 0.0246	0.163 0.4682	0.607 < 0.001	-0.11 0.5048	0.128 0.6926	0.327 0.1722	0.156 0.3695
	Elevation	Planar Curvature	Profile Curvature	Slope	Elevation	Planar Curvature	Profile Curvature	Slope

Figure 3.2 – Correlation matrix of yield vs. topography correlations and precipitation categories. The center number indicates the correlation between correlations coefficients and precipitation, with color indicating the direction of the relationship (red: negative, green: positive). The lower number is the p-value of the linear regression.

Table S3.1 - Studies included in the analysis, including number of site years, crop species, regions, and correlation type used. Xs in the topographic attribute columns indicate that a correlation between yield and topographic factor was present in that study.

Study	Crop	Region	Site Years	Correlation Type	Elevation	Slope	Planar Curvature	Profile Curvature
Anthony et al., 2012	Soybean	Minnesota	6	Pearsons	X	X		
Armstrong, 2013	Maize	Illinois	2	Pearsons	X	X		
Armstrong, 2013	Maize	Indiana	5	Pearsons	X	X		
Armstrong, 2013	Soybean	Illinois	2	Pearsons	X	X		
Armstrong, 2013	Soybean	Indiana	7	Pearsons	X	X		
Cox and Gerard, 2007	Soybean	Mississippi	12	Spearman	X	X	X	X
Jaynes et al., 2003	Maize	Iowa	6	Spearman	X	X	X	X
Jiang and Thelen, 2004	Maize	Michigan	4	Unknown	X			
Kaspar et al., 2003	Maize	Iowa	6	Unknown	X	X	X	X
Kitchen et al., 2003	Maize	Missouri	1	Pearsons	X	X		X
Kitchen et al., 2003	Soybean	Kansas	1	Pearsons	X	X		X
Kitchen et al., 2003	Soybean	Missouri	2	Pearsons	X	X		X
Kravchenko and Bullock, 2000	Maize	Illinois	7	Pearsons	X	X		X
Kravchenko and Bullock, 2000	Maize	Indiana	3	Pearsons	X	X		X
Kravchenko and Bullock, 2000	Soybean	Illinois	8	Pearsons	X	X		X
Kravchenko and Bullock, 2000	Soybean	Indiana	4	Pearsons	X	X		X
Leuthold et al., 2021*	Maize	Kentucky	4	Pearsons	X	X	X	X
Papiernik et al., 2005	Soybean	Minnesota	1	Pearsons		X		

*: Description of the methods of maize planting, maize harvest, and other field operations for Leuthold et al., 2021 are described in the Appendix.

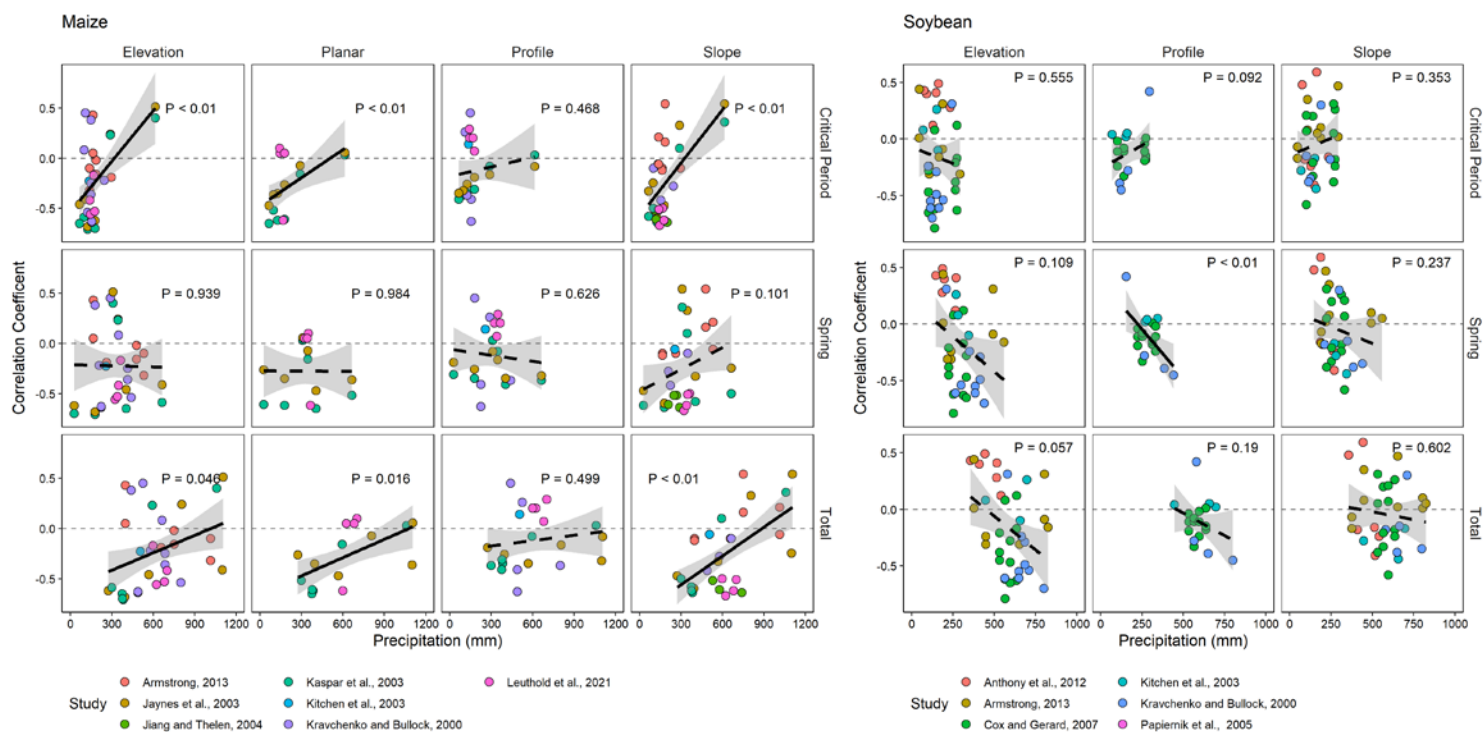


Figure S3.1 - Linear regressions of correlation coefficients between yield and topography characteristics (i.e., elevation, planar curvature, profile curvature, and slope), and cumulative precipitation during the three precipitation categories. Different points represent different site years, while different colors indicate different studies. The shaded area indicates the 90% confidence interval.

CHAPTER 4. COVER CROPS DECREASE MAIZE YIELD VARIABILITY IN SLOPING LANDSCAPES THROUGH INCREASED WATER DURING REPRODUCTIVE STAGES

4.1 Abstract

Rolling hill style topography is a common feature of agricultural land throughout the United States. Topographic complexity causes subfield variation in soil resources such as water and nutrients, leading to a mosaic of high- and low-productivity zones that can shift from one year to the next due to weather. Stabilizing yields across these productivity zones using agroecological methods may improve land use efficiency, prevent unnecessary cropland expansion, and reduce the environmental impact of these systems. Here, we hypothesized that cover crops may help to reduce soil water and nutrient losses and increase the stability of subsequent maize yields across time and space. We performed a field study to evaluate the effect of a cereal rye (*Secale Cereale* L.) cover crop on maize (*Zea mays* L.) yield at three landscape positions (summit, backslope, and toeslope) in Central KY in 2018-2019, and calibrated the DSSAT v4.7.0.001 computer simulation program to test our hypothesis across a thirty-year period. Our field trial showed pronounced variability in maize yield across different landscape positions, ranging from 6.3 Mg ha⁻¹ in the backslope, to 12.2 Mg ha⁻¹ in the toeslope. Model simulations were consistent with results from our field trial and indicated that low yields in the backslope were primarily due to water stress, with >10% yield reductions in 17 out of 30 simulated years relative to simulations under irrigated conditions where water was not limiting. In contrast, the toeslope and summit positions experienced >10% yield reductions due to water stress in only six of the 30 years. Growing a cereal rye cover crop before maize reduced the frequency of water stress and raised maize yields in the

backslope by 6% (500 kg ha^{-1}) on average, and 24% (1235 kg ha^{-1}) during dry years. The coefficient of variation across all weather conditions and landscape positions was reduced from 33% to 26% when maize followed a rye cover crop compared to fallow. The yield benefits of the cover crop were associated with decreased soil evaporation and runoff that increased water availability during anthesis and late maize reproductive phases. Crop model simulations allowed us to evaluate and parse out the fundamental drivers of the interaction between cover crops and complex topography under different weather scenarios. Overall, our study demonstrates the outsized potential of cover crops to increase and stabilize grain yields in rolling hill landscapes and emphasizes the value of cover crops as a tool for ecological intensification.

4.2 Introduction

Much of the rainfed crop production area of the United States is characterized by topographic variability. In complex terrain, downslope movement of fertile topsoil over time can decrease soil depth and fertility at upslope positions while increasing it in low-lying positions. In addition, low elevation landscape positions often have a water table closer to the soil surface, which slows decompositions and promotes soil organic matter accumulation. Variation in soil resources due to topographic effects can directly impact crop growth (Corre et al., 2002). Previous field-scale research has indicated that landscape position can explain up to 60% of spatial yield variability (Jiang and Thelen, 2004). A recent satellite-based regional analysis of crop yields demonstrated that sub-field variability in soil characteristics and topography is often more important than

management in explaining yield variability throughout the Central US (Lobell and Azzari, 2017).

The impact of topographic setting on crop yield varies from year to year in response to weather conditions (Kravchenko and Bullock, 2000; Kumhalova et al., 2011; Maestrini and Basso, 2018b). The accumulation of water in depressional areas gives rise to relatively high productivity during low-rainfall years, but can also lead to reduced yields via delayed emergence, decreased root growth, and nutrient uptake during wet years (Wankert et al., 1981). Conversely, crops grown in summit and sloping positions can be highly productive during wet years but experience water stress much earlier than foot- and toeslope positions during dry years due to lower soil water storage capacity and downslope losses. For instance, a study of grain yield response to landscape position in shallow, claypan soils indicated maize yields were significantly lower in backslope position than in the summit and toeslope during select years of the study. Further, the coefficient of variation for maize yields over time was 10 percent higher in maize grown on the backslope, compared to the deeper toeslope positions (Yost et al., 2016). Analyses of large-scale spatial datasets of the Central US indicate that 28% of active farmland, largely depressions and sloping uplands, can be classified as unstable, with yields varying by up to 33% from year to year (Basso et al., 2019; Martinez-Feria and Basso, 2020).

Spatiotemporal crop yield variability poses economic and environmental challenges. Yield loss in unstable zones costs an estimated 535M USD per year in lost production (Martinez-Feria and Basso, 2020). Additionally, low N use efficiency in heterogeneous cropland poses a risk to downstream ecosystem sustainability. When low yielding areas are fertilized at the same rate as high-yielding areas, fertilizer is at risk of not being taken

up by plants and instead being transported downstream, causing harm to the environment (Basso et al., 2016; Vitousek et al., 2013). The instability in spatial yield patterns from one year to the next make it challenging to predict economically and environmentally optimum N fertilizer rates for different areas within the same field. From the Central US alone, annual fertilizer loss from unstable cropland costs 485M USD, and adds 1.12 Tg of reactive N to the environment (Basso et al., 2019). The inefficiencies in nutrient cycling and water use that arise in areas of rolling cropland provide an opportunity to intensify agricultural production; if yields can be stabilized and nutrients conserved, these areas have potential to increase economic and environmental sustainability.

Ecological intensification aims to sustain or increase yields while reducing environmental impact by managing ecological processes (Bommarco et al., 2018, 2013). Cover crops may provide an avenue for ecological intensification of rolling cropland. By protecting topsoil against erosion, retaining soil nutrients, and creating a residue that conserves soil moisture (Kaye and Quemada, 2017), cover crops can reduce environmental impact while making cash crops less sensitive to topographic and weather variation. Working at the scale of a typical crop field, Munoz et al. (2014) found a cover crop was most beneficial for maize yield during dry years, and the positive effect was most pronounced in the summit and sloping positions of the landscape. Other multiple site-year studies have shown that cropping system diversification, which often includes cover crop integration, increases resilience to environmental stressors such as drought (Bowles et al., 2020; Gaudin et al., 2015). Thus, cover crops may offer a management option to sustain yields in the face of rising spatial yield heterogeneity (Lobell and Azzari, 2017) and weather variability (Wuebbles et al., 2017). However, because most assessments of

resilience occur post-hoc, the specific causes of the rotation effect remain poorly defined (Bennett et al., 2012; Bowles et al., 2020). Moreover, most research has been conducted in relatively uniform research plots that may misrepresent cropping system effects at field scale (Kravchenko et al., 2017).

Evaluating the role of cover crops in ecological intensification of rolling cropland requires several site-years of data on the rotation sequence, which are difficult to generate with field research alone due to time and cost constraints. Further, variables beyond the researcher's control, especially factors driven by weather such as the rate of biogeochemical processes, drainage, and crop evapotranspiration can vary dramatically and have large consequences on the results of two- to three-year long field trials. Well calibrated agricultural system models allow researchers to evaluate different management options across a range of environmental conditions. Crop models calibrated with data from empirically based-studies can integrate processes and study complex system dynamics to reveal management adaptations for the sustainable use of water (Dietzel et al., 2016; Ruíz-Nogueira et al., 2001; Saseendran et al., 2015; Singh et al., 2017), N fertilizer (Puntel et al., 2016; Salmerón et al., 2014; Sela et al., 2017), improving soil quality under competing uses of water (Chatterjee et al., 2020; Adhikari et al., 2017; Basche et al., 2016; Pinto et al., 2017), reducing environmental impact (Malone et al., 2017; Martinez-Feria et al., 2018, 2016) and increasing climate resilience (Battisti and Sentelhas, 2017; Sentelhas et al., 2015). There has been some application of process-based crop models to study sub-field variation in soil resources and spatially connected processes in complex topography (Albarenque et al., 2016; Basso et al., 2011; Basso and Ritchie, 2015; McNunn et al., 2019). However, crop model applications that focus on

cover crop management adaptations in rolling hill landscapes are still pending to our knowledge. Moreover, cover crop effects and optimal management recommendations are likely to be specific to edaphoclimatic conditions.

The goal of this study was to quantify the effect of a winter cover crop on maize yields and their variability over space and time, to evaluate the potential of this management adaptation in rolling hill terrain, and to inform future field experimental research and on-farm management decisions. We hypothesized that the addition of a cover crop would increase maize yields in particularly low-yielding settings by reducing crop water and N stress, thus reducing yield variability among landscape positions and among years. To test this hypothesis, we calibrated a cropping system model with data collected in 2019 in Lexington, KY from a winter fallow – maize system rotation with three landscape positions and different N fertilizer levels, and then conducted a simulation sensitivity analysis across 30 years (1989-2019) and two soil N fertility levels. By coupling field data and model simulations, we attempt to advance our knowledge of ecological intensification through cover crops in agroecosystems with complex terrain.

4.3 Materials and Methods

4.3.1 *Description of field trial*

From October 2018 through October 2019, a field trial was conducted to investigate the interactive effects of topography, cover crop use, and N fertilizer rate on maize yield. The trial took place at the University of Kentucky North Farm (38.123° N, -84.490° W), near Lexington, KY USA. The field site was selected to represent a hillslope setting found in producers' fields in this region. The topographic positions were delineated based on their elevation and slope (Figure 1). Soils at the summit position were classified as fine-silty,

mixed, active, mesic Typic Paleudalfs (Bluegrass series). Soils at the backslope position were classified as fine, mixed, active, mesic Mollic Hapludalfs (McAfee series). Soils in the toeslope position were classified as fine-silty, mixed, active, mesic Fluventic Hapludolls (Huntington series) (National Cooperative Soil Survey, 2020). The soils are formed in residuum of phosphatic limestone, which varies in depth by landscape position (depth to bedrock of 20 - 45 cm on the backslope, 100 cm on the summit, and >100 cm on the toeslope). Average annual precipitation at the site is 1088 mm and average annual temperature is 13.1 °C (1981-2010, <http://weather.uky.edu/>).

The field was in long term hay production prior to cultivation. In October 2018, the field was sprayed with glyphosate, moldboard plowed, and then disked to prepare the seedbed for the cover crop planting. Between April 2018 and April 2019, lime and potash were applied according to soil test results and University of Kentucky recommendations for optimum maize production. No other nutrients were considered suboptimal for maize growth according to the soil test.

The experimental plots were arranged in a split-split plot randomized complete block design, with three replications. The main plot factor was landscape position ($n = 3$), the sub-plot factor was cover crop treatment ($n = 2$), and the sub-sub-plot factor was N rate ($n = 4$) (**Figure 4.1**). A cereal rye cover crop was drill-seeded in the fall of 2018. Fallow plots were left bare throughout the winter, and weeds in these plots were not chemically controlled during cover crop growth. The cover crop was chemically terminated at the Feekes 7 growth stage (Knott, 2016), and left on the soil surface. Following cover crop termination, maize was no-till planted. Nitrogen fertilizer treatments consisted of four rates (0, 90, 180, and 270 kg N ha⁻¹), with 45 kg N ha⁻¹ applied at planting in all

treatments receiving N fertilizer, and the remainder applied at the V5 growth stage.

Further details concerning field management activities can be found in **Table 4.1**.

4.3.2 *Experimental data collection and analysis*

Two days prior to chemical termination of the cover crop, a random 0.25 m² aboveground biomass sample containing cereal rye and/or weeds was collected from each experimental unit (i.e., the sub-sub-plot level, n = 72). Maize biomass samples were collected at R1 (7/18/2019) by removing six plants from the center two rows in the plots receiving 0 kg N ha⁻¹ and 270 kg N ha⁻¹ (n = 36), and at R6 (9/11/2019), by removing eight plants from the center two rows of all plots (n = 72). All biomass samples were dried, weighed, ground, and analyzed for C and N concentrations via dry combustion. Maize biomass on an area basis was calculated based on the measured plant population from each plot. Maize grain yield was determined by hand harvesting ears from 6.1 m of the center two rows of each plot. Weight per ear, kernels per ear, and unit kernel weight were quantified from an eight-ear subsample. Maize populations were determined by counting plants in the hand-harvested area of each plot. Maize biomass on an area basis was calculated based on the measured plant population from each plot.

Volumetric soil water content was measured throughout the growing season using a Sentek Diviner 2000 Capacitance probe. Access tubes were installed in 270 kg N ha⁻¹ treatment plots (n = 15). Volumetric water content was measured at 10 cm increments down to 100 cm or bedrock, depending on the soil profile depth. Each measurement was taken as the average from three readings per sampling.

Soil samples from each landscape position were collected to a depth of 60 cm at cover crop planting, to determine bulk density, texture, pH, cation exchange capacity, and soil

organic C and N. Soil texture analysis was performed at the University of Kentucky Regulatory Services soil lab, using the micropipette method (Burt et al., 1993; Miller and Miller, 1987). Soil pH was measured using the Sikora Buffer method (Sikora, 2006). Cation exchange capacity was determined via ammonium saturation of exchange sites. Soil C and N concentrations were measured using a dry combustion analyzer. Soil samples were also collected to a depth of 60 cm at cover crop termination to establish inorganic N (Crutchfield and Grove, 2011) and soil water storage for model initialization. Treatment effects on maize yield during our experimental trial were evaluated using Type III sums of squares ANOVA using lme4 in R (v1.1-23 Bates et al., 2015). In the linear mixed model, cover crop, landscape position, and N fertilizer rate and their interactions were considered fixed effects, and replicate, replicate x landscape position interaction, and replicate x landscape position x cover crop interaction were considered random effects. Cover crop biomass and N content were analyzed in a similar manner, except that cover crop and N fertilizer rate were not included as factors in the model. Total soil water storage (mm) in 0-0.5 and 0.5-1 m soil profile depths was analyzed using a repeated measures ANOVA using lme4 in R (v1.1-23, Bates *et al.*, 2015). In the linear mixed model, total soil water storage was the response variable, cover crop and landscape position and their interaction were considered fixed effects, and sample date, replicate, and replicate x landscape position were random effects. To analyze the effect of the cover crop on soil water storage during key growth stages, soil water storage was averaged across dates during vegetative, anthesis, and reproductive growth periods. The data for each growth stage was then analyzed using a Type III sums of squares ANOVA using lme4 in R (v1.1-23, Bates et al., 2015), where cover crop, landscape position, and their

interaction were considered fixed effects, and replicate and replicate x landscape position were considered random effects.

4.3.3 *Simulation of field study*

4.3.3.1 *Description of software used and model settings*

The Decision Support System for Agro-technology Transfer (DSSAT) v.4.7.1.001 is a suite of dynamic, process-based modeling tools to simulate the C, N, and water balance in cropping systems (Jones *et al.*, 2003, Hoogenboom *et al.*, 2019). The Sequence option was used to simulate the CERES-Wheat and CERES-Maize models in rotation, with carryover of water, C, and N between the wheat and maize phases. Reference evapotranspiration was simulated following the FAO-56 approach (Allen *et al.*, 1998), and the Sulieman-Ritchie method was used to calculate soil evaporation (Ritchie *et al.*, 2009). The Suleiman-Ritchie method was selected based on best fit of observed soil moisture in the top 0 to 10 cm soil layer in fallow treatments. Soil organic C and N turnover were simulated using the CENTURY-based option in DSSAT (Parton *et al.*, 1988, 1994).

Simulations require management, weather, genotype, and soil input data. Management inputs were chosen to reflect the management of the field site, including the dates of cover crop planting, cover crop termination, maize planting and fertilization, as well as the methods of planting and fertilization.

Daily weather inputs of precipitation, relative humidity, and minimum and maximum air temperature were retrieved from the University of Kentucky Agricultural Weather Center (<http://weather.uky.edu/>), a nearby weather station located at the same experimental farm.

Solar radiation data were estimated using the DSSAT Weatherman 4.7.0.0 tool (Richardson, 1981, Jones, 2003). Daily wind speed data were obtained from the Lexington Bluegrass Airport, located approximately 13.7 km from the field site.

4.3.3.2 Soil physical parameter calibration

Soil parameterization at each landscape position was based on soil samples for the top 0 – 60 cm, and soil survey for the deeper layers (**Table 4.1**; Soil Survey Staff, 2020). Soil saturated hydraulic conductivity (K_{sat}), volumetric water content at drained upper limit (DUL), lower limit (LL), and at saturation (SAT) were calculated from DSSAT pedotransfer functions, and further optimized by 10 cm soil layer to minimize error in prediction of observed soil water storage data. Slope was estimated based on analysis of LIDAR imaging from the Kentucky Department of Agriculture (Kentucky Division of Geographic Information, 2017), and drainage class, curve number, soil albedo, and runoff potential were obtained from the USDA-NRCS (Soil Survey Staff, 2020). DSSAT simulates water run-off using these topographic inputs, but the model does not account for run-on from surrounding land. Thus, in the simulations, we assumed that all landscape positions received equal amounts of water input based only on the daily precipitation levels. The lack of water transport from one landscape position to another in the simulations likely matches a lack of water redistribution in the field study as well, which included sod buffers between the cropped areas at each landscape position (**Figure 4.1**). However, the toeslope position in both the field study and in simulations may underestimate conditions of saturation under high precipitation and run-on in continuous cropland.

4.3.3.3 Parameterization of the DSSAT-Century for soil N mineralization

The treatment receiving 0 kg N ha⁻¹ after winter fallow at each landscape position was used to parametrize DSSAT-CENTURY. The CENTURY model requires parametrization of a stable, intermediate, and microbial organic C and N pools (Parton et al., 1994). The model requires input of the total organic C and N, and the fraction of stable organic C. The microbial C pool is calculated as 5% of the total non-stable C pool (1 – Percent Stable C). The intermediate pool is then calculated as the difference between 1 and the stable and microbial C pools. To initialize simulations, the stable fraction of C according to each soil texture and field cropping history was selected from recommended values in DSSAT v.4.7.1.001. Thereafter, the stable organic C pool was modified to minimize error in the prediction of total aboveground N content in maize at R1 and R6 in the treatment receiving 0 kg N ha⁻¹. To minimize carry-over of errors in the water and N balance during simulations of the fallow/cover crop-maize rotation, during calibration and model evaluation across all treatments, simulations were initialized at cover crop termination, and cover crop biomass and composition, as well as soil water storage and inorganic N at this time were provided as an input.

4.3.3.4 Calibration of crop coefficients

Cultivar coefficients for the CERES-Wheat model were calibrated to match the observed aboveground biomass and N content at cover crop termination. Cultivar NEWTON in DSSAT v.4.7.1.001 was used to initialize simulations. To better match the amount of biomass and N content, the length of optimum temperature required for vernalization (P1V) was set to 52 days. Standard mature tiller weight (G3) was increased to 2.2 g, and the interval between successive leaf tip appearance (PHINT) was increased to 143 growing degree days (GDD). The goal of this calibration was to obtain an amount of

biomass and N content similar to the observed but did not focus on having cultivar coefficients that closely described phenology, growth, and partitioning of a cereal rye crop.

Cultivar coefficients for CERES-Maize were calibrated utilizing data from the treatment receiving 270 kg N ha⁻¹ following a winter fallow at the toeslope. This was done to minimize confounding effects of water and N stress and obtain crop growth coefficients closest to the real genetic potential for the hybrid used in our study. In addition, simulations were initialized at the time of cover crop termination to minimize carry-over of error in the water and N balance from starting simulations the previous fall.

Calibration of maize crop growth coefficients in CERES-Maize consist of six parameters: thermal time from emergence until the reproductive stage (P1), the days of delay in development per hour increase in photoperiod above 12.5 h (P2), thermal time from silking to maturity (P5), the maximum number of kernels per plant (G2), and the kernel filling rate during the linear grain filling stage (G3). Parameter P1 was optimized to match the simulated time of anthesis with the observed. Parameter P2 was set to 0 assuming limited photoperiod sensitivity in modern maize hybrids. The P3 parameter was modified to match the observed timing of physiological maturity. The PHINT parameter was then adjusted to match more closely the observed aboveground biomass at R1 and R6. G2 was adjusted to minimize bias in the prediction of the number of kernels per plant. Finally, the G3 coefficient was adjusted to reduce bias in the prediction of kernel size and yield. The final set of maize cultivar coefficients after calibration were 285 GDD, 0 days, 800 GDD, 1070 kernels per plant, 8.20 mg day⁻¹, and 38 GDD, for P1, P2, P3, G2, G3, and PHINT, respectively.

4.3.3.5 Model evaluation

After calibration utilizing data from the winter fallow treatments (treatments receiving 0 and 270 kg N ha⁻¹), model performance predicting maize yield, kernel number, aboveground biomass and N content, and soil water storage was evaluated across the different N fertilizer levels within each landscape position following a cereal rye cover crop. The statistics used to evaluate model performance were the root mean square error (RMSE), normalized root mean square error (NRMSE), and the Nash-Sutcliffe Efficiency Index (NSE) between observed and simulated data (Equations 4.1, 4.2, and 4.3, respectively),

$$RMSE = \sqrt{\frac{\sum_{i=1}^n (Simulated_i - Observed_i)^2}{n}} \quad [4.1]$$

$$NRMSE = \frac{\sqrt{\frac{\sum_{i=1}^n (Simulated_i - Observed_i)^2}{n}}}{\frac{\sum (Observed)}{n}} \quad [4.2]$$

$$NSE = 1 - \frac{\sum_{i=1}^n (Simulated_i - Observed_i)^2}{\sum_{i=1}^n (Observed_i - Observed_{Av})^2} \quad [4.3]$$

where $Simulated_i$ is the simulated value for R1 aboveground biomass, R1 aboveground N, R6 aboveground biomass, R6 aboveground N, maize yield, grain N content, unit kernel weight, or kernels per square meter, and $Observed_i$ is the respective observed value. $Observed_{Av}$ is the mean of the observed values for a respective parameter, and n is the number of observations. Lower values of the RMSE and NRMSE indicate greater agreement between modeled and observed data. The NSE can range from 1 to negative

infinity, with positive values indicating the model is a better predictor than the average value of the observed data. Model evaluation and the calculation of model statistics was performed in R, using the base R functions and the HydroGOF package (Version 0.4.0, Zambrano, 2020).

4.3.4 *Sensitivity analysis with historical weather*

Following calibration, a sensitivity analysis was performed using the DSSAT v.4.7.1.001 Sequence module to simulate crop rotations. Simulations were run using historical weather data from 1989 to 2019 with soil profiles for each of the three landscape positions in our field study. In addition, simulations were conducted under different soil N fertility levels, which were generated by varying N fertilizer rates and soil organic matter levels. The two N fertilizer scenarios consisted of the Kentucky recommendations for maize crops on well drained soils (Recommended N, 155 kg N ha⁻¹) and the highest rate present in our study (High N, 270 kg N ha⁻¹). The soil organic matter levels consisted of the baseline, which reflected the conditions present at our site (Baseline Fertility, 1.9-2.2% OC in top 15 cm), and a site with ~50% less soil organic C and N (Low Fertility, 1.2% OC in top 15 cm). Simulations started with cover crop planting in the fall each year and ended at maize harvest the following year. Simulations lasted only one rotation, and soil water storage and inorganic N were reinitialized before the start of the next simulation based on observed soil samples collected from our field trial in October 2018. Planting date and date of fertilizer applications were kept fixed on the same day of the year across all model runs. The model was not run continuously for the thirty-year period, but rather reinitialized in the fall of every year for a total of 30 one-year rotations. Thus,

our study is intended to evaluate the seasonal effect of cover crops and not long-term rotational effects.

To study the effect of years with lower vs. greater precipitation than the average, we classified years into three categories based on the summer precipitation: wet, average, and dry. These distinctions were made according to the 33rd and 66th percentile of the cumulative maize growing season precipitation (from planting to harvest) for the thirty years of weather data. The specific precipitation thresholds were < 559 mm for dry, 559 – 697 mm for average, and > 697 mm for wet. As temperature and precipitation are inherently linked, we did not set a temperature threshold when categorizing individual years. To quantify which factors explained a greater amount of the yield variability in simulations, the simulated yield for both the low and baseline soil organic matter scenarios were analyzed using an ANOVA with landscape position, cover crop, N fertilizer level, precipitation category and their interactions considered as fixed effects in the model, and year of the simulation considered as a random factor. Analysis was performed using the aov function from the stats package in R (v 4.0.2, R Core Team, 2020).

Based on the results of this sensitivity analysis, we decided to focus on the baseline soil organic matter conditions under the recommended N application to investigate spatial and temporal yield variability. We examined the coefficient of variation (CV) in simulated yield across all landscape positions and weather years under both cover cropping scenarios. We also examined the CV in simulated yield within specific landscape positions and precipitation categories. To quantify the yield gap due to water limitation and the percentage of years that underwent water stress, the sensitivity analysis was re-

run under automatic irrigation when actual crop available water in the top 30 cm of soil dropped below 60% of available capacity. In the soils that were calibrated for this simulation, the 60% thresholds that triggered irrigation were 11.35 cm of water in the summit, 9.74 cm of water in the backslope, and 11.79 cm of water in the backslope. When the amount of water dipped below these thresholds, irrigation automatically raised the amount of soil water to the DUL. Irrigated and non-irrigated treatments were then compared, and years that experienced a yield loss greater than 10% were considered to have undergone yield penalizing water stress and characterized as such.

4.4 Results

4.4.1 Model performance and comparison to field experiment

4.4.1.1 Cover crop biomass and N content

The cereal rye cover crop in our field experiment accumulated an average of 3,225 kg dry matter ha⁻¹ and 60 kg N ha⁻¹ prior to termination in 2019 (Figure 2A). Cover crop biomass and N content were similar across landscape positions in our experimental year ($P = 0.31$ and 0.34 , respectively). After calibration of the cultivar coefficients for CERES-Wheat, the model simulated aboveground biomass and N content values that were within one standard deviation of the observed means for 2019 (**Figure 4.2A**). Simulations across 30 years of weather data showed large interannual variability in cover crop biomass, ranging from 1051 kg ha⁻¹ to 7485 kg ha⁻¹. Averaged across 30 years, the simulated cover crop biomass production was 16% higher in the toeslope than the summit and backslope positions (**Figure 4.2A**).

4.4.1.2 Maize growth and N content

Maize grain yield in our field experiment varied significantly among landscape positions ($P < 0.001$), ranging from 6.3 Mg ha⁻¹ on the backslope to 12.2 Mg ha⁻¹ on the toeslope (Figure 2B). There were no effects of cover crop ($P = 0.30$) or N fertilizer rate ($P = 0.28$) on maize yield. Following calibration of CERES-Maize crop growth coefficients with treatments under winter fallow, the model simulated maize grain yield values that were within one standard deviation of the observed means for 2019 (Figure 2B). In addition, maize aboveground biomass, kernel number, and yield in the calibration dataset (i.e., the winter fallow treatment) were predicted with a relatively low nRMSE ranging from 8 to 9% and a positive model efficiency ranging from 0.32 to 0.86 (**Figure 4.3A**). When the model was evaluated in treatments following a cereal rye cover crop, nRMSE in the prediction of aboveground biomass, kernel number and yield increased in all cases compared to calibration, but the values were still within acceptable levels (nRMSE = 12-21%; **Figure 4.3B**).

After soil organic matter pools in DSSAT-CENTURY were optimized using the data from fallow treatments receiving 0 kg N ha⁻¹, the model predicted aboveground N content with an acceptable nRMSE across all N fertilizer rates and landscape positions in maize after fallow (13.7% - 18.3%) (**Figure 4.3A**). The model was more efficient at capturing the increase in aboveground N after fertilizer application at R1 (NSE = 0.86) than at R6 (NSE = -0.20). However, the overall RMSE in prediction of aboveground N at R6 was still low (40.6 kg ha⁻¹) and mainly associated with an over prediction of N content in treatments receiving the highest N fertilizer rate (Figure 3A). Similar to fallow treatments, the model was more efficient at predicting maize aboveground N at R1 (NSE = 0.86) than at R6 (NSE = 0.17) in maize following the cereal rye cover crop. Overall,

the model was efficient at predicting difference in yield and R1 and R6 biomass, and aboveground N at R1 across treatments. However, predicted aboveground N content at R6 and grain N content showed a larger response to the N fertilizer rates applied than the observed data and were over predicted on average under the highest N fertilizer applications.

4.4.1.3 Soil moisture dynamics

Landscape position and cover crop significantly affected soil water storage in our field experiment ($P < 0.001$). The cover crop treatment had significantly higher soil water storage in the top 0.5 m than the winter fallow treatment (**Figure 4.4**). As soil water storage decreased during the summer of 2019, soil water was higher during late maize reproductive stages in the backslope and toeslope positions when following a cereal rye cover crop (**Figure 4.4, Supplemental Figure S4.1**). Calibration and evaluation model simulations captured well the decrease in soil water during the maize growing season with a low RMSE ranging from 5 to 23 mm. Model simulations also captured the greater soil water storage following cereal rye early in the maize season, but not during seed filling, when both cover crop and fallow treatments had similar simulated soil moisture (**Figure 4.4**). In the maize after fallow treatment used for calibration, the NSE for the prediction of soil water storage ranged from 0.89 to 0.91 in the top 0.5 m, and from 0.68 to 0.79 in the lower 0.5 m. In the maize after cover crop treatment, NSE values ranged from 0.89 to 0.96 in the top 0.5 m, and 0.61 to 0.68 in the lower depths, with the summit outlier NSE value of -3.7. Soil water storage at lower depths experienced less variability throughout the year, which led to decreased NSE values relative to the top 0.5 m, but low NRMSE and RMSE values in lower depths indicate strong model agreement. having an

outlier NSE value of -3.7. Soil water storage at lower depths experienced less variability throughout the year, which led to decreased NSE values relative to the top 0.5 m, but low NRMSE and RMSE values in lower depths indicate strong model agreement.

4.4.2 *Sensitivity analysis of weather and management effects on simulated maize yield*

Variation in simulated yields across 30 years was attributed mainly to the weather classification based on precipitation (i.e., dry, average, wet), which accounted for 32-35% of the total sums of squares (SS) in the ANOVA (**Figure 4.5**). Landscape position, and its interaction with precipitation category, were the second and third most important factors in determining maize yields under the baseline soil organic matter scenario, and the second and fourth most important factor in explaining yield variability in the low soil organic matter scenario. The effect of landscape position and its associated interactions accounted for 28 and 31% of the total SS for the baseline and low fertility soil organic matter soil, respectively. The cover crop main effect and its interactions with other factors explained more variability under the baseline soil organic matter model than in the low soil organic matter model (0.8% and 0.5%, respectively). Interestingly, N fertilizer rate and its interactions with other factors did not explain yield variability in the baseline soil conditions (0.2% of total SS). Under the low fertility model, the effect of N rate and its interaction with other factors increased (2.8% of total SS), but still explained a relatively low percentage of the yield variability compared to the effects of landscape position, precipitation category, and their interactions. Full ANOVA tables for the low and baseline soil organic matter level analyses can be found in Supplemental Table S4.1.

Because precipitation category and landscape position were the most important sources of variation while N fertilizer level had a minor impact, subsequent discussion of results is focused on the landscape position x weather x cover crop interaction under a single baseline soil condition and a common recommended maize N rate for our study region, 155 kg N ha⁻¹.

4.4.2.1 Cover crop effects on simulated maize yield and yield stability

Simulated maize yield averaged 10.7 Mg ha⁻¹ across weather years, landscape positions, and cover crop treatments. Average simulated maize yields were 12% higher and 25% lower during wet and dry years, respectively. Across weather scenarios and cover crop treatments, the toeslope was consistently the highest yielding landscape position (12.9 Mg ha⁻¹), followed by the summit (10.7 Mg ha⁻¹), and then the backslope (8.5 Mg ha⁻¹) (**Figure 4.6**). Across the 30-year dataset, the addition of the cover crop increased the average yield by 2.2%, though the magnitude of this effect varied by landscape position. Simulated yields increased by 6.1% in the backslope and by 1.1% in the toeslope for maize following the cereal rye relative to the winter fallow and were similar between cover crops and winter fallow in the summit position. When averaged across landscape positions, the cover crop treatment increased maize yield by 10.9% during dry years, 1.4% during average years, and decreased yields by 2.3 % during wet years. The greatest benefit of the cover crop on simulated maize yields was during dry years on the backslope (24% increase), while the greatest reduction in yield due to the cover crop was during wet years on the backslope (4% decrease).

The yield-variance plots revealed that while maize yields shifted slightly when following a cover crop, the variance in yield among years was reduced for all landscape positions

(**Figure 4.7A**), and the variance among landscape positions was reduced in dry and average years (**Figure 4.7A and 4.7B**). Across all precipitation categories, the stabilizing effect of the cover crop on interannual yield variability was strongest on the backslope position and was similar on the summit and the toeslope positions (**Figure 4.7C**). When combined spatial and interannual variability were examined for each precipitation category, the greatest reduction in CV was observed during dry conditions. There was a moderate reduction in CV during average precipitation years, and the rye cover crop had no effect on maize yield CV during wet years (**Figure 4.7D**). The coefficient of variation for yields among all landscape positions and weather years decreased from 33% to 26% when a rye cover crop was added to the rotation (**Figure 4.7E**).

4.4.2.2 Cover crop effect on frequency and size of simulated water-stress yield gap

Our weather classification in wet, average, and dry years based on relative precipitation amounts did not consider if the maize crop experienced water stress. Thus, simulations under automatic irrigation during the maize growing season were used to calculate the yield gap due to water stress relative to non-irrigated simulations. Our results indicated that the summit and toeslope positions experienced a water-stress yield reduction greater than 10% in 6 out of the 30 years examined (**Figure 4.8A**). The backslope position was much more prone to water stress, undergoing >10% yield reductions in 17 of the 30 years of weather data in maize following fallow. The addition of a cover crop into the rotation reduced the percentage of years with a >10% water-stress yield gap by four years in the backslope, but did not reduce frequency of water stress in the summit or toeslope positions (**Figure 4.8A**). In addition to decreasing the frequency of water stress, the presence of a cover crop decreased average water stress yield gap in all three landscape

positions, reducing average yield loss by 985 kg ha⁻¹ yr⁻¹ (34% of average water-stress yield loss) in the backslope, 296 kg ha⁻¹ yr⁻¹ (26% of average water-stress yield loss) in the summit, and 198 kg ha⁻¹ yr⁻¹ (17% of average water-stress yield loss) in the toeslope position (**Figure 4.8B**).

4.4.2.3 Cover crop effects on simulated water balance and water stress

Cover crop transpiration during the winter growing season reduced the amount of soil water at cover crop termination by 8.8 mm in the top 50 cm of soil on average compared to winter fallow. However, this small deficit was typically overcome by the time of maize planting two weeks later via spring precipitation (**Supplemental Figure S4.2**).

The presence of cover crop residue reduced water losses through evaporation during the maize growing season by 72 to 91 mm depending on the landscape position and precipitation category. The largest reduction in evaporation occurred during wet years (87 mm reduction). During dry and average years, the reduction in total soil evaporative loss was similar across all landscape positions (74 mm and 79 mm reductions, respectively) (**Table 4.3**). In addition to the reduction of evaporation, the presence of cover crop residue also reduced the amount of runoff by 20 to 76 mm in the summit and backslope positions depending on weather class (**Table 4.3**). In contrast, runoff was similar across cover crop treatments in the toeslope (**Table 4.3**).

Averaged across the 30 years of weather conditions, the rye cover crop increased maize transpiration in each landscape position. The effect was greatest on the backslope (16.8 mm increase), moderate at the summit position (7.2 mm increase), and generally negligible at the toeslope (2.4 mm increase) (**Table 4.3**). The effect was greatest during

dry years, where the presence of cover crop residue increased transpiration by 18.4 mm across landscape positions. During average and wet years, the increased transpiration due to cover crop residue was only 7.7 mm and 0.2 mm, respectively. These average increases were driven largely by the cover crop effect in the backslope position across precipitation categories (**Table 4.3**). The presence of the cover crop residue increased the amount of soil water drainage from the bottom of the profile by 25 to 95 mm depending on the landscape position and precipitation categories (**Table 4.3**). Total drainage was greatest at the toeslope position, ranging from 60 mm in dry conditions under fallow to 190 mm during wet conditions under the cover crop. The greatest increase in drainage due to the cover crop was observed in the backslope (48 to 95 mm) and in wet years across landscape positions (50 to 85 mm).

Although the effect on maize total transpiration was relatively small in absolute terms, a consistent decrease in the growth water stress index, defined as a ratio between actual and potential evapotranspiration, was observed (**Figure 4.9**). Growing a rye cover crop decreased the intensity of water stress during maize flowering and grain filling under dry years. As precipitation during the maize growing season increased, the difference in water stress between the fallow and cover crop treatment was delayed till later in the season, but was still evident across landscape positions during average years, and in the backslope during all precipitation categories. During the vegetative stage of growth, the cover crop increased the excess water stress index indicating excessive soil water not conducive to plant growth. This occurred in the backslope across all precipitation categories during the vegetative phase, and in the summit and toeslope during average and wet years (**Figure 4.9**).

4.5 Discussion

4.5.1 *Applications of DSSAT to simulate topography x weather x cover crop interactions*

Crop model applications provide an opportunity to overcome limitations of agronomic trials by studying a wide array of management adaptations and environmental conditions. Our analysis, which focused on three contrasting landscape positions, indicated that process-based models can play a useful role in understanding and informing ecological processes that increase productivity and reduce sub-field variation in areas of complex topography. Our crop model simulations were particularly useful to overcome two main limitations in our field trial: i.) inability to test unlimited number of management options and soil fertility conditions, and ii.) inability to study the effect of year to year variability in environmental conditions. Our simulation study was also key to illustrating that spatial and temporal maize yield fluctuations in our study area are mainly associated with variability in water availability across years and landscape positions, and relatively less dependent on N cycling under recommended N fertilizer inputs, even under a low organic matter scenario and the presence of a cover crop. We used CERES-Wheat to simulate observed cereal rye cover crop growth in our study. Other studies have used crop models from different species than the cover crop to study water and N cycling in cover crop rotations (Adhikari et al., 2017; Li et al., 2008; Salmerón et al., 2014; Z. Qi et al., 2011). The CERES-Wheat module used in our study offered the advantage of simulating the detrimental effect of water excess on plant growth processes (Mearns et al., 1996; Thorp et al., 2010). Cereal rye cover crop biomass and N content at termination in our 30 year simulations were within the range of those reported in field trials for our study region

(Thapa et al., 2018), though timing of spring termination is a major source of variability when comparing biomass levels. Data from more years that include fall and spring destructive cover crop biomass and N sampling and soil water storage, including periods of excess water, would be beneficial to reduce uncertainty in cover crop predictions in our study area, where cover crops may experience high variability in soil moisture conditions ranging from water stress to saturation depending on the year and landscape position.

We found that the benefits of cover crop reported in our study were associated with increased water availability to maize during reproductive stages, due to a reduction of soil evaporation and runoff. While our observed data from 2019 showed a small 14 mm increase in soil water storage in the top 0.5 m of backslope and toeslope positions following the cover crop during late reproductive stages, this trend was not captured in our model simulations. Instead, model simulations in 2019 showed similar soil moisture across cover crop treatments (1 -2 mm higher following rye compared to fallow), but an increase in crop transpiration by 9-10 mm in the backslope and summit in maize after a cover crop compared to fallow. Precipitation during 2019 was insufficient to meet the crop evapotranspiration demand, leading to a pronounced depletion of soil water storage to a level close to the lower limit in the 0 to 0.5m soil depth. DSSAT model simulations will assume that water is similarly available across the range of plant available water without considering water tension, and it is possible that this simplification was not able to capture soil water storage dynamics when soil moisture decreases to values close to the lower limit. It is interesting to note that increased water availability in cover crop treatments in 2019 did not result in significantly greater maize yields. Our explanation

based on the simulations for this year, as well as observed soil moisture data and maize yield components, is that cover crop treatments experienced relatively greater excess water stress early on, that was compensated by greater water availability later in the season. This presumption is consistent with the higher incidence of excess water stress observed early in the season under cover crop treatments in our 30-year simulations. These results reveal an interesting interaction that should be further evaluated under different cover crop termination dates and residue management strategies. Optimized cover crop management recommendations may depend on different landscape positions to reduce the incidence of excess water stress while maximizing water savings for later in the season.

In our simulation results, the presence of the cover crop residue reduced soil water losses through runoff and evaporation. In particular, the presence of the cover crop residue led to a reduction in soil evaporation of 75 mm across landscape positions and climate conditions. This magnitude of decrease is consistent with another modeling study of a rye cover crop maize rotation using APSIM in a homogeneous field in Central Iowa (Basche *et al.* 2016). Other modeling studies also found a greater reduction in soil evaporation during wet years following a rye cover crop than following winter fallow (Qi *et al.*, 2011), similar to what we observed.

Soil water runoff is largely driven by the infiltration rate of soils and the time in which maximum infiltration is reached (Scarnecchia and Magdoff, 1994). Previous research has shown that the addition of a cover crop residue increases the time which maximum infiltration is reached, consequently decreasing runoff losses (Blanco-Canqui *et al.*, 2015). Results from our 30-year simulations showed a decrease in the amount of soil

water runoff in the summit and backslope positions of up to 70 and 50%, respectively, in maize after a cereal rye cover crop compared to fallow. This is in agreement with the effect of a rye cover crop on run-off rates found by Zhu et al. (1989), in which a grass cover crop decreased the seasonal run-off by 44-53% in a maize-soybean [*Glycine max* (L.) Merr] system. Beyond the immediate effects on soil water storage, this reduction in run-off provides additional benefits of reducing soil erosion and downslope nutrient losses that can occur during surface and subsurface runoff events, compounding the potential benefits of cover crops in sloping areas.

When following a rye cover crop, soil water drainage during the maize growing season increased by 37 -94 mm compared to the winter fallow treatment. This effect was unexpected, and a consequence of the reduced soil evaporation and runoff after a cover crop, and high intensity of precipitation events concentrated during short periods in the spring, when crop evapotranspiration demand is still low. This increase in drainage may have important implications on N leaching losses and show an interaction with timing of N fertilizer application depending on weather and landscape position that should be addressed in further studies. There has been considerable work done on the effects of cover crops and their ability to limit winter drainage and N loss through winter transpiration, both field studies (Kaspar et al., 2012; Meisinger and Ricigliano, 2017; Strock et al., 2004), and modeling (Li et al., 2008). However, field and modeling studies evaluating residual effects of cover crop on drainage and N leaching during the next cash crop growing season are less frequent (Brandi-Dohrn et al., 1997; McCracken et al., 1994; Salmerón et al., 2014, 2010; Tonitto et al., 2006). It is possible that drainage in our simulations was overpredicted overall due to the methodology employed by the DSSAT

model to capture downward water movement in the soil profile; a tipping bucket approach where water drains into lower layers as the upper limit of a given layer is reached (Jones et al., 2003). This methodology, though effective in capturing the soil water balance as a whole of a given system, may lead to error in drainage estimates (Meng and Quiring, 2008; Soldevilla-Martinez et al., 2013). This is especially relevant in humid climates where a large portion of spring rain is partitioned to drainage. However, further work to clarify and validate the effect of cover crop residue on drainage during the early stage of vegetative growth of the cash crop in humid and sub-humid regions is still needed, especially studies that employ weighing lysimeters or eddy-covariance flux towers. Similarly, well-balanced studies evaluating model predictions under different timing of water stress with observed data could further accelerate model evaluation and improvement to simulate yield variability in complex topography.

4.5.2 *Cover crops effect on maize yield*

We hypothesized that cover crops would reduce water and nutrient losses and increase productivity and yield stability in the rolling hill topography of our study region. Our simulation results support our original hypothesis, indicating that a cereal rye cover crop increased the 30-year average yield across landscape positions by 230 kg ha⁻¹, and reduced interannual variability in maize yields by increasing yields on the backslope by 6% across all years, and by 24% in dry years. Overall, the presence of cover crop residue reduced the CV in maize yields across landscape position and weather years from 33% to 26%. Only 5% of maize acreage in Kentucky is under irrigation, and thus maize grown in this area is highly subject to year-to-year variability in precipitation patterns and spatially varying soil characteristics. Our simulations indicate that, when following fallow, maize

yield would be reduced by water stress by 10% or more in 17 out of 30 years on the backslope, and in 6 out of 30 years on the summit and toeslope. The cover crop decreased the number of water-limited years to 13 years on the backslope. Thus, our results suggest that cover crops may be an important ecological intensification tool to increase productivity in rainfed environments with shallow soils.

Recent work on yield stability in maize cropping systems has identified topographic depressions as unstable zones due to near-average yields under low rainfall and below-average yields under high rainfall (Martinez-Feria and Basso, 2020). In contrast, we found that our lowest lying landscape position, the toeslope, was consistently the highest yielding landscape position, and had the lowest CV among landscape positions averaged across cover crop treatments. This discrepancy highlights that the landscape position effects on yield and temporal yield stability observed in one region may not transfer well to another. It is possible that our simulations under-predicted the potential negative effects of water saturation in the toeslope associated with run-on water during wet years. Also, the regional differences may be driven by differences in soil forming factors. For example, the soils of Kentucky are naturally well-drained because they are underlain by karst, while many soils in the Central US do not have well-developed drainage features and are therefore more prone to excess water. In our simulation studies, the incidence of stress caused by water excess increased under the cover crop treatments, although the overall effects of cover crops were positive due to increased water during seed filling. However, it is possible that cover crops may lead to yield losses in wet years and landscape positions with poor drainage or increased run-on.

It was interesting to find that winter transpiration of cover crops did not typically decrease water availability for maize, with differences in soil moisture between cover crops treatments usually disappearing before planting. However, this finding may not hold true in drier locations. Our study site in Central Kentucky is located in a sub humid climate zone and receives ~1100 mm of rainfall on average. Studies in more arid and semi-arid zones have indicated that the reduction in soil water loss through evaporation and run-off reduction does not make-up for the loss through cover crop transpiration and leads to increased water stress for the cash crop following a winter cover crop (Blanco-Canqui et al., 2015; Unger and Vigil, 1998). It is likely that maize grown at other locations within our study area that receive less precipitation may experience water stress after a cover crop in dry years. Cover crop management, in particular termination timing, could help palliate potential negative effects associated with water stress and increase yield stability in these locations (Alonso-Ayuso et al., 2014).

4.5.3 Study limitations and future research

Several research groups have pointed out that despite the benefits of cover crops, there are still barriers to adoption (Roesch-Mcnally et al., 2018). One key limitation to adoption is the perception that the integration of cover crops may decrease yields. The results of our simulation study indicate that the addition of a cover crop rarely has a detrimental effect on maize yields and can actually increase yields in areas of the landscape that are more prone to water limitation during especially dry years. The lack of substantial difference in yield between maize following a cover crop and maize following fallow at the summit and backslope during average years is in line with other studies that have researched the impact of cover crops on crop yields and have found little to no

effect under typical field settings (Basche et al., 2016; Martinez-Feria et al., 2016b). However, our simulation study does not account for the possibility of increased pest or disease pressure following rye, which can limit yields (Bakker et al., 2016), and could also underpredict yield reductions due to excess water. Farmers often experience reduced soil inorganic N after cover crops, and increased N stress due to the immobilization of plant available N during high C:N cover crop residue decomposition (Krueger et al., 2011). Our field site, because of its recent conversion from sod, did not appear to be substantially N limited. This allowed us to focus primarily on the hydrologic cycling aspect of the interactive effect of topography, cover crops, and climate. Further study is needed on how these three factors may influence biogeochemical cycling across space and time. When examined as a whole, our results highlight that cover crop experiments performed in uniformly high-yielding soils may underestimate the benefits of cover crops and make their use less appealing to producers. Continued research on the potential of cover crops to stabilize yields and increase resilience to climatic variability, especially in areas of complex topography, is critical to closing knowledge gaps about how these practices might function in large production settings.

4.6 Conclusions

In this study, we coupled field data and crop model simulations to quantify the effect of a winter cover crop on maize yields and their variability over space and time, to evaluate the potential of this management adaptation in rolling hill terrain, and to inform future experimental research. The majority of maize yield variability in our simulations was explained by weather and landscape position. The cereal rye cover crop reduced year to year variability in maize yield across all landscape positions, and increased average

yields on the backslope, particularly in dry years. Maize following a cover crop tended to have less water limitation during reproductive stages but sometimes excess water during vegetative growth compared to maize following fallow. Our results suggest that a rye cover crop is one route toward ecological intensification in rolling hill terrain and that cover crop research conducted in topographically uniform research trials may overlook important benefits. Continued research on the effect of cover crops on the water balance during the cash crop growing season in areas of variable soil depth and complex topography is paramount to adapting these management strategies for ecological intensification of agricultural land.

4.7 Chapter 4 tables and figures

Table 4.1 - Summary of field operations for cover crop and maize management in the 2019 field experiment.

Field Operation	Date	Management Details
Cover Crop Planting	10/12/2018	Cover crop was drill seeded into 19 cm rows with at a seeding rate of 70 kg ha ⁻¹ .
Cover crop termination	4/13/2019	Cover crop was chemically terminated with a combination of glyphosate and 2,4-D and left on the soil surface.
Maize planting	5/08/2019	Maize was no-till planted in 76 cm rows at a target population of 78,000 plants ha ⁻¹ . A 5 x 5 starter fertilizer was subsurface banded at 45 kg N ha ⁻¹ as 32% urea ammonium nitrate (UAN) in plots receiving N fertilizer.
Maize sidedress fertilization	6/04/2019	At the V5 stage, 32% UAN was dribbled on the soil surface to supply the remainder of the full N fertilizer rate.
Maize R1 sampling	7/18/2019	Six maize plants from the center two rows were removed at R1 for biomass and nutrient content measurements.
Maize harvest	9/11/2019	Maize was hand harvested from a 6.1-m section of each plot for yield calculations, and 8 plants were removed from the center two rows for biomass and nutrient content measurements.

Table 4.2 - Measured, estimated, and calculated characteristics of soils used in simulations. Soil layers were provided to the model in 10 cm increments but are average and combined in this table for brevity.

Profile	Measured Inputs						Estimated Inputs	Model Generated Inputs ^b				
	Depth ^a	Clay	Silt	Org. C	Org. N	Bulk Density	Stable C Fraction	LL	DUL	SAT	SRG F	K _{sat}
	cm	-----%-----				g cm ⁻³	%	-----% vol.-----			0-1	cm hr ⁻¹
Summit	0-30	21.7	68.7	1.6	0.14	1.3	40.0	0.115	0.362	0.455	0.775	1.200
	30-60	42.8	44.4	0.3	0.03	1.3	56.7	0.260	0.450	0.500	0.123	0.090
	60-100	30.9	61.8	0.4	0.03	1.4	70.0	0.240	0.431	0.479	0.036	0.150
Backslope	0-30	24.6	63.5	1.8	0.16	1.2	90.5	0.128	0.413	0.497	0.902	1.275
	30-50	47.0	36.0	0.3	0.02	1.2	94.0	0.200	0.480	0.507	0.607	0.060
Toeslope	0-30	19.1	71.5	2.2	0.19	1.2	62.5	0.098	0.379	0.443	0.975	1.065
	30-60	25.0	67.0	1.2	0.11	1.3	73.3	0.207	0.442	0.498	0.177	0.383
	60-90	25.0	65.0	0.8	0.07	1.3	80.0	0.330	0.450	0.485	0.057	0.173
	90-150	28.0	60.0	0.5	0.04	1.3	90.0	0.262	0.404	0.477	0.005	0.075

^a: Measured soil properties were derived from collected soil samples for the top 60 cm and estimated from Soil Survey data (Soil Survey Staff, 2020) for deeper layers.

^bLL: Lower limit, DUL: Drained upper limit, SAT: Saturated limit, SRGF: Soil root growth factor, K_{sat}: Saturated hydraulic conductivity

Table 4.3 - Simulated water balance components during maize growing season by landscape position, precipitation category, and cover crop treatment, and difference between cover treatments (cover crop – control).

Landscape Position	Precipitation Category	Treatment	Evaporation	Difference	Runoff	Difference	Transpiration	Difference	Drainage	Difference
			-----mm-----							
Summit	Dry	Fallow	133		28		294		44	
Summit	Dry	Rye Cover	58	-76	8	-20	310	16	82	37
Summit	Average	Fallow	154		37		354		56	
Summit	Average	Rye Cover	73	-80	10	-28	360	5	117	61
Summit	Wet	Fallow	147		78		356		120	
Summit	Wet	Rye Cover	60	-87	32	-46	356	0	205	85
Backslope	Dry	Fallow	133		75		236		22	
Backslope	Dry	Rye Cover	61	-72	36	-39	266	29	69	48
Backslope	Average	Fallow	159		105		307		26	
Backslope	Average	Rye Cover	79	-80	53	-52	325	19	95	69
Backslope	Wet	Fallow	148		180		335		59	
Backslope	Wet	Rye Cover	63	-86	104	-76	337	2	154	95
Toeslope	Dry	Fallow	124		9		311		60	
Toeslope	Dry	Rye Cover	51	-73	5	-4	321	10	86	26
Toeslope	Average	Fallow	138		11		361		85	
Toeslope	Average	Rye Cover	61	-77	10	-1	360	-1	124	38
Toeslope	Wet	Fallow	142		50		356		140	
Toeslope	Wet	Rye Cover	51	-91	54	4	355	-2	190	50

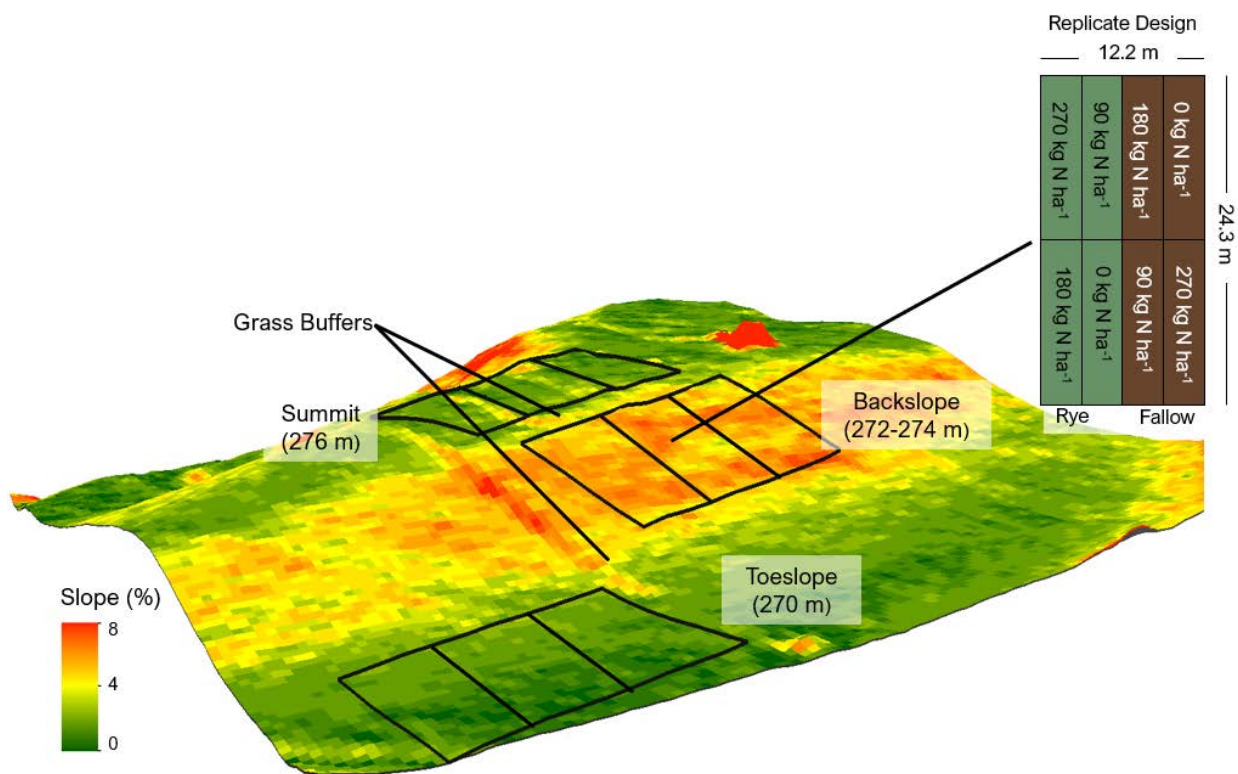


Figure 4.1 - Topographic map with % slope and experimental layout for field experiments in 2019.

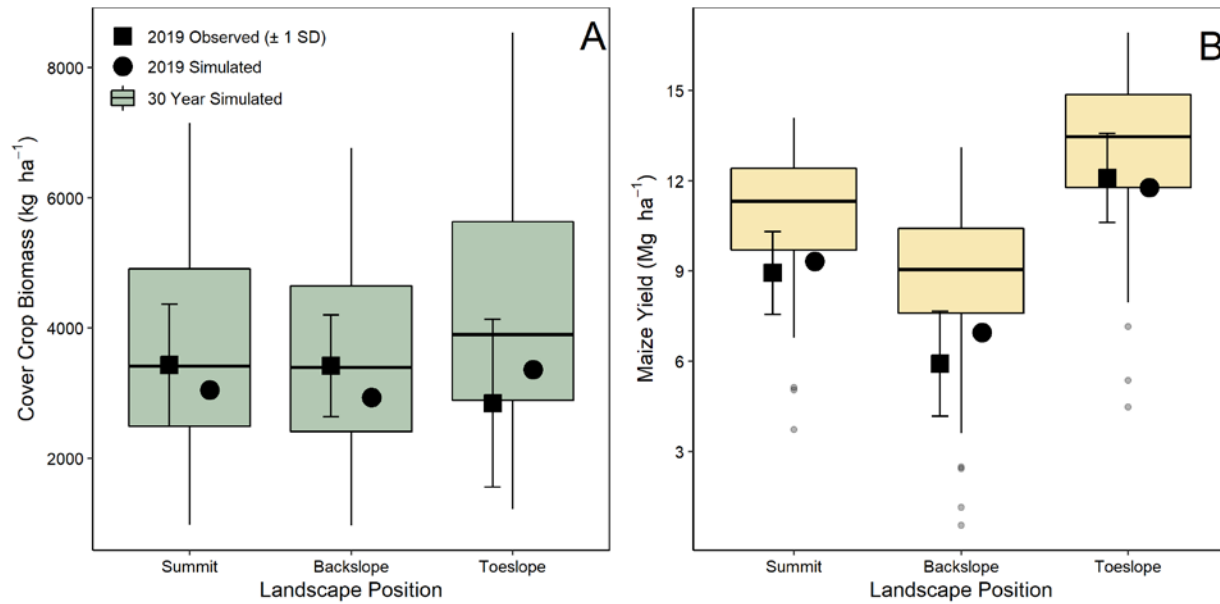


Figure 4.2 - Observed and simulated rye cover crop aboveground biomass at termination (A), and maize grain yield (B). Closed symbols represent observed and simulated data for experimental trials in 2019, error bars on observed data represent ± 1 standard deviation. Boxplots show data from 30-year simulations with historical weather data (1989 – 2019).

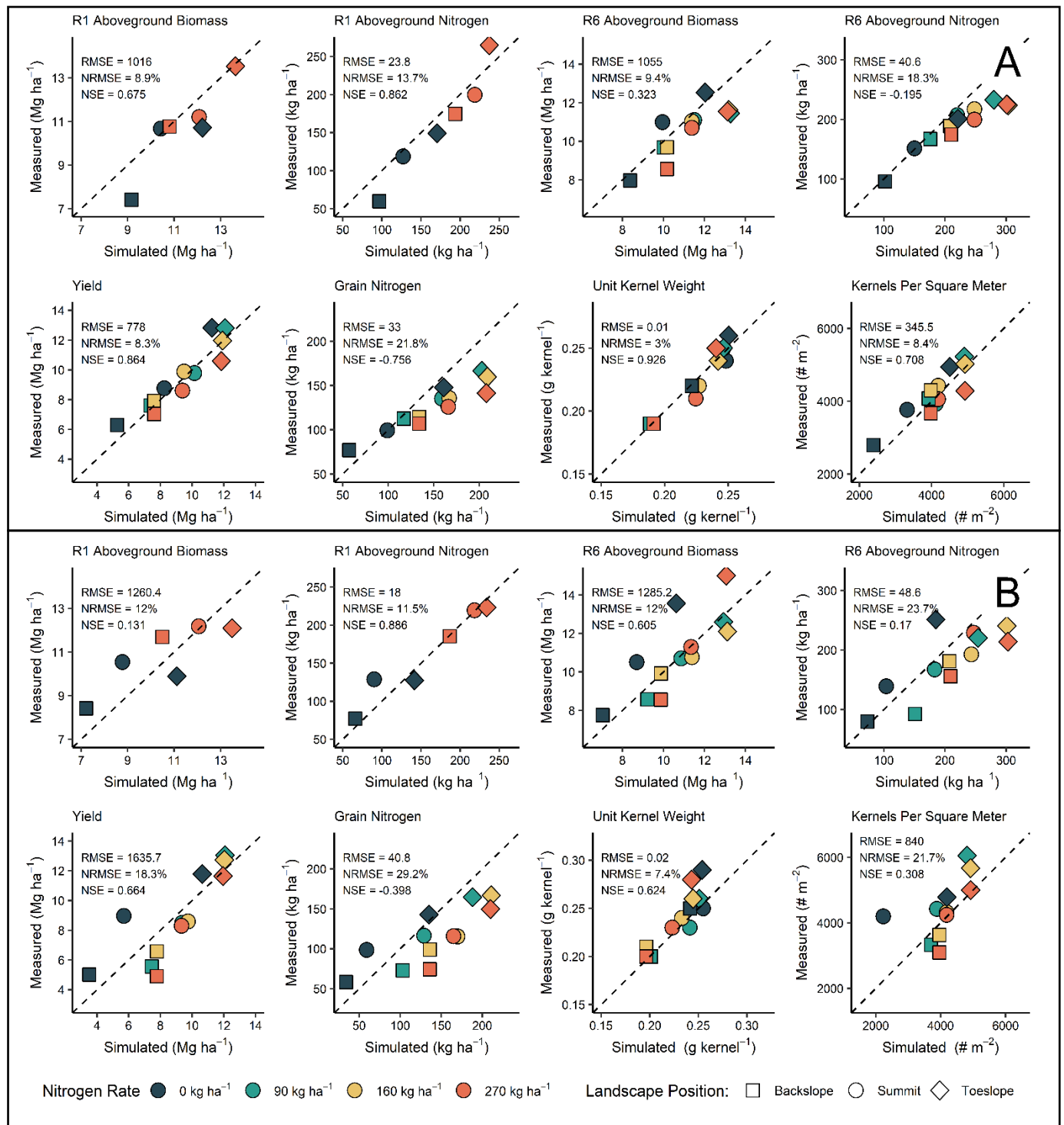


Figure 4.3 - Observed and simulated maize aboveground biomass and N content at R1 and R6, grain yield, grain N content, unit kernel weight, and kernels per square meter in maize after fallow (A) and maize after a cereal rye cover crop (B). Different symbols show data by landscape position and N rate. Maize aboveground biomass and N content at R1 was only sampled in treatments receiving 0 and 270 kg N ha⁻¹.

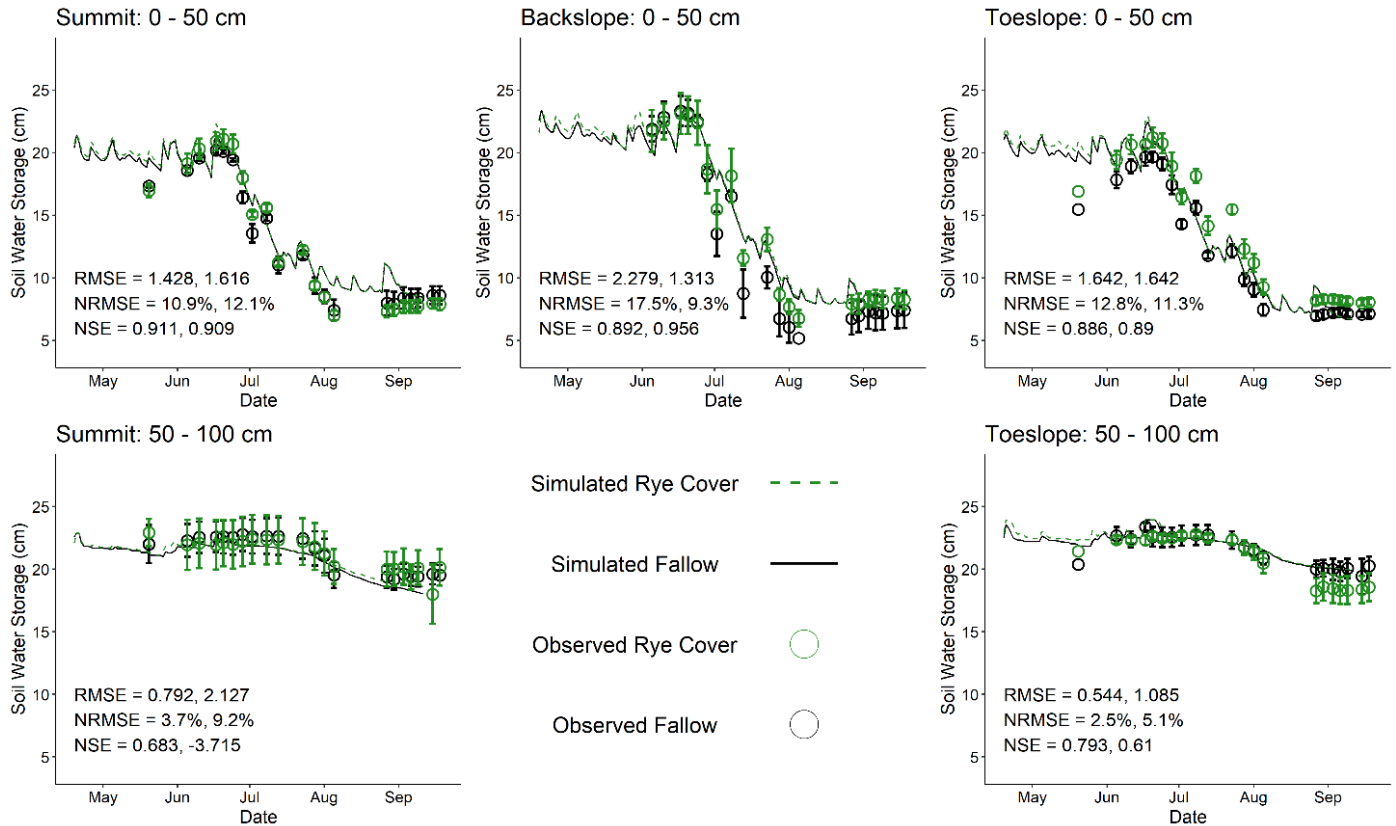


Figure 4.4 - Observed and simulated total soil water in the top (0-50 cm) and bottom (50-100 cm) soil profile at each landscape position in maize after fallow and after a cover crop during 2019 experimental trial. Soils in the backslope position did not extend beyond 50 cm. Error bars show the standard error in the observed data. Statistics for model performance are presented for fallow treatment and rye treatment, respectively.

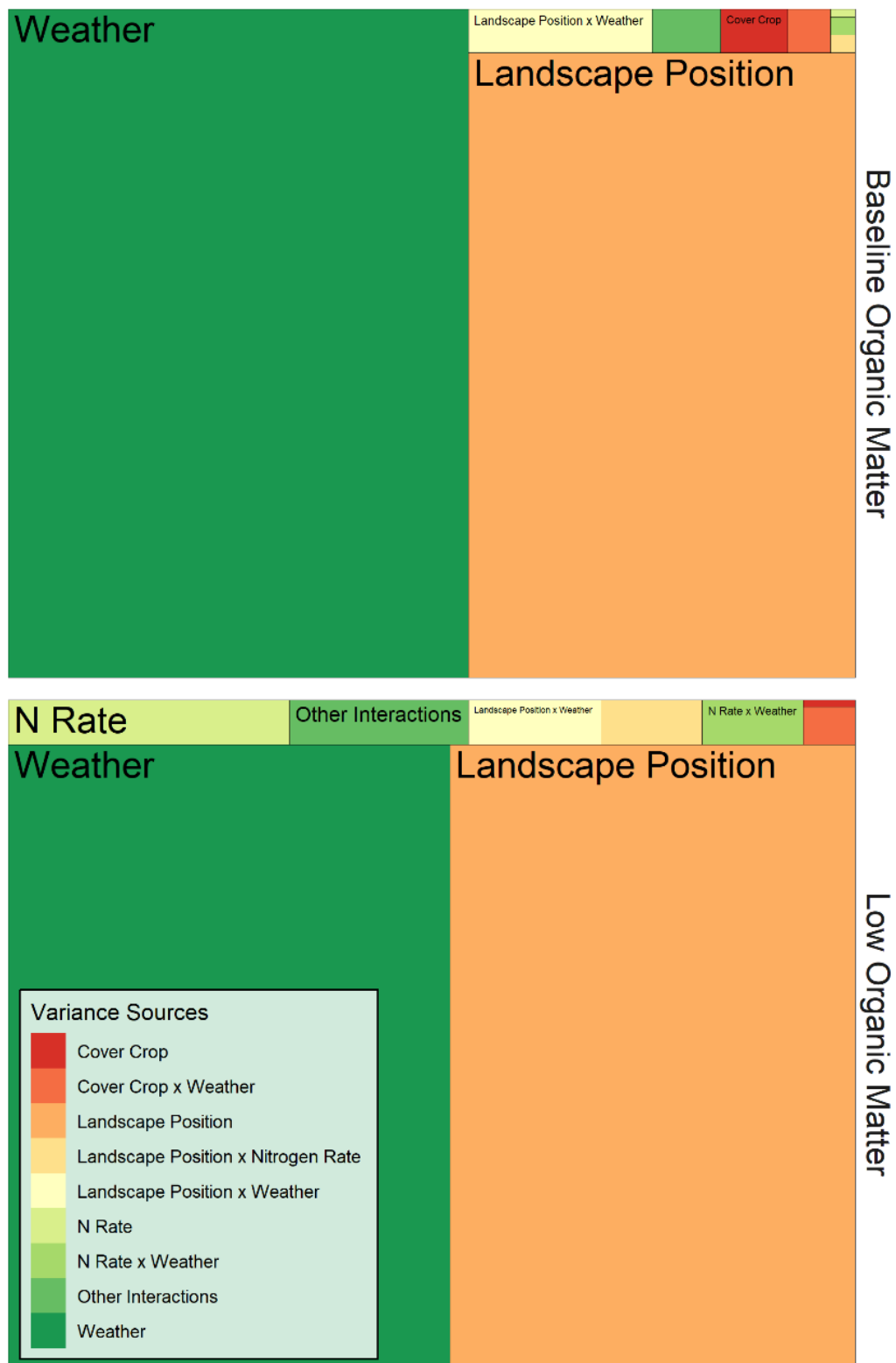


Figure 4.5 - Treemap indicating the apportionment of sums of squares within the ANOVA models for the baseline soil fertility and the low fertility treatments. Larger areas within the treemap correlate with greater percentage of sums of square apportioned to a particular model term.

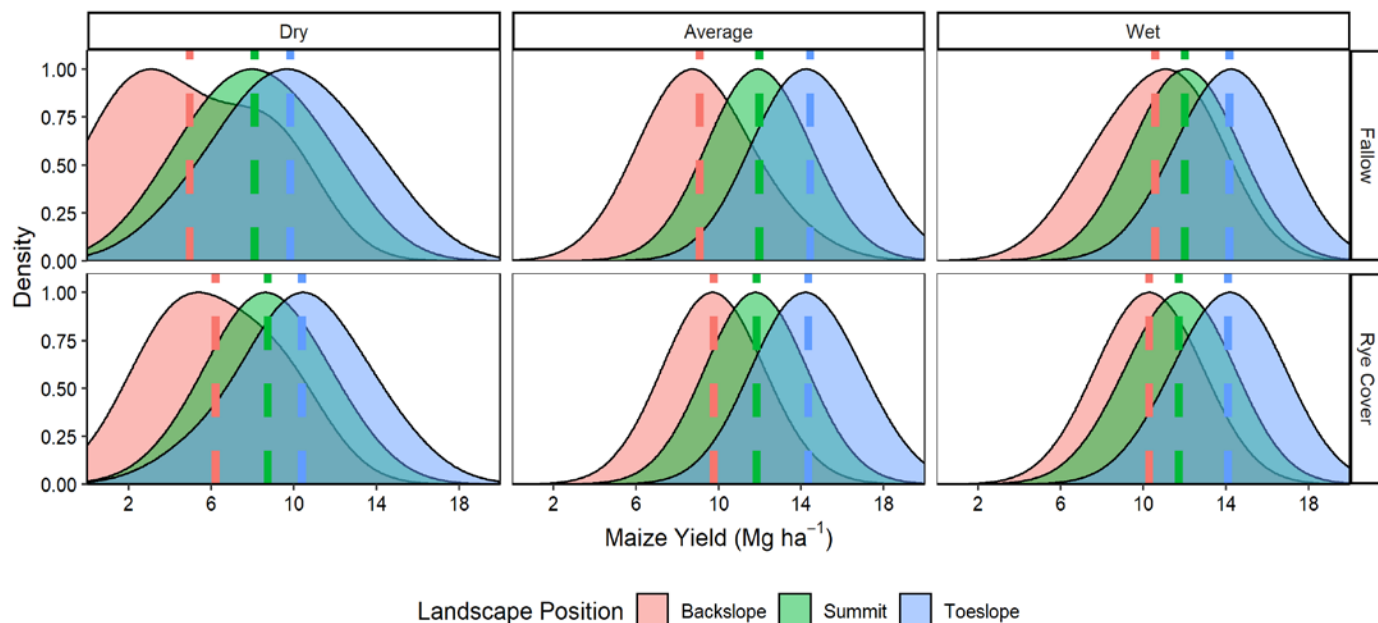


Figure 4.6 - Smoothed density plots of maize yield at different landscape positions for different cover crop treatments and precipitation categories. Dashed lines indicate the mean yields for each distribution.

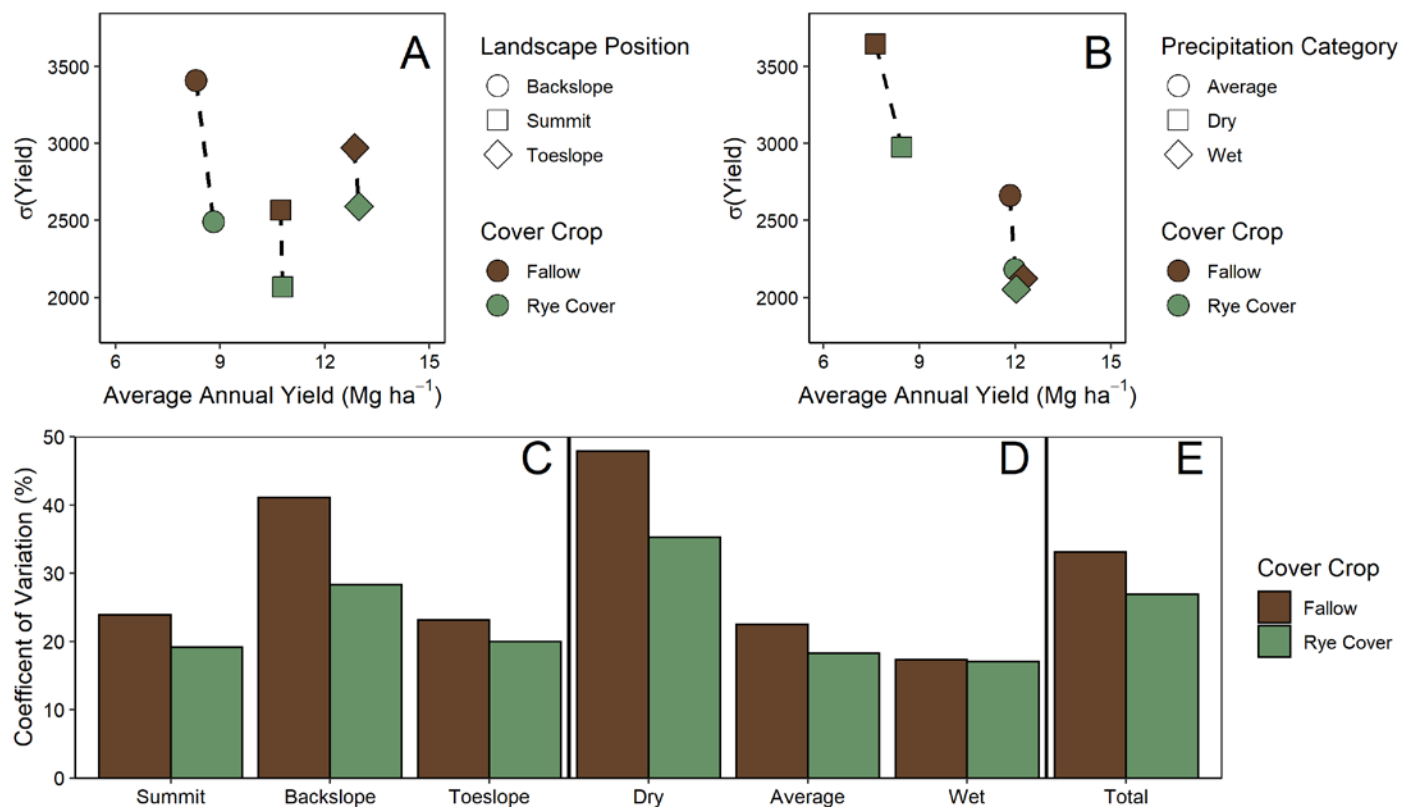


Figure 4.7 - Top: Maize grain yield vs. variance plot for the different landscape positions (A) and different precipitation categories (B). Dashed lines connect the fallow and cover cropped treatment within the same landscape position. $\sigma(\text{Yield})$ is equal to one standard deviation in kg ha⁻¹. Bottom: Yield coefficient of variation from 30-year simulations by landscape position (C), precipitation category (D), and total (E), of maize grown after fallow or after a cereal rye cover crop.

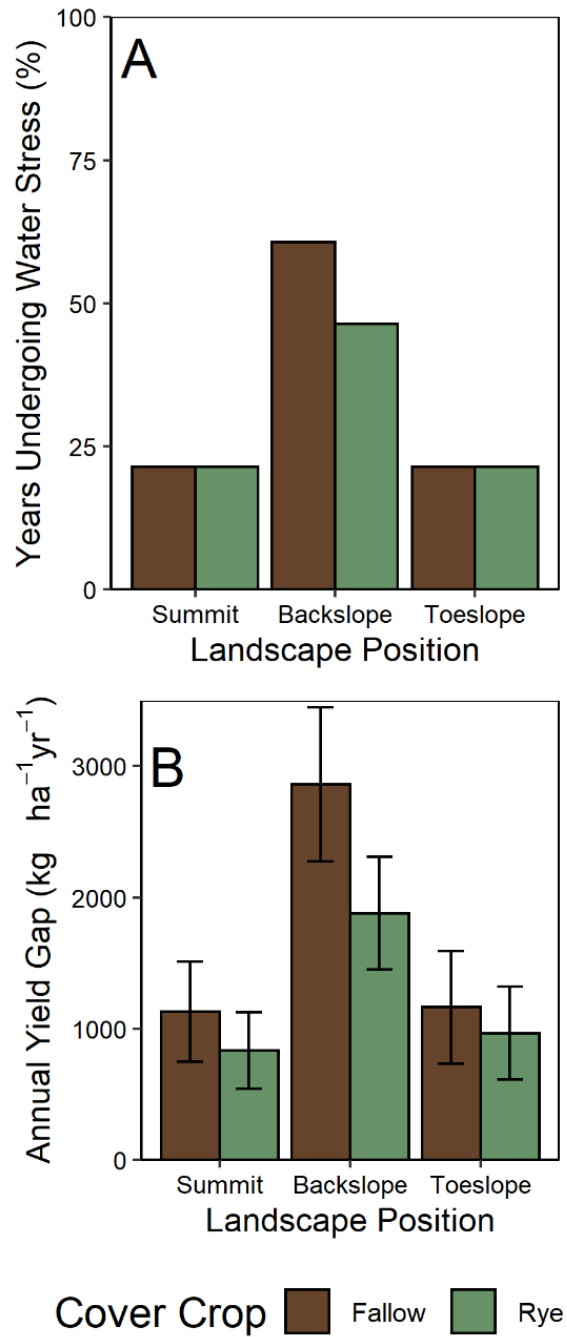


Figure 4.8 –Percentage of years undergoing 10% or greater yield reduction due to water stress (A) and average annual yield gap due to water stress across all simulation years (B) by landscape position and cover crop treatment. Error bars indicate ± 1 SE.

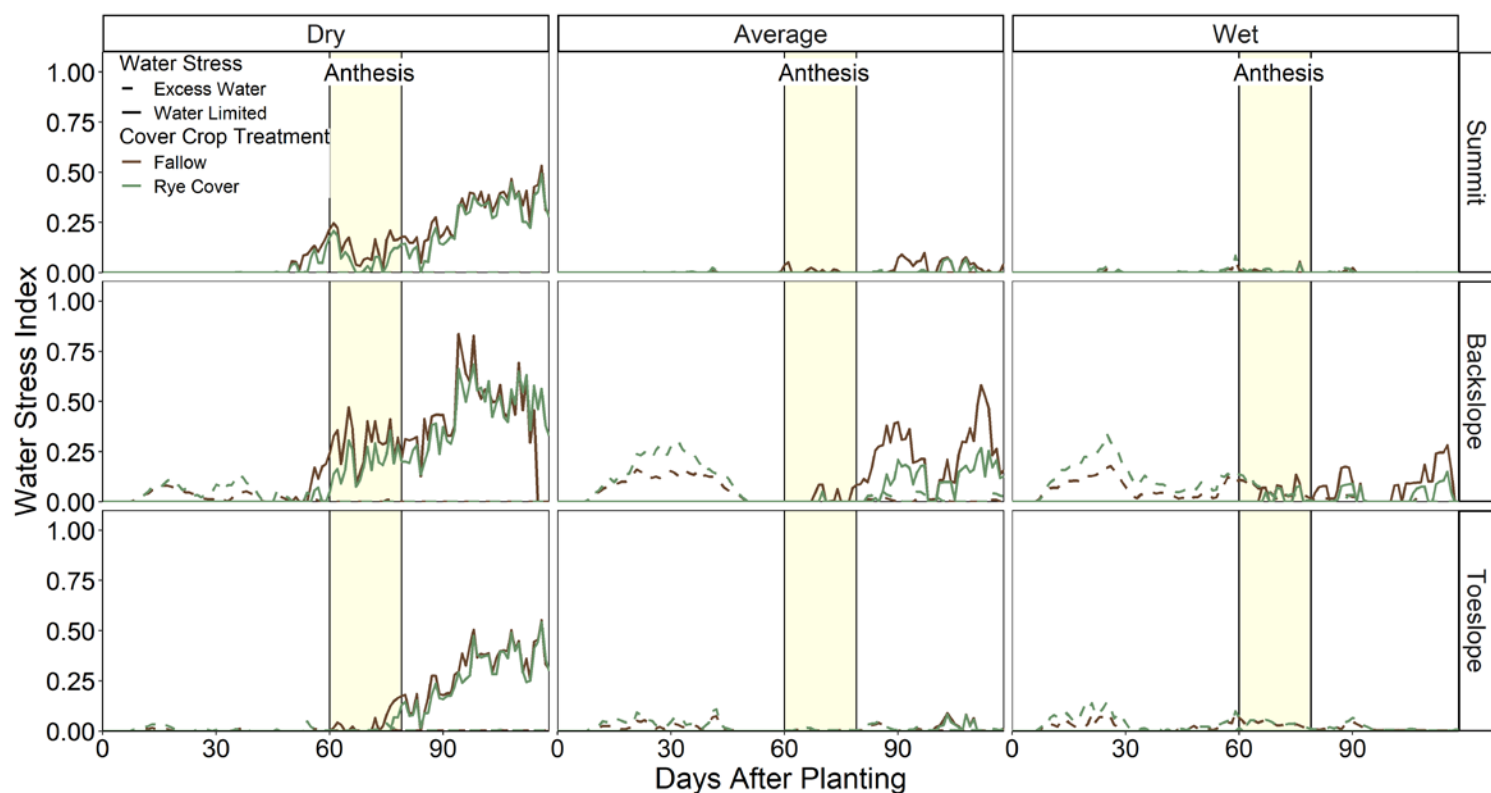


Figure 4.9 - Simulated daily excess and limited water stress index during the corn growing season by weather scenario (dry, average, and wet) and landscape position for each cover crop treatment. Data averaged across 30-year simulations. The shaded yellow bar indicates the range of simulated anthesis dates across the 30-year simulation study.

Table S 4.1 - Full ANOVA tables for yield sensitivity analysis. Top panel reflects results from baseline soil organic matter treatments, lower panel reflects low soil organic matter treatments. The percent sums of squares represent the fraction of sums of squares apportioned to the factor in question compared to the total sums of squares.

Baseline Soil Organic Matter

Factors	DF	Sums Sq	Mean Sq	F-value	P-Value	% Sums of Squares
Summer_Category	2	1286000000	643178746	14.58	6.34E-05	35.48%
Landscape_Position	2	1009000000	504296397	213.946	<2e-16	27.84%
Summer_Category:Landscape_Position	4	33550000	8388605	3.559	0.0125	0.93%
Cover_Crop	1	12233180	12233180	30.452	4.68E-07	0.34%
Summer_Category:Cover_Crop	2	7844370	3922185	9.763	0.00017	0.22%
Landscape_Position:Cover_Crop	2	7071966	3535983	8.802	0.000368	0.20%
Summer_Category:Landscape_Position:Cover_Crop	4	2513429	628357	1.564	0.192646	0.07%
Nitrogen_Rate	1	796576	796576	15.031	0.000158	0.02%
Summer_Category:Nitrogen_Rate	2	1842495	921248	17.383	1.62E-07	0.02%
Landscape_Position:Nitrogen_Rate	2	1846287	923144	17.419	1.58E-07	0.05%
Cover_Crop:Nitrogen_Rate	1	1237115	1237115	23.343	3.32E-06	0.05%
Summer_Category:Landscape_Position:Nitrogen_Rate	4	181149	45287	0.855	0.492906	0.03%
Summer_Category:Cover_Crop:Nitrogen_Rate	2	757748	378874	7.149	0.001082	0.00%
Landscape_Position:Cover_Crop:Nitrogen_Rate	2	607837	303918	5.735	0.003982	0.02%
Summer_Category:Landscape_Position:Cover_Crop:Nitrogen_Rate	4	148144	37036	0.699	0.593902	0.02%
Residuals: Year	150	7949436	52996	-	-	NA
Residuals: Year:Landscape_Position	25	1103000000	44100442	-	-	NA
Residuals: Year:Landscape_Position:Cover_Crop	75	30129284	401724	-	-	NA
Residuals: Within	50	117900000	2357123	-	-	NA
Total Residuals	-	1258978720	-	-	-	35%
Total	-	3624609016	-	-	-	100%

Low Soil Organic Matter

Factors	Df	Sum Sq	Mean Sq	F-Value	P-Value	% Sums of Squares
Summer_Category	2	1034000000	516844252	14.11	7.91E-05	32.58%
Landscape_Position	2	949101108	474550554	228.024	<2e-16	29.90%
Summer_Category:Landscape_Position	4	22253664	5563416	2.673	0.0425	0.70%
Cover_Crop	1	1383947	1383947	5.681	0.01969	0.04%
Summer_Category:Cover_Crop	2	7343723	3671862	15.071	3.15E-06	0.23%
Landscape_Position:Cover_Crop	2	3198037	1599018	6.563	0.00236	0.10%
Summer_Category:Landscape_Position:Cover_Crop	4	810485	202621	0.832	0.50925	0.03%
Nitrogen_Rate	1	47221504	47221504	256.248	< 2e-16	1.49%
Summer_Category:Nitrogen_Rate	2	16913441	8456721	45.891	2.82E-16	0.53%
Landscape_Position:Nitrogen_Rate	2	17052237	8526119	46.267	2.23E-16	0.54%
Cover_Crop:Nitrogen_Rate	1	4975193	4975193	26.998	6.55E-07	0.16%
Summer_Category:Landscape_Position:Nitrogen_Rate	4	3134875	783719	4.253	0.00274	0.10%
Summer_Category:Cover_Crop:Nitrogen_Rate	2	563520	281760	1.529	0.22012	0.02%
Landscape_Position:Cover_Crop:Nitrogen_Rate	2	130360	65180	0.354	0.70267	0.00%
Summer_Category:Landscape_Position:Cover_Crop:Nitrogen_Rate	4	190379	47595	0.258	0.90423	0.01%
Residuals - Year	25	915700000	36627934	-	-	NA
Residuals - Year:Landscape_Position	50	104057093	2081142	-	-	NA
Residuals - Year:Landscape_Position:Cover_Crop	75	18272293	243631	-	-	NA
Residuals - Within	1	27642049	1842	-	-	NA
Total Residuals	-	1065671435	-	-	-	34%
Total	-	3173943908	-	-	-	100%

Table S4.2 - Crop coefficient parameters for the wheat cultivar used to simulate a rye cover crop, and the maize cultivar used in this study

Wheat

	P1V	P1D	P5	G1	G2	G3	PHINT
NEWTON	52	0	500	15	23	2.2	143

Wheat Cultivar Coefficients: P1V – Days required for vernalization at optimum vernalizing temperature; P1D – Photoperiod response (Percent reduction in rate per drop in photoperiod); P5 – Grain filling phase duration in GDD; G1 – Kernel number per unit canopy weight at anthesis (Kernels/gram); G2 – Standard kernel size under optimum conditions (milligrams); G3 – Standard, non-stressed mature tiller weight (grams); PHINT – Phylochron interval, the interval in thermal time between successive leaf tip appearances.

Maize

	P1	P2	P5	G2	G3	PHINT	
PC0004	285	0	800	1070	8.20	38	

Maize Cultivar Coefficients: P1 - Time from seedling emergence to the end of the juvenile phase (GDD); P2 – Extent to which development (expressed as days) is delayed for each hour increase in photoperiod above the longest photoperiod at which development proceeds at a maximum rate (%); P5 – Thermal time from silking to physiological maturity (GDD); G2 - Maximum number of kernels per plant (#); G3 - Kernel filling rate during the linear grain filling stage and under optimum conditions (milligrams/day); PHINT – Phylochron interval, the interval in thermal time between successive leaf tip appearances.

For further discussion of DSSAT CSM Crop Coefficients, please see Jones et al., 2003

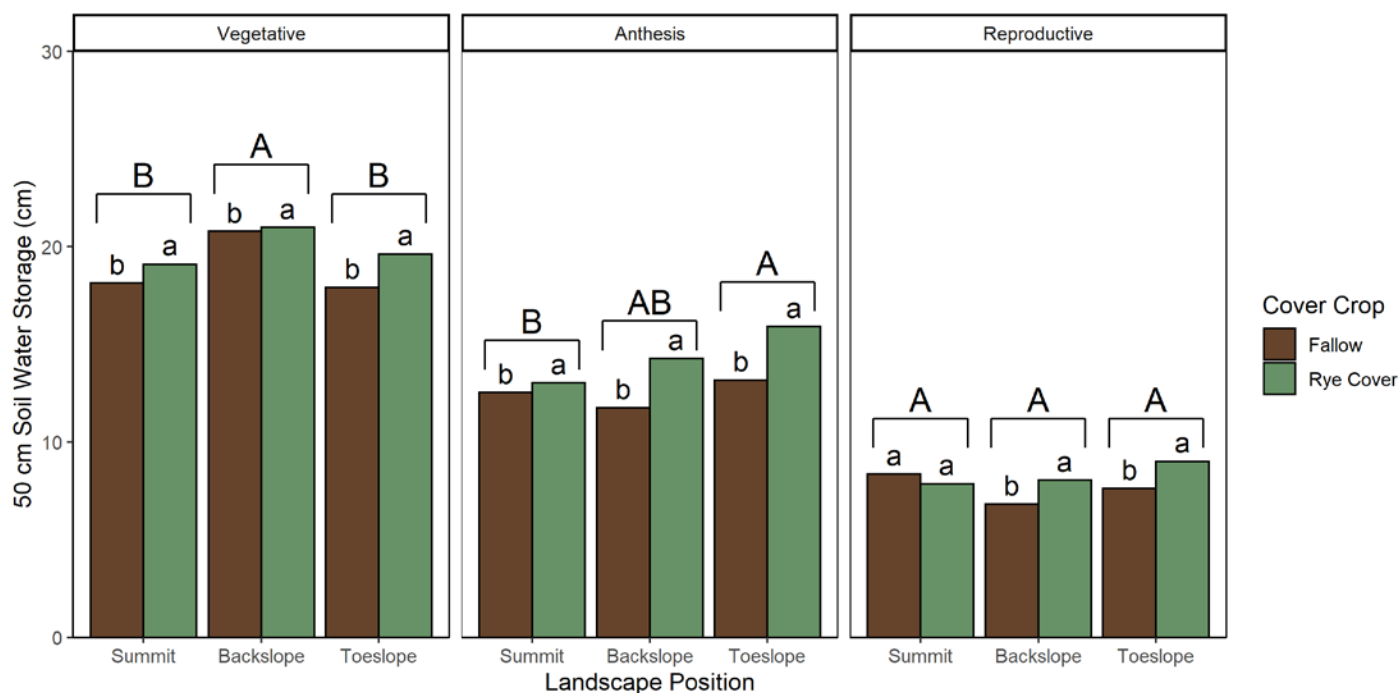


Figure S4.1 - Mean measured soil water storage across key developmental stage in the 2019 field experiment for different landscape positions and cover crop treatments. Capital letters indicate significant differences in soil water storage between landscape position, while lowercase letters indicate significant differences in soil water storage between cover crop treatments.

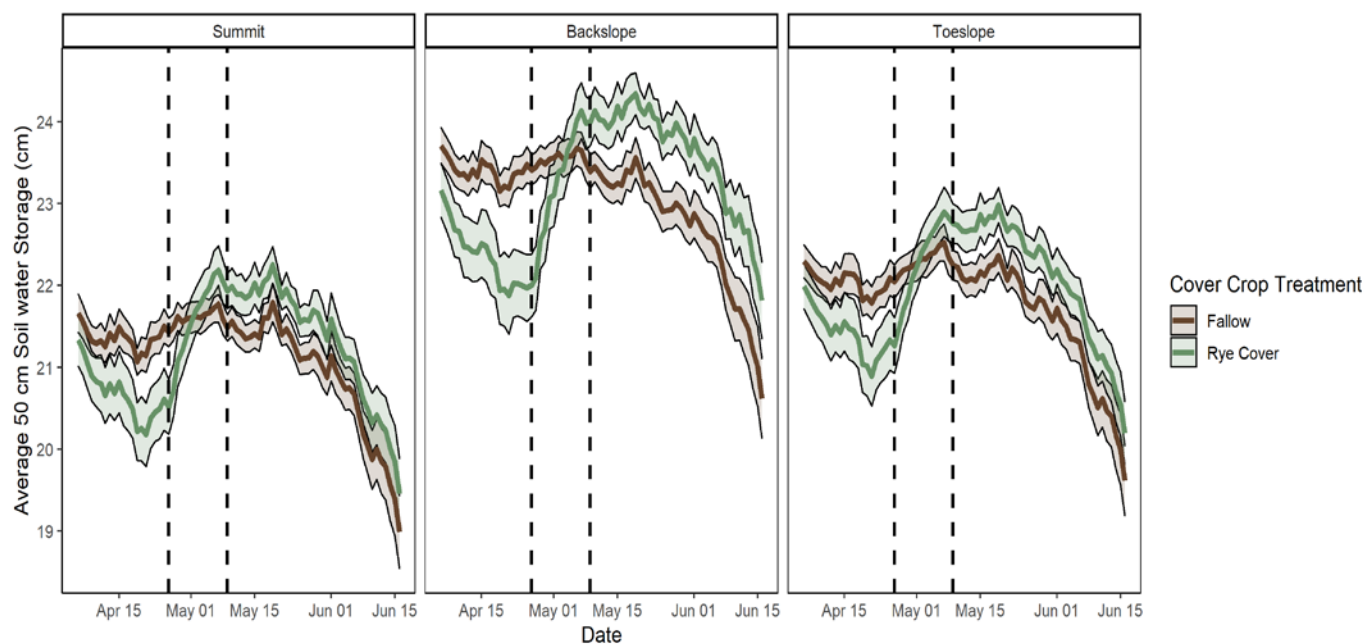


Figure S 4.2 - Average soil water storage across 30 years of data for both the cover crop treatments during spring planting period. The first vertical line indicates the date of cover crop termination, the second indicates the date of maize planting. Shaded areas surrounding the lines represent ± 1 SE.

Appendix

In 2019 and 2020, we conducted field experiments to investigate the interactive effects of cover crop treatment, nitrogen (N) fertilizer rate, and landscape position on maize (*Zea mays* L.) yield. We conducted this experiment at two locations, the Spindletop Research Farm in Lexington, KY (ST; 38.123° N, -84.490° W), and as part of an on-farm collaboration with a local producer outside of Glendale, KY (HC; 37.602° N, -85.906° W), over the course of two years, for a total of four-site years. In both years at the Spindletop sites, the field had been in pasture prior to cultivation for this experiment. At the Hardin County sites, the fields had been in long-term no-till maize-soybean (*Glycine max* (L.) Merr) rotations. In both years of our field trials at Hardin County, the field experiment followed the soybean phase of the rotation. Soil, topographic, and climate data for these sites can be found in Chapter 2 of this thesis.

Plots were arranged in a split-plot randomized complete block experimental design with three replicates at all field sites. At the ST locations all replicates were located on one hillslope each year, with cover crop treatments randomly assigned within a landscape position-replicate combination. At the HC sites, each replicate was placed on a separate hillslope within the producer's field each year, and cover crop treatments were continuous strips across landscape positions. The cover crop treatments included: a sole seeded cereal rye (*Secale cereale* L.), a cereal rye-crimson clover (*Trifolium incarnatum*) mixture, and a no-cover control.

The cover crop treatments were initiated in the preceding fall of each maize growing season (between October 9 and October 21, depending on site-year), chemically terminated in the spring, and left to decompose on the soil surface. Further discussion of cover crop management can be found in Chapter 2 of this thesis. Approximately two weeks after cover crop termination, maize was no-till planted in 76 cm rows at a target population of 76,500 plants ha⁻¹. Maize planting date ranged between April 29 and May 17, depending on site year. Four N rates were established ranging from 0 to 270 kg ha⁻¹. In all plots other than the 0 N treatments, 45 kg ha⁻¹ was applied at planting as 32% urea ammonium nitrate in a “5x5” configuration; 5 cm to the side of the seed, and 5 cm below the soil surface. The remaining amount of the full N fertilizer rate was dribbled on the soil surface as 32% UAN at the V5 growth stage of maize.

At the Spindletop sites, maize yield was measured by hand harvesting ears from two 3.05-m lengths of the center row in each plot s and recording the fresh weight. Eight ears were subsampled, weighed to obtain a fresh weight, and then placed in a 65 °C drier for up to two weeks or until weight did not continue to vary upon subsequent reweighing. A dry weight was obtained from the subsample, and the moisture content of the ears was applied to obtain a dry weight of the 6.1 m sample. The subsample was then shelled, and the cobs and grain weighed separately to obtain a kernel to cob ratio. This ratio was applied to the 6.1 m sample to obtain an estimate of dry grain weight, which was then scaled to a hectare basis. Dry grain weight was then adjusted to 15.5% moisture, consistent with regional commodity moisture content at harvest. At the Hardin County location, maize was harvested using a Wintersteiger Delta research plot combine, and grain yield and moisture were recorded with a HarvestMaster System. Following combining, we measured plot length to derive accurate area estimates of the combined area and

data were adjusted to 15.5% moisture and scaled to a hectare basis. Average maize yield across treatments is presented in Table A1.

Topographic data were generated in ArcMap 10.7.1, using elevation data retrieved from the Kentucky State LiDAR Data Repository (Kentucky Division of Geographic Information, 2017). Linear regression between maize yield and the topographic factors were calculated for each field site across cover crop landscape position treatments using R (R Core Team, 2020). In our analysis of response to topographic factors, we chose to use the N rate most closely aligned with University of Kentucky recommendations, 180 kg ha⁻¹. Topographic data was generated at the subplot scale, such that each regression consisted of 27 points. Pearson correlation coefficients were retrieved from the summary of each linear regression. The coefficient of variation was calculated in for each site as well as a measure of total spatial yield variability. Correlation coefficients and CV are presented in Table A1.

Weather data for Spindletop farm was collected from the University of Kentucky Ag Weather Center's weather monitoring station located ~ 1 km from both field sites which collects daily minimum, maximum, and average air temperature, as well as daily cumulative precipitation. Hardin County weather data was collected with a research grade weather station installed at the field site each year. Cumulative spring and growing season precipitation for each site-year is presented in Table A1.

Table A1 – Precipitation and yield data for each site year, and the Pearson correlation coefficients for each site-year of experimental field trials presented in Chapter 3.

Site	Year	Crop	Growing Season Rainfall (mm)	Spring Rainfall (mm)	Average Yield (Mg ha ⁻¹)	Yield CV	Slope Correlation	Elevation Correlation	Planar Curvature Correlation	Profile Curvature Correlation
Spindletop	2019	Maize	624	323	11.10	31.9	-0.67	-0.56	0.05	0.20
Spindletop	2020	Maize	599	365	14.14	14.1	-0.50	-0.17	-0.62	0.20
Hardin County	2019	Maize	701	350	11.61	29.3	-0.41	-0.42	0.10	0.29
Hardin County	2020	Maize	681	341	15.92	14.1	-0.62	-0.53	0.05	0.07

Growing season precipitation encompasses the period between March 1 and August 31; Spring rainfall is defined as the period between March 1 and May 31.

REFERENCES

- Abendroth, L.J., Elmore, R.W., Boyer, M.J., Marlay, S.K., 2011. Corn Growth and Development, 1st ed. Iowa State University, Ames, IA.
- Adhikari, P., Omani, N., Ale, S., DeLaune, P.B., Thorp, K.R., Barnes, E.M.,
Hoogenboom, G., 2017. Simulated effects of winter wheat cover crop on cotton production systems of the Texas rolling plains. *Trans. ASABE* 60, 2083–2096.
<https://doi.org/10.13031/trans.12272>
- Albarenque, S.M., Basso, B., Caviglia, O.P., Melchiori, R.J.M., 2016. Spatio-temporal nitrogen fertilizer response in maize: Field study and modeling approach. *Agron. J.* 108, 2110–2122. <https://doi.org/10.2134/agronj2016.02.0081>
- Allen, R.G., Pereira, L.S., Raes, D., Smith, M., 1998. Crop Evapotranspiration-
Guidelines for computing crop water requirements. FAO Irrig. Drain. Pap. No. 56.
- Alonso-Ayuso, M., Gabriel, J.L., Quemada, M., 2014. The kill date as a management tool for cover cropping success. *PLoS One* 9. <https://doi.org/10.1371/journal.pone.0109587>
- Ampontuah, E.O., Robinson, J.S., Nortcliff, S., 2006. Assessment of soil particle redistribution on two contrasting cultivated hillslopes. *Geoderma* 132, 324–343.
<https://doi.org/10.1016/j.geoderma.2005.05.014>
- Anthony, P., Malzer, G., Sparrow, S., Zhang, M., 2012. Soybean yield and quality in relation to soil properties. *Agron. J.* 104, 1443–1458.
<https://doi.org/10.2134/agronj2012.0095>

- Armstrong, K., 2013. Evalutayion of Reclaimed coal-mined prime farmland based on soil characteristics in lieu of the current yield based approach. Universtiy of Illinois at Urbana-Champaign.
- Bakker, M.G., Acharya, J., Moorman, T.B., Robertson, A.E., Kaspar, T.C., 2016. The potential for cereal rye cover crops to host corn seedling pathogens. *Phytopathology* 106, 591–601. <https://doi.org/10.1094/PHYTO-09-15-0214-R>
- Basche, A., DeLonge, M., 2017. The Impact of Continuous Living Cover on Soil Hydrologic Properties: A Meta-Analysis. *Soil Sci. Soc. Am. J.* 81, 1179–1190. <https://doi.org/10.2136/sssaj2017.03.0077>
- Basche, Andrea D, Archontoulis, S. V, Kaspar, T.C., Jaynes, D.B., Parkin, T.B., Miguez, F.E., 2016. Simulating long-term impacts of cover crops and climate change on crop production and environmental outcomes in the Midwestern United States. *Agric. Ecosyst. Environ.* 218, 95–106. <https://doi.org/10.1016/j.agee.2015.11.011>
- Basche, Andrea D., Kaspar, T.C., Archontoulis, S. V., Jaynes, D.B., Sauer, T.J., Parkin, T.B., Miguez, F.E., 2016. Soil water improvements with the long-term use of a winter rye cover crop. *Agric. Water Manag.* 172, 40–50. <https://doi.org/10.1016/j.agwat.2016.04.006>
- Basso, B., Dumont, B., Cammarano, D., Pezzuolo, A., Marinello, F., Sartori, L., 2016. Environmental and economic benefits of variable rate nitrogen fertilization in a nitrate vulnerable zone. *Sci. Total Environ.* 545–546, 227–235. <https://doi.org/10.1016/j.scitotenv.2015.12.104>
- Basso, B., Ritchie, J.T., 2015. Simulating Crop Growth and Biogeochemical Fluxes in

- Response to Land Management Using the SALUS Model. *Ecol. Agric. Landscapes*
Long term Res. path to Sustain. 252–274.
- Basso, B., Ritchie, J.T., Cammarano, D., Sartori, L., 2011. A strategic and tactical
management approach to select optimal N fertilizer rates for wheat in a spatially
variable field. *Eur. J. Agron.* 35, 215–222. <https://doi.org/10.1016/j.eja.2011.06.004>
- Basso, B., Shuai, G., Zhang, J., Robertson, G.P., 2019. Yield stability analysis reveals
sources of large-scale nitrogen loss from the US Midwest. *Sci. Rep.* 1–9.
<https://doi.org/10.1038/s41598-019-42271-1>
- Bates, D., Mächler, M., Bolker, B.M., Walker, S.C., 2015. Fitting Linear Mixed-Effects
Models Using lme4. *J. Stat. Softw.* 67, 1–48. <https://doi.org/10.18637/jss.v067.i01>
- Battisti, R., Sentelhas, P.C., 2017. Improvement of soybean resilience to drought through
deep root system in Brazil. *Agron. J.* 109, 1612–1622.
<https://doi.org/10.2134/agronj2017.01.0023>
- Beehler, J., Fry, J., Negassa, W., Kravchenko, A., 2017. Impact of cover crop on soil
carbon accrual in topographically diverse terrain. *J. Soil Water Conserv.* 72, 272–
279. <https://doi.org/10.2489/jswc.72.3.272>
- Bennett, A.J., Bending, G.D., Chandler, D., Hilton, S., Mills, P., 2012. Meeting the
demand for crop production: The challenge of yield decline in crops grown in short
rotations. *Biol. Rev.* 87, 52–71. <https://doi.org/10.1111/j.1469-185X.2011.00184.x>
- Blanco-Canqui, H., Shaver, T.M., Lindquist, J.L., Shapiro, C.A., Elmore, R.W., Francis,
C.A., Hergert, G.W., 2015. Cover Crops and Ecosystem Services: Insights from

- Studies in Temperate Soils. *Agron. J.* 107, 2449–2474.
<https://doi.org/10.2134/agronj15.0086>
- Blesh, J., 2019. Feedbacks between nitrogen fixation and soil organic matter increase ecosystem functions in diversified agroecosystems. *Ecol. Appl.* 29, 1–12.
<https://doi.org/10.1002/eap.1986>
- Blesh, J., 2018. Functional traits in cover crop mixtures : Biological nitrogen fixation and multifunctionality. *J. Appl. Ecol.* 55, 38–48.
- Bommarco, R., Kleijn, D., Potts, S.G., 2013. Ecological intensification: Harnessing ecosystem services for food security. *Trends Ecol. Evol.* 28, 230–238.
<https://doi.org/10.1016/j.tree.2012.10.012>
- Bommarco, R., Vico, G., Hallin, S., 2018. Exploiting ecosystem services in agriculture for increased food security. *Glob. Food Sec.* 17, 57–63.
<https://doi.org/https://doi.org/10.1016/j.gfs.2018.04.001>
- Bowles, T.M., Mooshammer, M., Socolar, Y., Schmer, M.R., Strock, J., Grandy, A.S., 2020. Long-Term Evidence Shows that Crop-Rotation Diversification Increases Agricultural Resilience to Adverse Growing Conditions in North America Article Long-Term Evidence Shows that Crop-Rotation Diversification Increases Agricultural Resilience to Adverse G. *One Earth* 2, 1–10.
<https://doi.org/10.1016/j.oneear.2020.02.007>
- Brandi-Dohrn, F.M., Hess, M., Selker, J.S., Dick, R.P., Kauffman, S.M., Hemphill, D.D., 1997. Nitrate Leaching under a Cereal Rye Cover Crop. *J. Environ. Qual.* 26, 181–188. <https://doi.org/10.2134/jeq1997.00472425002600010026x>

Brubaker, S.C., Jones, A.J., Lewis, D.T., Frank, K., 1990. Soil Properties Associated with Landscape Position 235–239.

Burke, I.C., Elliott, E.T., Cole, C.V., Ecological Applications, 1995. Influence of Macroclimate , Landscape Position , and Management on Soil Organic Matter in Agroecosystems Authors (s): Ingrid C . Burke , Edward T . Elliott and C . Vernon Cole Published by : Wiley Stable URL : <http://www.jstor.org/stable/1942057> REFERENCE 5, 124–131.

Burt, R., Reinsch, T.G., Miller, W.P., 1993. A micro-pipette method for water dispersible clay. Commun. Soil Sci. Plant Anal. 24, 2531–2544.
<https://doi.org/10.1080/00103629309368975>

Canessa, R., Brink, L., Saldaña, A., Rios, R.S., Hättenschwiler, S., Mueller, C.W., Prater, I., Tielbörger, K., Bader, M.Y., 2020. Relative effects of climate and litter traits on decomposition change with time, climate and trait variability. J. Ecol. 0–2.
<https://doi.org/10.1111/1365-2745.13516>

Cavigelli, M.A., Lengnick, L.L., Buyer, J.S., Fravel, D., Handoo, Z., McCarty, G., Millner, P., Sikora, L., Wright, S., Vinyard, B., Rabenhorst, M., 2005. Landscape level variation in soil resources and microbial properties in a no-till corn field. Appl. Soil Ecol. 29, 99–123. <https://doi.org/10.1016/j.apsoil.2004.12.007>

Chen, B., Liu, E., Tian, Q., Yan, C., Zhang, Y., 2014. Soil nitrogen dynamics and crop residues. A review. Agron. Sustain. Dev. 34, 429–442.
<https://doi.org/10.1007/s13593-014-0207-8>

Chi, B.-L., Bing, C.-S., Walley, F., Yates, T., 2009. Topographic Indices and Yield

- Variability in a Rolling Landscape of Western Canada. *Pedosphere* 19, 362–370.
[https://doi.org/10.1016/S1002-0160\(09\)60127-2](https://doi.org/10.1016/S1002-0160(09)60127-2)
- Clark, A., 2007. *Managing Cover Crops Properly*, 3rd ed. Sustainable Agriculture Research and Education, College Park, MD.
- Coppens, F., Garnier, P., De Gryze, S., Merckx, R., Recous, S., 2006. Soil moisture, carbon and nitrogen dynamics following incorporation and surface application of labelled crop residues in soil columns. *Eur. J. Soil Sci.* 57, 894–905.
<https://doi.org/10.1111/j.1365-2389.2006.00783.x>
- Corre, M.D., Schnabel, R.R., Stout, W.L., 2002. Spatial and seasonal variation of gross nitrogen transformations and microbial biomass in a Northeastern US grassland. *Soil Biol. Biochem.* 34, 445–457.
- Cox, M.S., Gerard, P.D., 2007. Soil management zone determination by yield stability analysis and classification. *Agron. J.* 99, 1357–1365.
<https://doi.org/10.2134/agronj2007.0041>
- Craine, J.M., Fierer, N., McLauchlan, K.K., 2010. Widespread coupling between the rate and temperature sensitivity of organic matter decay. *Nat. Geosci.* 3, 854–857.
<https://doi.org/10.1038/ngeo1009>
- Crews, T.E., Peoples, M.B., 2005. Can the synchrony of nitrogen supply and crop demand be improved in legume and fertilizer-based agroecosystems? A review. *Nutr. Cycl. Agroecosystems* 72, 101–120. <https://doi.org/10.1007/s10705-004-6480-1>

- Crutchfield, J.D., Grove, J.H., 2011. A New Cadmium Reduction Device for the Microplate Determination of Nitrate in Water, Soil, Plant Tissue, and Physiological Fluids. *J. AOAC Int.* 94, 1896–1905. <https://doi.org/10.5740/jaoacint>
- De Baets, S., Poesen, J., Meersmans, J., Serlet, L., 2011. Cover crops and their erosion-reducing effects during concentrated flow erosion. *Catena* 85, 237–244. <https://doi.org/10.1016/j.catena.2011.01.009>
- Desclaux, D., Huynh, T.-T., Roumet, P., 2000. Identification of Soybean Plant Characteristics That Indicate the Timing of Drought Stress. *Crop Sci.* 40, 716–722.
- Dharmakeerthi, R.S., Kay, B.D., Beauchamp, E.G., 2005. Factors Contributing to Changes in Plant Available Nitrogen across a Variable Landscape. *Soil Sci. Soc. Am. J.* 69, 453–462. <https://doi.org/10.2136/sssaj2005.0453>
- Dietzel, R., Liebman, M., Ewing, R., Helmers, M., Horton, R., Jarchow, M., Archontoulis, S., 2016. How efficiently do corn- and soybean-based cropping systems use water? A systems modeling analysis. *Glob. Chang. Biol.* 22, 666–681. <https://doi.org/10.1111/gcb.13101>
- Findeling, A., Garnier, P., Coppens, F., Lafolie, F., Recous, S., 2007. Modelling water, carbon and nitrogen dynamics in soil covered with decomposing mulch. *Eur. J. Soil Sci.* 58, 196–206. <https://doi.org/10.1111/j.1365-2389.2006.00826.x>
- Finney, D.M., Kaye, J.P., 2017. Functional diversity in cover crop polycultures increases multifunctionality of an agricultural system 509–517. <https://doi.org/10.1111/1365-2664.12765>

- Finney, D.M., Murrell, E.G., White, C.M., Baraibar, B., Barbercheck, M.E., Bradley, B.A., Cornelisse, S., Hunter, M.C., Kaye, J.P., Mortensen, D.A., Mullen, C.A., Schipanski, M.E., 2017. Ecosystem Services and Disservices Are Bundled in Simple and Diverse Cover Cropping Systems. *Agric. Environ. Lett.* 2, 170033.
<https://doi.org/10.2134/ael2017.09.0033>
- Finney, D.M., White, C.M., Kaye, J.P., 2016. Biomass Production and Carbon/Nitrogen Ratio Influence Ecosystem Services from Cover Crop Mixtures.
<https://doi.org/10.2134/agronj15.0182>
- Florence, A.M., McGuire, A.M., 2020. Do diverse cover crop mixtures perform better than monocultures? A systematic review. *Agron. J.* 112, 3513–3534.
<https://doi.org/10.1002/agj2.20340>
- Galloway, J.N., Aber, J.D., Erisman, J.W., Seitzinger, S.P., Howarth, R.W., Cowling, E.B., Cosby, B.J., 2003. The nitrogen cascade. *Bioscience* 53, 341–356.
[https://doi.org/10.1641/0006-3568\(2003\)053\[0341:TNC\]2.0.CO;2](https://doi.org/10.1641/0006-3568(2003)053[0341:TNC]2.0.CO;2)
- Gaudin, A.C.M., Tolhurst, T.N., Ker, A.P., Janovicek, K., Tortora, C., 2015. Increasing Crop Diversity Mitigates Weather Variations and Improves Yield Stability. *PLoS One* 10, 1–20. <https://doi.org/10.1371/journal.pone.0113261>
- Green, T.R., Erskine, R.H., 2004. Measurement , scaling , and topographic analyses of spatial crop yield and soil water content. *Hydrol. Process.* 18, 1447–1465.
<https://doi.org/10.1002/hyp.1422>
- Guretzky, J.A., Moore, K.J., Burras, C.L., Brummer, E.C., 2004. Distribution of legumes along gradients of slope and soil electrical conductivity in pastures. *Agron. J.* 96,

547–555. <https://doi.org/10.2134/agronj2004.5470>

- Haddix, M.L., Gregorich, E.G., Helgason, B.L., Janzen, H., Ellert, B.H., Francesca Cotrufo, M., 2020. Climate, carbon content, and soil texture control the independent formation and persistence of particulate and mineral-associated organic matter in soil. *Geoderma* 363, 114160. <https://doi.org/10.1016/j.geoderma.2019.114160>
- Hanna, A.Y., Harlan, P.W., Lewis, D.T., 1982. Soil Available Water as Influenced by Landscape Position and Aspect 1. *Agron. J.* 74, 999–1004. <https://doi.org/10.2134/agronj1982.00021962007400060016x>
- Harmony, K.R., Moore, K.J., Brummer, E.C., Lee Burras, C., George, J.R., 2001. Spatial legume composition and diversity across seeded landscapes. *Agron. J.* 93, 992–1000. <https://doi.org/10.2134/agronj2001.935992x>
- Hothorn, T., Bretz, F., Westfall, P., 2008. Simultaneous Inference in General Parametric Models. Technical Report Number 019. *Biometrical J.* 50, 346–363.
- Huang, X., Wang, L., Yang, L., Kravchenko, A.N., 2008. Management Effects on Relationships of Crop Yields with Topography Represented by Wetness Index and Precipitation. *Agron. J.* 100, 1463–1471. <https://doi.org/10.2134/agronj2007.0325>
- Jaynes, D.B., Kaspar, T.C., Colvin, T.S., James, D.E., 2003. Cluster Analysis of Spatiotemporal Corn Yield Patterns in an Iowa Field. *Agron. J.* 95, 574. <https://doi.org/10.2134/agronj2003.0574>
- Jiang, P., Thelen, K.D., 2004. Effect of Soil and Topographic Properties on Crop Yield in a North-Central Corn – Soybean Cropping System. *Agron. J.* 96, 252–258.

- Jones, J., Hoogenboom, G., Porter, C., Boote, K., Batchelor, W., Hunt, L., Wilkens, P., Singh, U., Gijsman, A., Ritchie, J., 2003. The DSSAT cropping system model. *Eur. J. Agron.* 18, 235–265. [https://doi.org/10.1016/S1161-0301\(02\)00107-7](https://doi.org/10.1016/S1161-0301(02)00107-7)
- Kaspar, T.C., Colvin, T.S., Jaynes, D.B., 2003. Relationship Between Six Years of Corn Yields and Terrain Attributes 87–101.
- Kaspar, T.C., Jaynes, D.B., Parkin, T.B., Moorman, T.B., Singer, J.W., 2012. Effectiveness of oat and rye cover crops in reducing nitrate losses in drainage water. *Agric. Water Manag.* 110, 25–33. <https://doi.org/10.1016/j.agwat.2012.03.010>
- Kaspar, T.C., Pulido, D.J., Fenton, T.E., Colvin, T.S., Karlen, D.L., Jaynes, D.B., Meek, D.W., 2004. Relationship of Corn and Soybean Yield to Soil and Terrain Properties 709, 700–709.
- Kassambara, A., Mundt, F., 2020. factoextra: Extract and Visualize the results of Multivariate Data Analyses.
- Kaye, J.P., Finney, D., White, C., Bradley, B., Schipanski, M., Alonso-ayuso, M., Hunter, M., Burgess, M., Mejia, C., 2019. Managing nitrogen through cover crop species selection in the U.S. mid-Atlantic. *PLoS One* 14, 1–23.
- Kaye, J.P., Quemada, M., 2017. Using cover crops to mitigate and adapt to climate change . A review. *Agron. Sustain. Dev.* 37, 1–17.
- Kentucky Division of Geographic Information, 2017. KYAPED Kentucky 5 foot Digital Elevation Model (DEM). Frankfort, Kentucky.
- Khakural, B.R., Robert, P.C., Mulla, D.J., 1996. Relating Corn/Soybean Yield to

- Variability in Soil and Landscape Characteristics, in: Robert, P.C., Rust, R.H., Larson, W.E. (Eds.), Proceedings of the Third International Conference on Precision Agriculture. ASA-CSSA-SSSA, Madison, WI.
- <https://doi.org/https://doi.org/10.2134/1996.precisionagproc3.c12>
- Kitchen, N.R., Drummond, S.T., Lund, E.D., Sudduth, K.A., Buchleiter, G.W., 2003. Soil Electrical Conductivity and Topography Related to Yield for Three Contrasting Soil–Crop Systems. *Agron. J.* 95, 483–495.
- Knott, C.A., 2016. Identifying Wheat Growth Stages. University Kentucky Ext. Bull. AGR-224, 1–8.
- Kravchenko, A.N., Bullock, D.G., 2000. Correlation of Corn and Soybean Grain Yield with Topography and Soil Properties. *Agron. J.* 92, 75–83.
- Kravchenko, A.N., Robertson, G.P., Thelen, K.D., Harwood, R.R., 2005. Management, Topographical, and Weather Effects on Spatial Variability of Crop Grain Yields. *Agron. J.* 97, 514–523.
- Kravchenko, A.N., Snapp, S.S., Robertson, G.P., 2017. Field-scale experiments reveal persistent yield gaps in low-input and organic cropping systems. *Proc. Natl. Acad. Sci. U. S. A.* 114, 926–931. <https://doi.org/10.1073/pnas.1612311114>
- Krueger, E.S., Ochsner, T.E., Porter, P.M., Baker, J.M., 2011. Winter rye cover crop management influences on soil water, soil nitrate, and corn development. *Agron. J.* 103, 316–323. <https://doi.org/10.2134/agronj2010.0327>
- Kumhalova, J., Kumhala, F., Kroulik, M., Matejkova, S., 2011. The impact of

- topography on soil properties and yield and the effects of weather conditions. *Precis. Agric.* 12, 813–830. <https://doi.org/10.1007/s11119-011-9221-x>
- Kumhálová, J., Kumhála, F., Kroulík, M., Matějková, Š., 2011. The impact of topography on soil properties and yield and the effects of weather conditions. *Precis. Agric.* 12, 813–830. <https://doi.org/10.1007/s11119-011-9221-x>
- Kuo, S., Jellum, E.J., 2002. Influence of winter cover crop and residue management on soil nitrogen availability and corn. *Agron. J.* 94, 501–508. <https://doi.org/10.2134/agronj2002.5010>
- Lacey, C., Nevins, C., Camberato, J., Kladvík, E., Sadeghpour, A., Armstrong, S., 2020. Carbon and nitrogen release from cover crop residues and implications for cropping systems management. *J. Soil Water Conserv.* jswc.2020.00102. <https://doi.org/10.2489/jswc.2020.00102>
- Ladoni, M., Basir, A., Robertson, P.G., Kravchenko, A.N., 2016. Scaling-up : cover crops differentially influence soil carbon in agricultural fields with diverse topography. *Agric. Ecosyst. Environ.* 225, 93–103. <https://doi.org/10.1016/j.agee.2016.03.021>
- Ladoni, M., Kravchenko, A.N., Robertson, G.P., 2015. Topography Mediates the Influence of Cover Crops on Soil Nitrate Levels in Row Crop Agricultural Systems. *PLoS One* 10, 1–17. <https://doi.org/10.1371/journal.pone.0143358>
- Leuthold, S.J., Salmerón, M., Wendroth, O., Poffenbarger, H., 2021. Cover crops decrease maize yield variability in sloping landscapes through increased water during reproductive stages. *F. Crop. Res.* 265, 108111. <https://doi.org/10.1016/j.fcr.2021.108111>

- Li, L., Malone, R.W., Ma, L., Kaspar, T.C., Jaynes, D.B., Saseendran, S.A., Thorp, K.R., Yu, Q., Ahuja, L.R., 2008. Winter cover crop effects on nitrate leaching in subsurface drainage as simulated by RZWQM-DSSAT. *Trans. ASABE* 51, 1575–1583.
- Lobell, D.B., Azzari, G., 2017. Satellite detection of rising maize yield heterogeneity in the U . S . Midwest Satellite detection of rising maize yield heterogeneity in the U . S . Midwest. <https://doi.org/10.1088/1748-9326/aa5371>
- Lupwayi, N.Z., Clayton, G.W., O'Donovan, J.T., Harker, K.N., Turkington, T.K., Rice, W.A., 2004. Decomposition of crop residues under conventional and zero tillage. *Can. J. Soil Sci.* 84, 403–410. <https://doi.org/10.4141/S03-082>
- Ma, L., Peterson, G.A., Ahuja, L.R., Sherrod, L., Shaffer, M.J., Rojas, K.W., 1999. Decomposition of surface crop residues in long-term studies of dryland agroecosystems. *Agron. J.* 91, 401–409. <https://doi.org/10.2134/agronj1999.00021962009100030008x>
- Maestrini, B., Basso, B., 2018a. Predicting spatial patterns of within-field crop yield variability. *F. Crop. Res.* 219, 106–112. <https://doi.org/10.1016/j.fcr.2018.01.028>
- Maestrini, B., Basso, B., 2018b. Drivers of within-field spatial and temporal variability of crop yield across the US Midwest. *Sci. Rep.* 8, 14833. <https://doi.org/10.1038/s41598-018-32779-3>
- Malone, R.W., Kersebaum, K.C., Kaspar, T.C., Ma, L., Jaynes, D.B., Gillette, K., 2017. Winter rye as a cover crop reduces nitrate loss to subsurface drainage as simulated by HERMES. *Agric. Water Manag.* 184, 156–169.

<https://doi.org/10.1016/j.agwat.2017.01.016>

Martinez-Feria, R.A., Basso, B., 2020. Unstable crop yields reveal opportunities for site-specific adaptations to climate variability. *Sci. Rep.* 10.

<https://doi.org/10.1038/s41598-020-59494-2>

Martinez-Feria, R.A., Castellano, M.J., Dietzel, R.N., Helmers, M.J., Liebman, M., Huber, I., Archontoulis, S. V, 2018. Linking crop- and soil-based approaches to evaluate system nitrogen-use efficiency and tradeoffs. *Agric. Ecosyst. Environ.* 256, 131–143. <https://doi.org/10.1016/j.agee.2018.01.002>

Martinez-Feria, R.A., Dietzel, R., Liebman, M., Helmers, M.J., Archontoulis, S. V, 2016. Rye cover crop effects on maize : A system-level analysis. *F. Crop. Res.* 196, 145–159. <https://doi.org/10.1016/j.fcr.2016.06.016>

McCracken, D. V., Smith, M.S., Grove, J.H., Blevins, R.L., MacKown, C.T., 1994. Nitrate Leaching as Influenced by Cover Cropping and Nitrogen Source. *Soil Sci. Soc. Am. J.* 58, 1476. <https://doi.org/10.2136/sssaj1994.03615995005800050029x>

McNunn, G., Heaton, E., Archontoulis, S., Licht, M., VanLoocke, A., 2019. Using a Crop Modeling Framework for Precision Cost-Benefit Analysis of Variable Seeding and Nitrogen Application Rates. *Front. Sustain. Food Syst.* 3, 1–15. <https://doi.org/10.3389/fsufs.2019.00108>

Mearns, L.O., Rosenzweig, C., Goldberg, R., 1996. The effect of changes in daily and interannual climatic variability on cereals-wheat: A sensitivity study. *Clim. Change* 32, 257–292. <https://doi.org/10.1007/BF00142465>

- Meisinger, J.J., Ricigliano, K.A., 2017. Nitrate Leaching from Winter Cereal Cover Crops Using Undisturbed Soil-Column Lysimeters. *J. Environ. Qual.* 46, 576–584. <https://doi.org/10.2134/jeq2016.09.0372>
- Meng, L., Quiring, S.M., 2008. A comparison of soil moisture models using soil climate analysis network observations. *J. Hydrometeorol.* 9, 641–659. <https://doi.org/10.1175/2008JHM916.1>
- Miller, K.S., Geisseler, D., 2018. Temperature sensitivity of nitrogen mineralization in agricultural soils. *Biol. Fertil. Soils* 54, 853–860. <https://doi.org/10.1007/s00374-018-1309-2>
- Miller, W.P., Miller, D.M., 1987. Micro-pipette method for soil mechanical analysis. *Commun. Soil Sci. Plant Anal.* 18, 1–15.
- Munoz, J.D., Steibel, J.P., Snapp, S., Kravchenko, A.N., 2014. Cover crop effect on corn growth and yield as influenced by topography. *Agric. Ecosyst. Environ.* 189, 229–239. <https://doi.org/10.1016/j.agee.2014.03.045>
- Negassa, W., Price, R.F., Basir, A., Snapp, S.S., Kravchenko, A., 2015. Cover crop and tillage systems effect on soil CO₂ and N₂O fluxes in contrasting topographic positions. *Soil Tillage Res.* 154, 64–74. <https://doi.org/10.1016/j.still.2015.06.015>
- Nevens, C.J., Lacey, C., Armstrong, S., 2020. The synchrony of cover crop decomposition, enzyme activity, and nitrogen availability in a corn agroecosystem in the Midwest United States. *Soil Tillage Res.* 197, 104518. <https://doi.org/10.1016/j.still.2019.104518>

- Nolan, B.T., Ruddy, B.C., Hitt, K.J., Helsel, D.R., 1997. Risk of nitrate in groundwaters of the United States - A national perspective. *Environ. Sci. Technol.* 31, 2229–2236. <https://doi.org/10.1021/es960818d>
- Osipitan, O.A., Dille, J.A., Assefa, Y., Knezevic, S.Z., 2018. Cover crop for early season weed suppression in crops: Systematic review and meta-analysis. *Agron. J.* 110, 2211–2221. <https://doi.org/10.2134/agronj2017.12.0752>
- Paltineanu, I.C., Starr, J.L., 1997. Real-time Soil Water Dynamics Using Multisensor Capacitance Probes: Laboratory Calibration. *Soil Sci. Soc. Am. J.* 61, 1576–1585. <https://doi.org/10.2136/sssaj1997.03615995006100060006x>
- Papiernik, S.K., Lindstrom, M.J., Schumacher, J.A., Farenhorst, A., Stephens, K.D., Schumacher, T.E., 2005. Variation in soil properties and crop yield across an eroded prairie landscape.
- Parr, J.F., Papendick, R.I., 1978. Factors Affecting the Decomposition of Crop Residues by Microorganisms, in: *Crop Residue Management Systems*. ASA, CSSA, SSSA, Madison, WI, pp. 101–129. <https://doi.org/10.2134/asaspecpub31.c6>
- Parton, W., Stewart, J.W., Cole, C.V., 1988. Dynamics of C , N , P and S in grassland soils: a model. *Biogeochemistry* 5, 109–131.
- Parton, W.J., Ojima, D.S., Cole, C.V., Schimel, D.S., 1994. A General Model for Soil Organic Matter Dynamics : Sensitivity to Litter Chemistry , Texture and Management, in: *Quantitative Modeling of Soil Forming Processes*. Soil Science Society of America, Madison, WI, pp. 147–167.

- Pietikäinen, J., Pettersson, M., Bååth, E., 2005. Comparison of temperature effects on soil respiration and bacterial and fungal growth rates. *FEMS Microbiol. Ecol.* 52, 49–58. <https://doi.org/10.1016/j.femsec.2004.10.002>
- Pinto, P., Fernández Long, M.E., Piñeiro, G., 2017. Including cover crops during fallow periods for increasing ecosystem services: Is it possible in croplands of Southern South America? *Agric. Ecosyst. Environ.* 248, 48–57. <https://doi.org/10.1016/j.agee.2017.07.028>
- Poffenbarger, H.J., Mirsky, S.B., Weil, R.R., Kramer, M., Spargo, J.T., Cavigelli, M.A., 2015. Legume Proportion, Poultry Litter, and Tillage Effects on Cover Crop Decomposition. *Agron. J.* 107, 2083–2096. <https://doi.org/10.2134/agronj15.0065>
- Puntel, L.A., Sawyer, J.E., Barker, D.W., Dietzel, R., Poffenbarger, H., Castellano, M.J., Moore, K.J., Thorburn, P., Archontoulis, S. V., 2016. Modeling long-term corn yield response to nitrogen rate and crop rotation. *Front. Plant Sci.* 7, 1–18. <https://doi.org/10.3389/fpls.2016.01630>
- Quemada, M., 2004. Predicting crop residue decomposition using moisture adjusted time scales. *Nutr. Cycl. Agroecosystems* 70, 283–291. <https://doi.org/10.1007/s10705-004-0531-5>
- Quemada, M., Cabrera, M.L., 1997. Temperature and moisture effects on C and N mineralization from surface applied clover residue. *Plant Soil* 189, 127–137. <https://doi.org/10.1023/A:1004281804058>
- Ranells, N.N., Waggoner, M.G., 1996. Nitrogen Release from Grass and Legume Cover Crop Monocultures and Bicultures. *Agron. J.* 782, 777–782.

- Reyes, W.M., Epstein, H.E., Li, X., McGlynn, B.L., Riveros-Iregui, D.A., Emanuel, R.E.,
2017. Complex terrain influences ecosystem carbon responses to temperature and
precipitation. *Global Biogeochem. Cycles* 31, 1306–1317.
<https://doi.org/10.1002/2017GB005658>
- Ritchie, J.T., Porter, C.H., Jones, J.W., Sulieman, A., 2009. Extension of an Existing
Model for Soil Water Evaporation and Redistribution under High Water Content
Conditions. *Soil Sci. Soc. Am. J.* 73, 792–801.
<https://doi.org/10.2136/sssaj2007.0325>
- Roesch-Mcnally, G.E., Basche, A.D., Arbuckle, J.G., Tyndall, J.C., Miguez, F.E.,
Bowman, T., Clay, R., 2018. The trouble with cover crops: Farmers’ experiences
with overcoming barriers to adoption. *Renew. Agric. Food Syst.* 33, 322–333.
<https://doi.org/10.1017/S1742170517000096>
- Rosenbloom, N.A., Doney, S.C., Schimel, D.S., 2001. Geomorphic evolution of soil
texture and organic matter in eroding landscapes. *Global Biogeochem. Cycles* 15,
365–381. <https://doi.org/10.1029/1999GB001251>
- Rosenzweig, C., Tubiello, F.N., Goldberg, R., Mills, E., Bloomfield, J., 2002. Increased
crop damage in the US from excess precipitation under climate change. *Glob.*
Environ. Chang. 12, 197–202. [https://doi.org/10.1016/S0959-3780\(02\)00008-0](https://doi.org/10.1016/S0959-3780(02)00008-0)
- Ruis, S.J., Blanco-Canqui, H., Creech, C.F., Koehler-Cole, K., Elmore, R.W., Francis,
C.A., 2019. Cover crop biomass production in temperate agroecozones. *Agron. J.*
111, 1535–1551. <https://doi.org/10.2134/agronj2018.08.0535>
- Ruíz-Nogueira, B., Boote, K.J., Sau, F., 2001. Calibration and use of CROPGRO-

- soybean model for improving soybean management under rainfed conditions. *Agric. Syst.* 68, 151–173. [https://doi.org/10.1016/S0308-521X\(01\)00008-7](https://doi.org/10.1016/S0308-521X(01)00008-7)
- Sadras, V.O., Calviño, P.A., 2001. Quantification of Grain Yield Response to Soil Depth in Soybean, Maize, Sunflower, and Wheat. *Agron. J.* 93, 577–583. <https://doi.org/10.2134/agronj2001.933577x>
- Salmerón, M., Cavero, J., Isla, R., Porter, C.H., Jones, J.W., Boote, K.J., 2014. DSSAT nitrogen cycle simulation of cover crop-maize rotations under irrigated mediterranean conditions. *Agron. J.* 106, 1283–1296. <https://doi.org/10.2134/agronj13.0560>
- Salmerón, M., Cavero, J., Quílez, D., Isla, R., 2010. Winter cover crops affect monoculture maize yield and nitrogen leaching under irrigated Mediterranean conditions. *Agron. J.* 102, 1700–1709. <https://doi.org/10.2134/agronj2010.0180>
- Salvagiotti, F., Cassman, K.G., Specht, J.E., Walters, D.T., Weiss, A., Dobermann, A., 2008. Nitrogen uptake, fixation and response to fertilizer N in soybeans: A review. *F. Crop. Res.* 108, 1–13. <https://doi.org/10.1016/j.fcr.2008.03.001>
- Saseendran, S.A., Ahuja, L.R., Ma, L., Timlin, D., Stöckle, C.O., Boote, K.J., Hoogenboom, G., 2015. Current Water Deficit Stress Simulations in Selected Agricultural System Models. ASA, CSSA, SSSA, Madison, WI. <https://doi.org/10.2134/advagricsystmodell.c1>
- Sauer, T.J., Horton, R., 2005. Soil Heat Flux, in: Hatfield, J.L., Baker, J. (Eds.), *Micrometeorology in Agricultural Systems*. American Society of Agronomy, Madison, WI, pp. 131–154. <https://doi.org/10.2134/agronmonogr47.c7>

- Scarnecchia, D.L., Magdoff, F., 1994. Building Soils for Better Crops. Organic Matter Management. *J. Range Manag.* 47, 315. <https://doi.org/10.2307/4002554>
- Schipanski, M.E., Drinkwater, L.E., 2012. Nitrogen fixation in annual and perennial legume-grass mixtures across a fertility gradient. *Plant Soil* 357, 147–159. <https://doi.org/10.1007/s11104-012-1137-3>
- Schipanski, M.E., Drinkwater, L.E., 2011. Nitrogen fixation of red clover interseeded with winter cereals across a management-induced fertility gradient. *Nutr. Cycl. Agroecosystems* 90, 105–119. <https://doi.org/10.1007/s10705-010-9415-z>
- Schipanski, M.E., Drinkwater, L.E., Russelle, M.P., Artile, R., 2010. Understanding the variability in soybean nitrogen fixation across agroecosystems. *Plant Soil* 329, 379–397. <https://doi.org/10.1007/s11104-009-0165-0>
- Schlesinger, W.H., Bernhardt, E.S., 2013. Biogeochemistry, 3rd ed. Elsevier, Waltham, MA, USA. <https://doi.org/10.1016/C2010-0-66291-2>
- Sela, S., van Es, H.M., Moebius-Clune, B.N., Marjerison, R., Moebius-Clune, D., Schindelbeck, R., Severson, K., Young, E., 2017. Dynamic Model Improves Agronomic and Environmental Outcomes for Maize Nitrogen Management over Static Approach. *J. Environ. Qual.* 46, 311–319. <https://doi.org/10.2134/jeq2016.05.0182>
- Sentelhas, P.C., Battisti, R., Câmara, G.M.S., Farias, J.R.B., Hampf, A.C., Nendel, C., 2015. The soybean yield gap in Brazil - Magnitude, causes and possible solutions for sustainable production. *J. Agric. Sci.* 153, 1394–1411. <https://doi.org/10.1017/S0021859615000313>

Sievers, T., Cook, R.L., 2018. Aboveground and Root Decomposition of Cereal Rye and Hairy Vetch Cover Crops. *Soil Sci. Soc. Am. J.* 82, 147–155.

<https://doi.org/10.2136/sssaj2017.05.0139>

Sikora, F.J., 2006. A Buffer that Mimics the SMP Buffer for Determining Lime Requirement of Soil. *Soil Sci. Soc. Am. J.* 70, 474–486.

<https://doi.org/10.2136/sssaj2005.0164>

Singh, G., Williard, K., Schoonover, J., Nelson, K.A., Kaur, G., 2019. Cover Crops and Landscape Position Effects on Nitrogen Dynamics in Plant-Soil-Water Pools. *Water* 11, 1–18. <https://doi.org/10.3390/w11030513>

Singh, S., Boote, K.J., Angadi, S. V., Grover, K.K., 2017. Estimating water balance, evapotranspiration and water use efficiency of spring safflower using the CROPGRO model. *Agric. Water Manag.* 185, 137–144.

<https://doi.org/10.1016/j.agwat.2017.02.015>

Smith, R.G., Menalled, F.D., Robertson, G.P., 2007. Temporal Yield Variability under Conventional and Alternative Management Systems 1629–1634.

<https://doi.org/10.2134/agronj2007.0096>

Snapp, SS, Labarta, S., Mutch, R., Black, D., Leep, R., Nyiraneza, J., O’Neil, K., 2005. Evaluating cover crops for benefits, costs and performance within cropping system niches. *Agron. J.* 97, 322–332. <https://doi.org/10.2134/agronj2005.0322>

Snapp, Sieglinde, Swinton, S., Labarta, R., Black, R., 2005. Evaluating Cover Crops for Benefits, Costs and Performance within Cropping System Niches. *Agron. J.* 97, 322–332.

Soil Survey Staff, 2020. Web Soil Survey.

Soldevilla-Martinez, M., López-Urrea, R., Martínez-Molina, L., Quemada, M., Lizaso, J.I., 2013. Improving Simulation of Soil Water Balance Using Lysimeter Observations in a Semiarid Climate. *Procedia Environ. Sci.* 19, 534–542. <https://doi.org/10.1016/j.proenv.2013.06.060>

Steiner, J.L., Schomberg, H.H., Unger, P.W., Cresap, J., 1999. Crop Residue Decomposition in No-Tillage Small-Grain Fields. *Soil Sci. Soc. Am. J.* 63, 1817–1824. <https://doi.org/10.2136/sssaj1999.6361817x>

Stott, D.E., Elliott, L.F., Papendick, R.I., Campbell, G.S., 1986. Low temperature or low water potential effects on the microbial decomposition of wheat residue. *Soil Biol. Biochem.* 18, 577–582. [https://doi.org/10.1016/0038-0717\(86\)90078-7](https://doi.org/10.1016/0038-0717(86)90078-7)

Strock, J.S., Porter, P.M., Russelle, M.P., 2004. Cover Cropping to Reduce Nitrate Loss through Subsurface Drainage in the Northern U.S. Corn Belt. *J. Environ. Qual.* 33, 1010. <https://doi.org/10.2134/jeq2004.1010>

Suriyavirun, N., Krichels, A.H., Kent, A.D., Yang, W.H., 2019. Microtopographic differences in soil properties and microbial community composition at the field scale. *Soil Biol. Biochem.* 131, 71–80. <https://doi.org/10.1016/j.soilbio.2018.12.024>

Team, R.C., 2020. R: A language and environment for statistical computing.

Thapa, R., Poffenbarger, H., Tully, K.L., Ackroyd, V.J., Kramer, M., Mirsky, S.B., 2018. Biomass production and nitrogen accumulation by hairy vetch–cereal rye mixtures: A meta-analysis. *Agron. J.* 110, 1197–1208.

<https://doi.org/10.2134/agronj2017.09.0544>

Thelemann, R., Johnson, G., Sheaffer, C., Banerjee, S., 2010. The Effect of Landscape Position on Biomass Crop Yield 513–522. <https://doi.org/10.2134/agronj2009.0058>

Thorp, K.R., Hunsaker, D.J., French, A.N., White, J.W., Clarke, T.R., 2010. Evaluation of the CSM-CROPSIM-CERES-Wheat model as a tool for crop water management. *Trans. ASABE* 53, 87–102.

Tonitto, C., David, M.B., Drinkwater, L.E., 2006. Replacing bare fallows with cover crops in fertilizer-intensive cropping systems: A meta-analysis of crop yield and N dynamics. *Agric. Ecosyst. Environ.* 112, 58–72.
<https://doi.org/10.1016/j.agee.2005.07.003>

Unger, P.W., Vigil, M.F., 1998. Cover crop effects on soil water relationships. *J. Soil Water Conserv.* 53, 200 LP – 207.

van Rij, J., Wieling, M., Baayen, R., van Rijn, H., 2020. itsadug: Interpreting Time Series and Autocorrelated Data Using GAMMs.

Vitousek, P.M., Aber, J.D., Horwath, R.W., Likens, G.E., Matson, P., Schindler, D., 4bvn, S., 1997. Human alteration of the global nitrogen cycle: sources and consequences. *Ecol. Appl.* 7, 737–750. [https://doi.org/https://doi.org/10.1890/1051-0761\(1997\)007\[0737:HAOTGN\]2.0.CO;2](https://doi.org/https://doi.org/10.1890/1051-0761(1997)007[0737:HAOTGN]2.0.CO;2)

Vitousek, P.M., Menge, D.N.L., Reed, S.C., Cleveland, C.C., Vitousek, P.M., 2013. Biological nitrogen fixation : rates , patterns and ecological controls in terrestrial ecosystems. *Philos. Trans. R. Soc.* 386, 1–9.

- Wankert, W., Fausey, N.R., Watters, H.D., 1981. Flooding responses in Zea Mays L. *Plant Soil* 62, 351–366.
- Wendroth, O., Reuter, H.I., Kersebaum, K.C., 2003. Predicting yield of barley across a landscape : a state-space modeling approach. *J. Hydrol.* 272, 250–263.
[https://doi.org/https://doi.org/10.1016/S0022-1694\(02\)00269-X](https://doi.org/https://doi.org/10.1016/S0022-1694(02)00269-X)
- White, C.M., DuPont, S.T., Hautau, M., Hartman, D., Finney, D.M., Bradley, B., LaChance, J.C., Kaye, J.P., 2017. Managing the trade off between nitrogen supply and retention with cover crop mixtures. *Agric. Ecosyst. Environ.* 237, 121–133.
<https://doi.org/10.1016/j.agee.2016.12.016>
- Williams, C.L., Liebman, M., Edwards, J.W., James, D.E., Singer, J.W., Arritt, R., Herzmann, D., 2008. Patterns of regional yield stability in association with regional environmental characteristics. *Crop Sci.* 48, 1545–1559.
<https://doi.org/10.2135/cropsci2006.12.0837>
- Wood, S.N., 2011. Fast stable restricted maximum likelihood and marginal likelihood estimation of semiparametric generalized linear models. *J. R. Stat. Soc.* 73, 3–36.
- Wortman, S.E., Francis, C.A., Lindquist, J.L., 2012. Cover crop mixtures for the western Corn Belt: Opportunities for increased productivity and stability. *Agron. J.* 104, 699–705. <https://doi.org/10.2134/agronj2011.0422>
- Wuebbles, D.J., Fahey, D.W., Hibbard, K.A., DeAngelo, B., Doherty, S., Hayhoe, K., Horton, R., Kossin, J.P., Taylor, P.C., Waple, A.M., Weaver, C.P., 2017. Executive summary. *Clim. Sci. Spec. Rep. Fourth Natl. Clim. Assessment, Vol. I* 10–34.
<https://doi.org/10.7930/J0DJ5CTG.U.S.>

- Yost, M.A., Kitchen, N.R., Sudduth, K.A., Sadler, E.J., Baffaut, C., Volkmann, M.R., Drummond, S.T., 2016. Long-Term Impacts of Cropping Systems and Landscape Positions on Claypan-Soil Grain Crop Production. *Agron. J.* 108, 713–725. <https://doi.org/10.2134/agronj2015.0413>
- Yu, Y., Stomph, T.J., Makowski, D., Zhang, L., van der Werf, W., 2016. A meta-analysis of relative crop yields in cereal/legume mixtures suggests options for management. *F. Crop. Res.* 198, 269–279. <https://doi.org/10.1016/j.fcr.2016.08.001>
- Z. Qi, M. J. Helmers, R. W. Malone, K. R. Thorp, 2011. Simulating Long-Term Impacts of Winter Rye Cover Crop on Hydrologic Cycling and Nitrogen Dynamics for a Corn-Soybean Crop System. *Trans. ASABE* 54, 1575–1588. <https://doi.org/10.13031/2013.39836>

VITA

Samuel John Leuthold

Education

Montana State University

December 2017

B.S. Soil and Water Sciences (Minor: GIS)

Professional Positions Held

Graduate Research Assistant

January 2019 - Current

University of Kentucky Plant and Soil Sciences Dept.

Research Associate

December 2016 – August 2018

Montana State University Soil Biogeochemistry Lab

Biological Science Technician

May 2016 – August 2016

USGS GECSC

Scholastic and Professional Honors

Plant and Soil Science Outstanding Continuing MS Student

May 2020

2nd place MS Student Oral Presentation – Southern Regional
ASA Meeting

February 2020

1st place Graduate Student Oral Presentation – National ASA
Nutrient Management Division

November 2019

North Central Soil Fertility Council Outstanding Graduate
Student Award

November 2019

Professional Publications

Leuthold, S., Salmeron, M., Wendroth, O., Poffenbarger, H. (2021) Cover crops decrease maize yield variability in sloping landscapes through increased water during reproductive stages. Field Crops Research. In-Press.

Leuthold, S.J., Ewing, S.A., Payn, R.A., Miller, F.R., Custer, S.G. (2021) Seasonal connections between meteoric water and streamflow generation along a mountain headwater stream. Hydrol. Process. 1–17. <https://doi.org/10.1002/hyp.14029>

Miller, F.R., Ewing, S.A., Payn, R.A., Paces, J.B., **Leuthold, S.J.**, Custer, S.G., (2020) Sr and U isotopes reveal the influence of lithologic structure on groundwater contributions along a mountain headwater catchment (Hyalite Canyon, MT). J. Hydrol. <https://doi.org/10.1016/j.jhydrol.2020.125653>